August 2020

Development of a Novel Sequential Injection-Proton NMR Method for Determining Cathinones in Forensic Samples

Malati Thapa
University of Wisconsin-Milwaukee

DEVELOPMENT OF A NOVEL SEQUENTIAL INJECTION-PROTON NMR METHOD FOR DETERMINING CATHINONES IN FORENSIC SAMPLES

by

Malati Thapa

A Thesis Submitted in

Partial Fulfillment of the

Requirements for the Degree of

Master of Science

in Chemistry

at

The University of Wisconsin-Milwaukee

August 2020

ABSTRACT

DEVELOPMENT OF A NOVEL SEQUENTIAL INJECTION-PROTON NMR METHOD FOR DETERMINING CATHINONES IN FORENSIC SAMPLES

by

Malati Thapa

The University of Wisconsin-Milwaukee, 2020
Under the Supervision of Professor Joseph Howard
Aldstadt III

A novel method was developed for the determination of low levels of Cathinones in authentic samples by interfacing Sequential Injection Analysis (SIA) to Proton Nuclear Magnetic Resonance Spectroscopy (NMR). In the first part of this study, solid phase extraction (SPE) was studied by SIA to preconcentrate the sample and remove matrix interferences. Phenylpropanolamine (PPA), Phenylephrine (PEP), and Methylephedrine (MEP) were studied as simulants for the Cathinones, representing primary, secondary, and tertiary amines, respectively. A variety of stationary, mobile, and eluent phases for several column geometries were examined, and a wide cylindrical column (20 mm×6.6 mm) with a bed volume of 2.7 mL with a strong cation exchange (SCX) resin was selected for further study. The method was

applied to authentic samples at the Wisconsin State Crime Lab (WSCL) in Milwaukee. A range of samples were analyzed that differed in the Cathinones (Methcathinone, Methylone, and N-Ethylpentylone) and interferences (Mannitol and Caffeine) that were present. Measurements were done by SIA-NMR as well as directly by NMR. When SIA-NMR was performed, the interferences were efficiently removed. However, tertiary amines were found to be more difficult to quantitatively elute than primary and secondary amines.

For the second part of the study, the SPE-SIA method was optimized by application of Plackett-Burman (P-B) screening (11 factor design) and Simplex optimization (7 factor design) methods. The optimized SPE-SIA method had the following conditions: 800 μL sample volume, 21 μL/s sample aspiration flowrate, 18 μL/s carrier load flowrate, 25 μL/s elution flowrate, 100 mM phosphate buffer (pH 6.00) mobile phase, 215 mM NaCl / 60 mM HCl eluent, and 1565 μL eluent volume. For the optimized method, the Limit of Detection was 0.023 mM (70% improvement) and the precision, measured for 0.25 mM PPA (n=3), was 0.10% (93% improvement).

In the final part of the study, the optimized SIA-NMR method was applied to a new set of confiscated samples provided by the WSCL in which (N-Ethylpentylone and N-Ethylhexedrone) were present. The optimized method was effective in the determination of low levels of Cathinones in the confiscated samples for all three types of amines. Predicted proton spectra of the Cathinones were then created using

the MNova software program and compared to the observed spectra. The number of peaks in the observed and predicted spectra generally agreed, but differences in the chemical shifts and multiplicities of the protons were observed.

To

Mother: Laxmi Devi Manandhar,

Father: Madhukar Singh Thapa,

Husband: Resham Rana,

and Son: Martin Rana

TABLE OF CONTENTS

LIST OF FIGURES

LIST OF TABLES

ACKNOWLEDGEMENTS

Studying abroad is always a challenge. Change in climate, culture, education system, and many more new events were on the way when I joined UWM as a graduate student. Thanks to all my loved ones, I successfully completed my journey in obtaining a master's degree in analytical chemistry with comfort and joy in my heart. I would like to thank Dr. Aldstadt for his generous time and energy in helping me put this work together. His trust that I could lift myself from point zero on the learning curve learning curve to where I am is appreciated beyond words. I would like to thank my one-year old son, Martin Rana for being my greatest strength. I would also like to thank my husband, Resham Rana, for his help during my journey as graduate student in UWM and for the endless hours in listening to me practice my seminar, milestone meeting talk and defense speech. I would like to thank my mother, Laxmi Devi Manandhar, my father, Madhukar Singh Thapa and my mother-in-law, Nanu Maya Rana, for letting me be what I am today, taking care of my son from the day one of his birth and helping me to continue my education. I would also like to thank my sister, Mala Thapa, and my brother, Manish Thapa, for their love, trust, and support.

I would also like to thank my friends in Milwaukee for their suggestions. I would

Chapter 1

Introduction

1.1 Background

The emergence of new psychoactive substances (NPS) is increasing rapidly with time, thereby presenting continued challenges in forensic analytical chemistry. Normally, NPS represent a diverse range of substances that were originally designed to mimic the effect of established illicit drugs such as cannabis, lysergic acid diethylamide (LSD), cocaine, or amphetamines [1]. NPS are manufactured to replace those drugs which are banned, which also means that the chemical structure of the drugs is changed constantly so that criminals can stay ahead of the law [2]. They are untested and unregulated and, thus, are particularly dangerous. NPS are controlled under federal law which makes their synthesis or distribution a prosecutable offense, even if it is sold as an over-the-counter item [3]. Until December 2019, more than 950 substances have been reported to the UNODC Early Warning Advisory (EWA) on NPS by governments, laboratories, and partner organizations [4].

Over the past decade, Cathinones have emerged as a common NPS [5]. Cathinones (Figure 1.1) are β-keto amphetamines that are derived from monoamine alkaloids found in the leaves of a shrub called Catha edulis ("Khat") [6]. Synthetic Cathinones have been placed on Schedule I of the Controlled Substance Act [7]. Commonly known as "Bath Salts", a variety of street names are used for variants, such as: Bloom, Ivory Wave, Vanilla Sky, White Lightning, Red Dove, Cloud 9, Cotton Cloud, Snow Day, and Ocean Snow [8]. The general pattern of behavior that emerges after ingestion of Cathinones is a feeling of euphoria that is experienced for several hours, followed by a depressive stage that includes irritability, loss of appetite, and insomnia [9]. Gum disease or oral cancer, depression, and cardiovascular disease could also be the result of long-term usage of Cathinones.

The analytical strategy that forensic labs typically use is to initially conduct "presumptive (screening) tests" followed by confirmatory testing using more sophisticated analytical techniques [10]. Common presumptive tests, such as colorimetry, infrared spectroscopy (IR), and thin-layer chromatography (TLC), are intended to primarily provide qualitative information. They are fast, inexpensive, and can be performed by relatively inexperienced technicians. However, they are notoriously error-prone — they are generally imprecise and inaccurate [10]. Colorimetry is very commonly used in presumptive testing but is prone to false negative, and false positive results. IR has

poor sensitivity and requires the constant update of spectral libraries for positive identification. TLC is relatively non-selective, and thus interferences in confiscated samples can be a problem [11]. There is thus a pressing need for more reliable screening methods [12].

For confirmatory testing, gas chromatography-mass spectrometry (GC-MS) is the most common technique that is used [10]. However, GC-MS is time consuming, expensive, and requires an experienced analyst. Furthermore, some NPS compounds are regulated as isomers, and it is impossible to discriminate between them because they have identical mass spectra [13].

In the present work, a novel method was developed interfacing Sequential Injection Analysis (SIA) with Nuclear Magnetic Resonance (NMR) Spectroscopy to provide solution to this problem. The goal of this automated method is to selectively measure relatively low levels (<100 mM) of Cathinones in minimum time (<10 min), and to then demonstrate the method using authentic casework samples provided by the Wisconsin State Crime Lab in Milwaukee.

1.2   Nuclear Magnetic Resonance (NMR)

An alternative to existing techniques used in crime labs that could potentially be used for both screening and confirmation is NMR, a technique that is unparalleled in elucidating molecular structures [14]. NMR is a non-destructive technique and has wide application in medicine, biology, agriculture, environment, and many more [15, 16]. NMR was discovered by I. I. Rabi who received Nobel Prize in Physics in 1944 [17]. He successfully made accurate measurements of nuclear magnetic moments using magnetic resonance absorption of a molecular beam. Later, F. Block and E.M. Purcell successfully demonstrated NMR for condensed matter, and shared the Noble Prize in Physics in 1952 [18].

Atomic nuclei carry a charge and this charge spins on the nuclear axis. This circulation will generate a magnetic moment diplole along the axis (Figure 1.2) [19]. Without an externally applied magnetic field, the nuclear spins are random. But when an external magnetic field is applied, the nuclei will align either with or against the external field. The frequency at which the protons spin is called precession frequency. The protons that align with the external field are in the α spin states and have lower energies. The protons that align against the external magnetic field are in the β spin state and have higher energies (Figure 1.3). The difference in energy between the two energy states is dependent upon the strength of the applied magnetic field. If the sample is

4

placed in the magnetic field and irradiated at the same frequency as the precession frequency, the spin "flips" from the β spin state to the α spin state. During this process, electromagnetic signals are emitted. The proton NMR spectrometer then measures these signals and creates a spectrum of frequency versus intensity.

For a given molecule, the NMR spectrum is unique "fingerprint" of its structure. One of the key advantages of NMR is that it generates a signal for each functional group relative to neighboring substituents. Because of this capability, one can distinguish among isomers of Cathinones. An example is the NMR spectrum of 3-Fluorometh Cathinone and 4-Fluorometh Cathinone (Figure 1.4). In the NMR spectra, the number of signals show different types of protons that are present, the location of protons shows how shielded or deshielded the protons are, the intensity of the signal shows the number of protons of that type, and signal splitting shows the number of protons on adjacent atoms.

Proton NMR spectrometers have been reported in forensic analysis applications, particularly for drugs of abuse [20]. Because relatively large amount of sample in pure form are required, these methods suffer from both poor sensitivity and severe matrix effects [21]. For this project, however, the design of the picoSpin80 instrument allows one to address these issues because, unlike conventional instrument designs in which samples are introduced discretely ("batch") using borosilicate tubes, the picoSpin80 has a flow-through sample cell. Therefore, integration of the picoSpin80 to "upstream"

liquid flow techniques is made possible. Thus, techniques such as Liquid Chromatography (LC), Capillary Electrophoresis (CE), and Flow-Injection Analysis (FIA) can be directly coupled to the picoSpin80 instrument. If pre-concentration is performed "upstream", the intrinsic insensitivity of NMR can also be addressed. Solid-Phase Extraction (SPE) is well-suited to this task.

1.3   Solid Phase Extraction (SPE)

Solid phase extraction (SPE) has established itself as an effective sample preparation technique for isolating analytes of interest in a variety of matrices, including urine, blood, natural waters, beverages, soil, and animal tissue [22]. SPE is a chromatographic technique in which displacement rather than elution is the means by which solutes emerge [14]. SPE chemically separates different components based upon their displacement from the stationary phase by a liquid eluent. SPE generally requires less time, uses smaller amount of solvents, and produces cleaner extracts than elution chromatography [23].SPE is often applied as a means to "clean up" a sample before quantifying the amount of analyte(s) in the sample. Modern SPE typically uses a liquid mobile phase which is passed through a stationary phase in which liquid adsorbed onto a solid support.If the desired analyte is retained by the stationary phase, an eluent is passed through the stationary phase to displace the analyte (or class of similar analytes).

SPE consists of four primary steps (Figure 1.5). The first step is the pre-treatment of the stationary phase to remove any contaminants in the packing material. This step "conditions" the stationary phase to improve the efficiency of analyte retention, and remove any air present in the column by filling the void volume with solvent. The second step is the loading of sample onto the stationary phase. Care must be taken to not allow the stationary phase to dry during the conditioning, and the sample treatment steps, which would cause inefficient retention of analyte, and result in poor recoveries. The third step is the washing step. In this step, unretained material passes through the column to waste. In the fourth step, the stationary phase is washed with eluent to release the analyte of interest. The composition, volume, and flow rate of eluent are optimized so that quantitative recovery of the analyte is achieved with low dilution [24].

For this thesis, strong cation exchange (SCX) sorbents containing aliphatic sulfonic acid groups were used. SCX ligands are negatively charged in aqueous solution across a broad pH range. A basic analyte, such as a Cathinone, will be retained by the SCX sorbent, and the eluent then neutralizes the ionic interaction between the analyte and the sorbent. One of the advantages of SPE is that it can be readily coupled to analytical techniques such as NMR [25, 26]. Because the stationary phase is a sorbent with an average particle size in μm, it provides a large surface area per unit bed mass, and thus, SPE can be conducted at higher flow rates [27]. SPE can be operated with smaller

elution volumes and yield extracts with fewer matrix interferences if optimization of the bed mass to reduce non-specific matrix adsorption is done [27]. Integrating SPE directly to NMR in a continuous flow, on-line approach is possible using Sequential Injection Analysis (SIA).

1.4   Sequential Injection analysis (SIA)

SIA is a variation of FIA which was reported in 1990 by J. Ruzicka & G. Marshall as a novel approach to process analysis, and laboratory assays [28]. SIA can be coupled with various detection methods including UV–visible absorption spectrometry, electrochemistry, NMR spectroscopy, and luminescence emission spectroscopy for a wide variety of bioprocess, immunoassay, forensic, pharmaceutical, environmental, and agricultural applications [29–31].

The flow diagram of a simple SIA system is shown in Figure 1.6. SIA is minimally comprised of a bi-directional pump, holding coil (HC), multi-position valve (MPV), reaction coil (RC), and a detector. The heart of the system is the MPV which draws sample, mobile phase, eluent, and other reagents and standards sequentially into the HC, thereby establishing a "stack" of zones. The stacked zones are then pumped (in the opposite direction) to the detector by the bi-directional pump. As the adjacent zones move through the RC, the zones are mixed, and a detectable species is formed

and is recorded as a peak by the detector [32]. Figure 1.7 shows the radial, and axial (bidirectional) profiles in SIA that enable dispersion of the zones within the system [33].

The simple example of operation of SIA (Figure 1.6) is the method for quantification of amoxicillin in pharmaceuticals using SIA with UV molecular absorption detectionusing a diode-array spectrophotometric detector [34]. The stacked zone in this experiment was as follows : carrier (water) aspiration, sample aspiration, and eluent (NaOH) aspiration with flowrate of 1 mL/min for all steps. The resultant absorbance spectra of Amoxicillin is shown in Figure 1.8.

SIA instruments have key advantages in this application. They are simple in design and versatile. Different sample pre-treatment processes such as preconcentration, filtration, and separation can be performed [35]. SIA can be operated with small sample volumes (1-100 μL) in a short amount of time (<5 min). Practical advantages include the generation of low volumes of waste and a small footprint. A computer interface is required for instrument control and data acquisition. For the project, SPE-SIA method was developed to preconcentrate the sample. SPE-SIA has been widely used for detection of variety of compounds Table 1.1.

9

1.5 Research goals

The goal of the project was to develop a novel method for detection of low levels of Cathinones in confiscated samples by interfacing SPE-SIA to NMR. For the first part of the project, the SPE-SIA method was developed using three different Cathinone simulants. To effectively pre-treat the sample by SPE, factors were considered which could directly or indirectly affect the desired response, including different SPE resins, column geometries, and eluents. In the second phase, the method was optimized by application of the Plackett-Burman screening method, and Simplex methods. For the third part of the work, the SPE-SIA method was integrated to NMR, and figures of merit were determined. The SIA-NMR method was then applied to confiscated samples from the WSCL. Finally, the proton NMR spectra of Cathinones were analyzed to determine why there were differences between predicted and observed spectra.

1.6 Figures and Tables
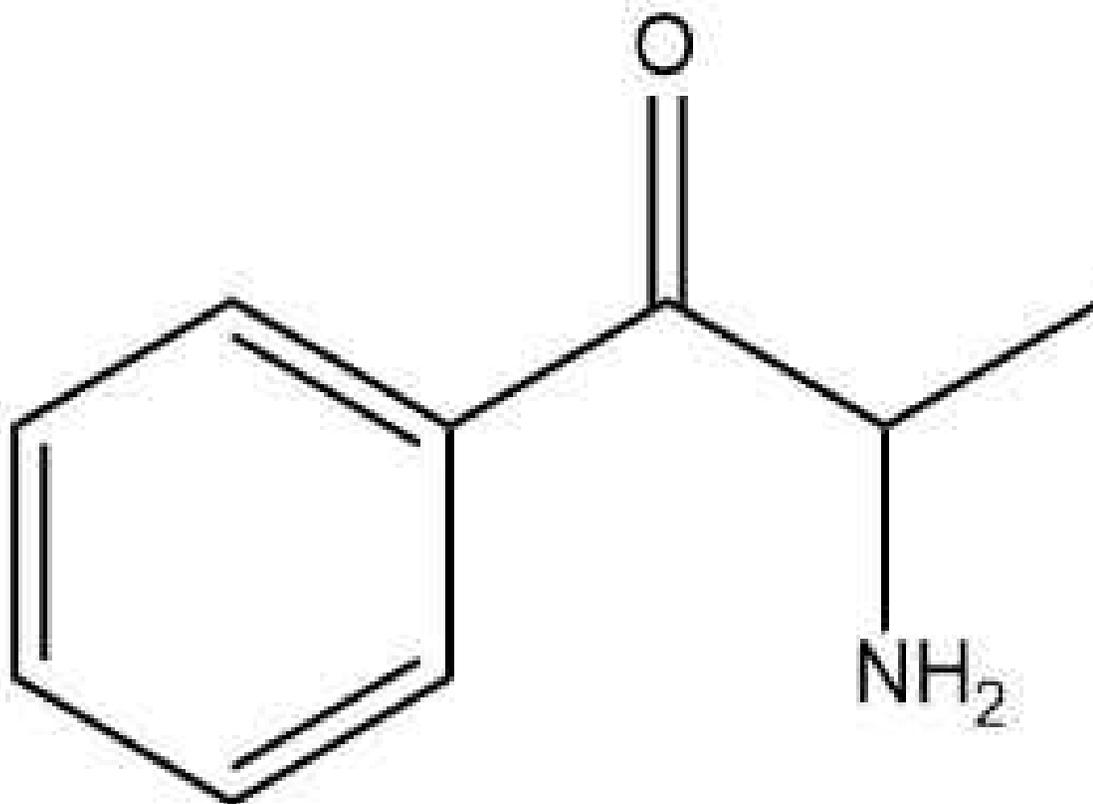
FIGURE 1.1: The structure of Cathinone.
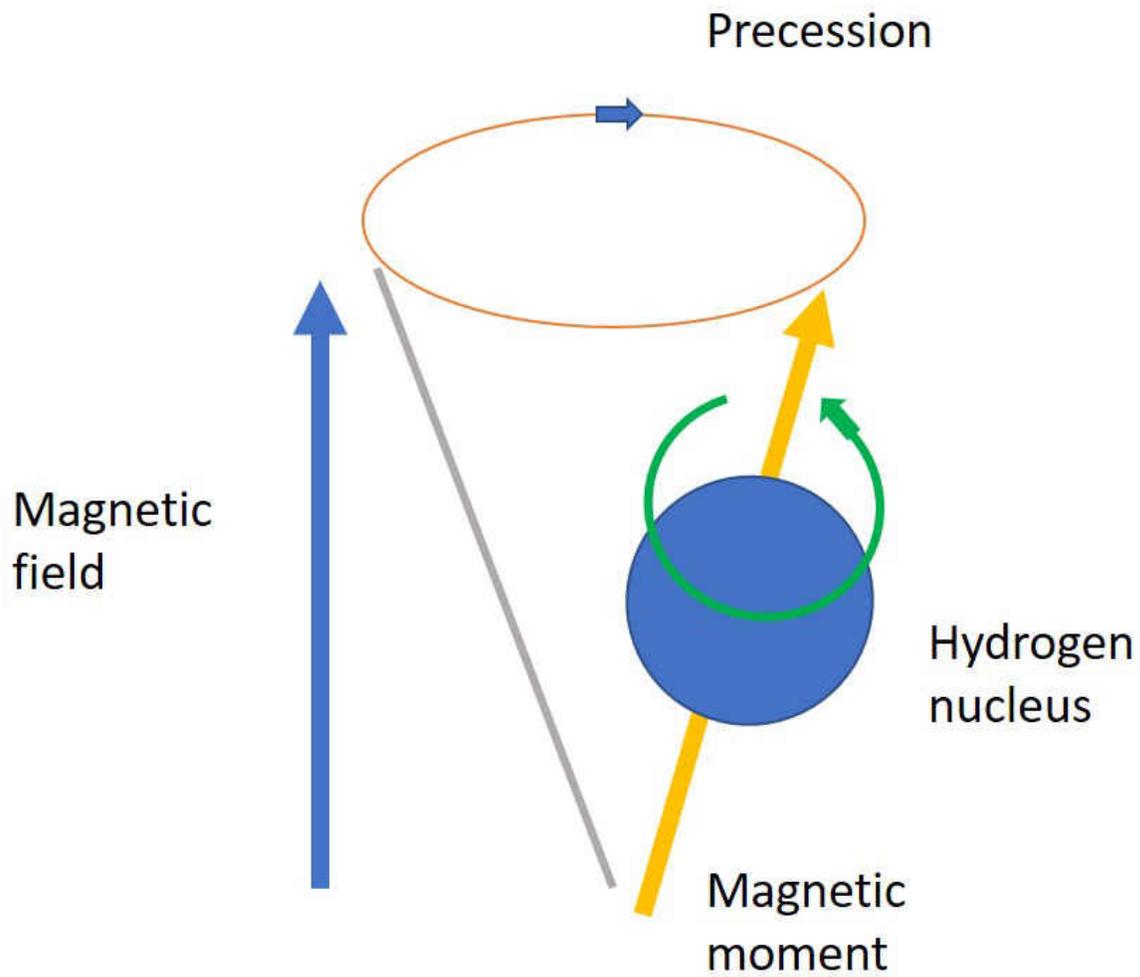
FIGURE 1.2: Schematic depiction of the phenomenon that is the basis of proton NMR. Adapted from [36].
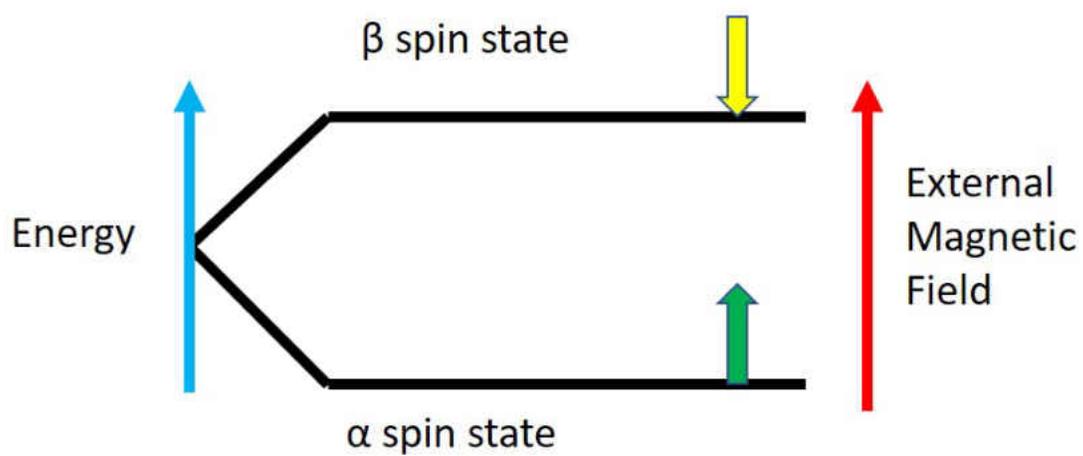
FIGURE 1.3: The two proton energy levels studied by proton NMR. Adapted from [36].
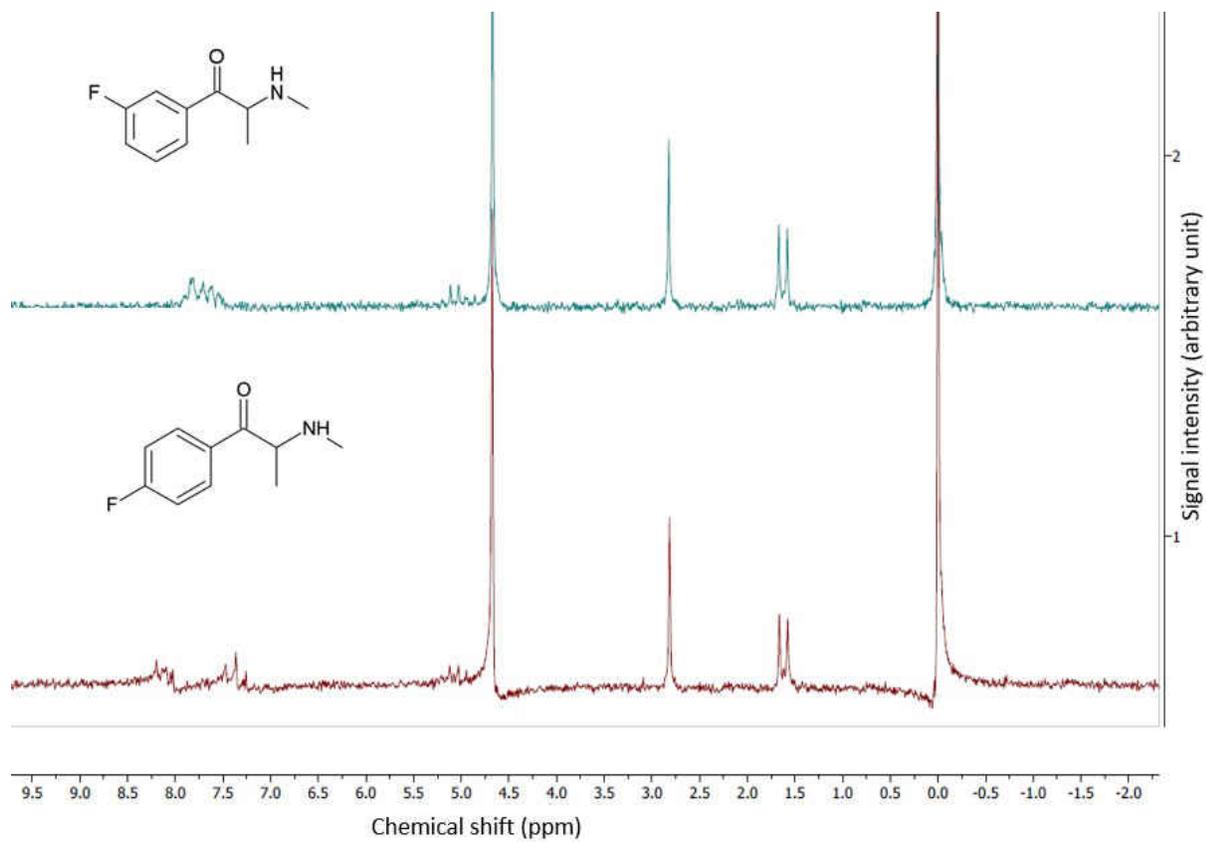
FIGURE 1.4: Proton NMR spectrum of 4-Fluorometh Cathinone(top) and 3-Fluorometh Cathinone (bottom). The different isomers can be identified by the spectral pattern at a chemical shift of approximately 8.0 ppm.
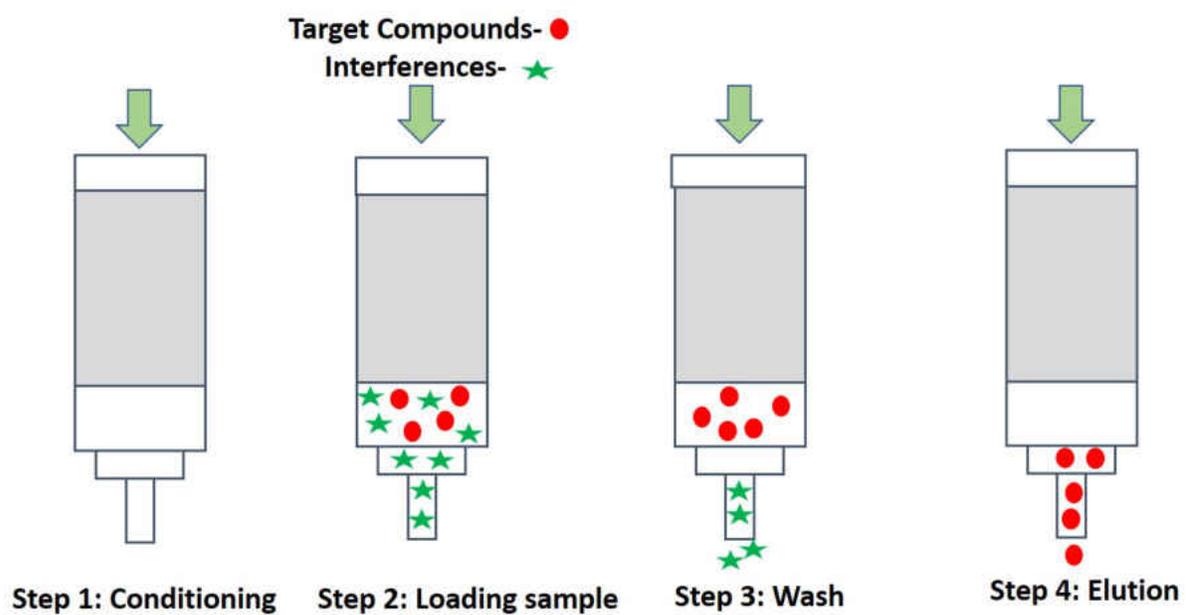
FIGURE 1.5: A schematic diagram showing the four primary steps in the SPE procedure. Adapted from [37].
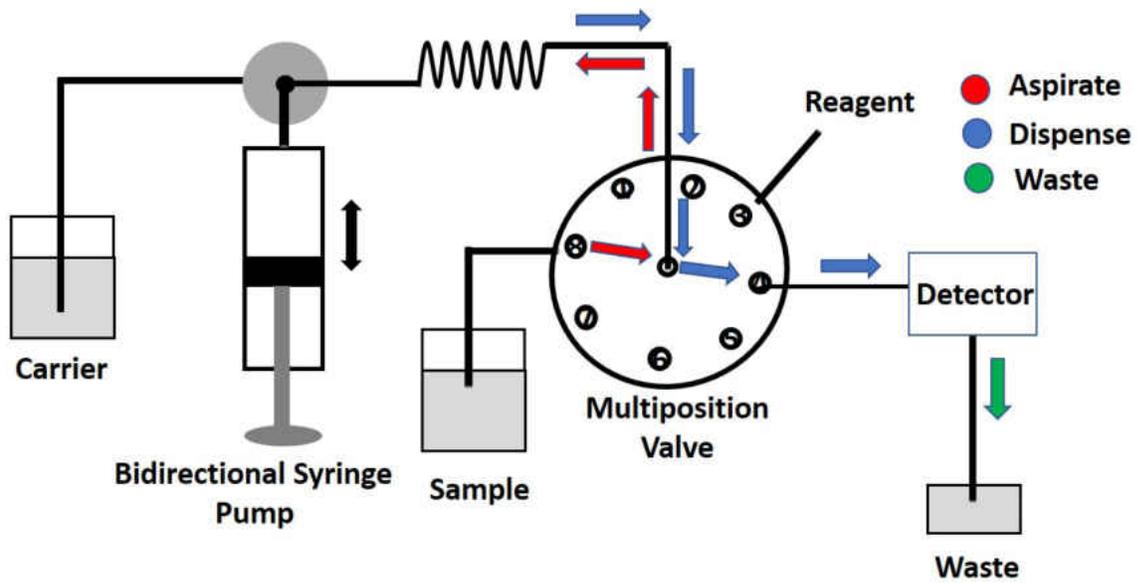
FIGURE 1.6: A schematic diagram showing a typical SIA manifold.
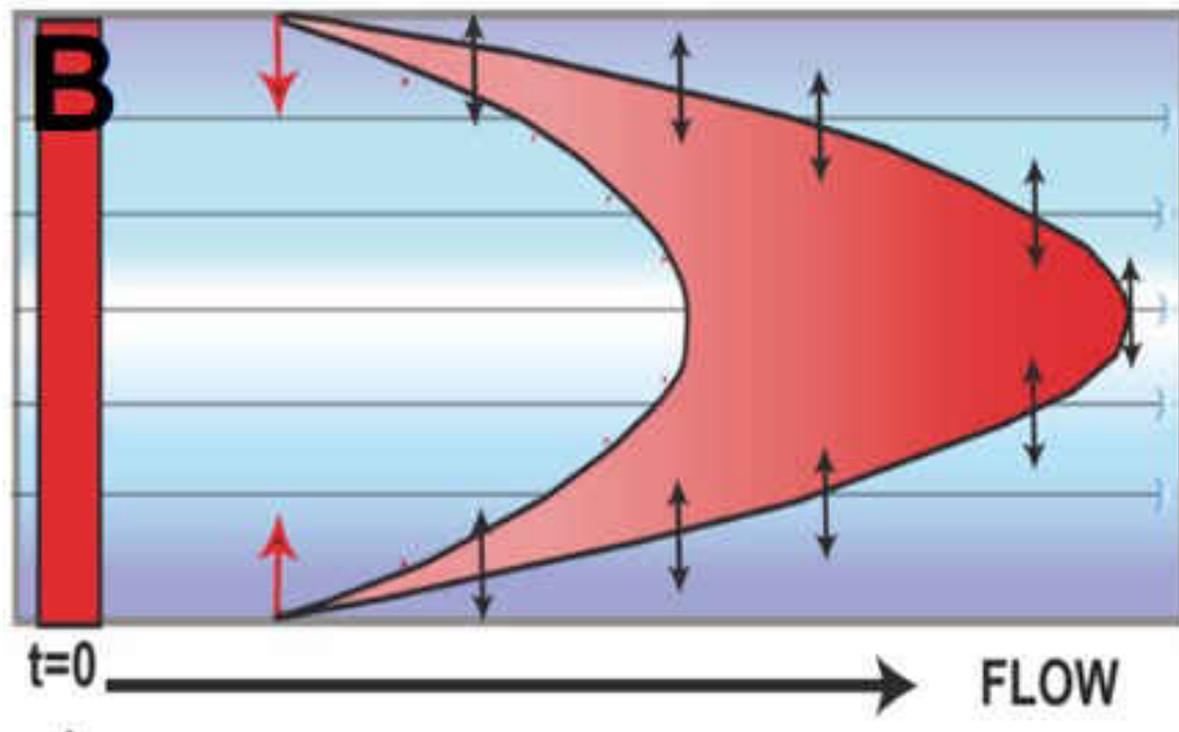
FIGURE 1.7: Cross-sectional view of the flow profile in SIA. The disperion of a zone in the conduit is the result of a combination of diffusive and convective forces. Adapted from [33].
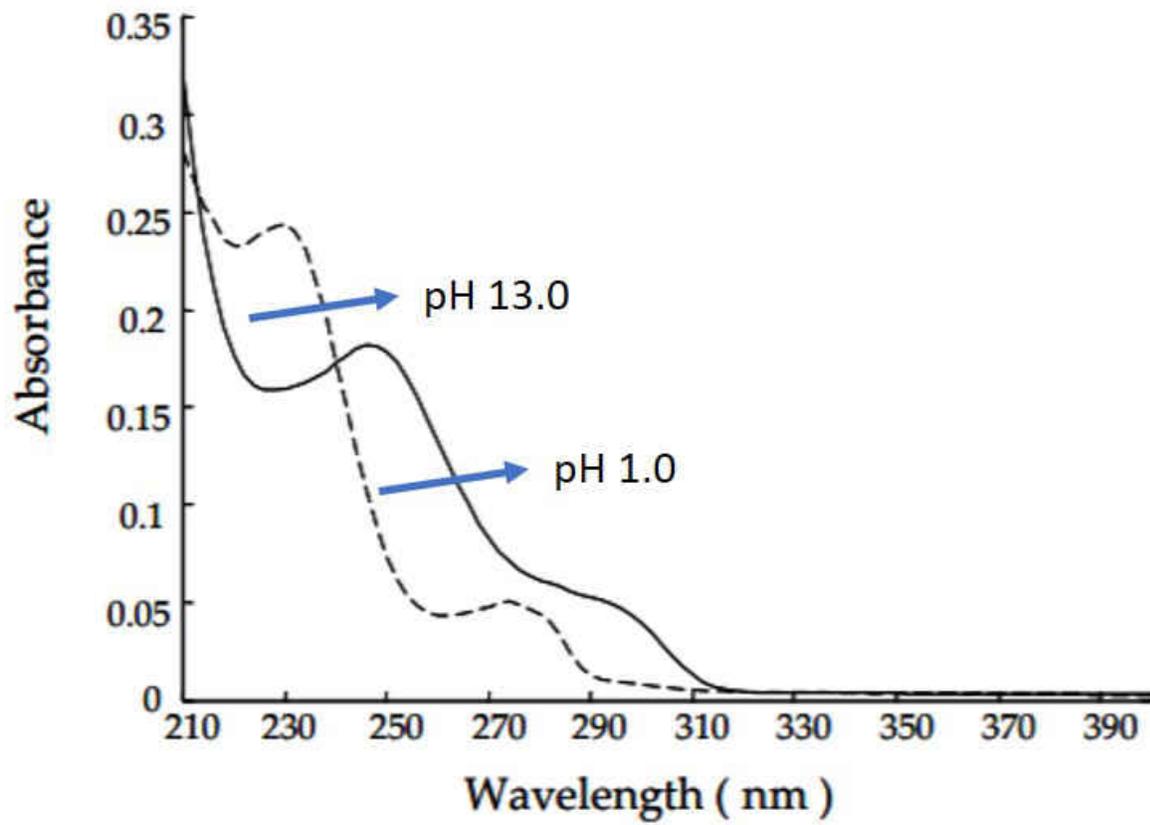
FIGURE 1.8: UV spectra of a solution of amoxillin at pH 13.0 and pH 1.0. Adapted from [34]

Sample	Sample aspiration flowrate	Peak Elution flowrate	LOD	Reference
Morphine	10.0 μL/s	20 μL/s	0.0230 μg/mL	[38]
Trifluoperazine	10.0 μL/s	20 μL/s	18.2 ng/mL	[39]
Fluroquinolone	100 μL/s	100 μL/s	0.0130 mg/L	[40]
Cimetidine	1.00 mL/min	0.30 mL/min	8.00 μgŁ	[41]
Citalopram	2.50 mL/min	2.50 mL/min		[42]
Thioridazine	0.60 mL/min	0.60 mL/min	5.50 ng/mL	[43]
Caffeine	0.80 mL/min	0.80 mL/min	NA	[44]
Rutin Trihydrate	10.0 μL/s	10.0 μL/s	NA	[45]
β blockers	1.00 mL/min	0.50 mL/min	0.005 μg/L	[46]
Amiloride	20.0 μL/s	20.0 μL/s	0.050 μg/L	[47]

TABLE 1.1: Application of SPE-SIA for detection of various samples.

References

[1] K. E. Champion, M. Teesson, and N. C. Newton, "Development of a universal internet-based prevention program for ecstasy and new psychoactive substances," *Open Journal of Preventive Medicine* 2015, 5, 01, 23.

[2] S. Bright, "New and emerging drugs," *Melbourne: Australian Drug Foundation* 2013.

[3] *Synthetic Drugs*, Accessed April 11, 2020, URL `https://www.deadiversion.usdoj.govsynthetic-drugs/index.html`.

[4] U. E. W. Advisory, "New psychoactive substances (nps)," *NPS (accessed Jan 11, 2019)* URL `https://www. unodc. org/LSS/Home`.

[5] L. D. Simmler and M. E. Liechti, *Neuropharmacology of New Psychoactive Substances (NPS)*, Springer, New York, 2016.

[6] N. Patel, "Mechanism of action of cathinone: the active ingredient of khat (catha edulis," *East African Medical Journal* 2000, 77, 6.

[7] J. A. Fass, A. D. Fass, and A. S. Garcia, "Synthetic cathinones (bath salts): legal status and patterns of abuse," *Annals of Pharmacotherapy* 2012, 46, 3, 436–441.

[8] J. A. Gershman and A. D. Fass, "Synthetic cathinones ('bath salts'): legal and health care challenges," *Pharmacy and Therapeutics* 2012, 37, 10, 571.

[9] A. Al-Motarreb, K. Baker, and K. J. Broadley, "Khat: pharmacological and medical aspects and its social use in yemen," *Phytotherapy Research: An International Journal Devoted to Pharmacological and Toxicological Evaluation of Natural Product Derivatives* 2002, 16, 5, 403–413.

[10] S. Bell, *Forensic chemistry*, Pearson, New York, 2014.

[11] L. A. Broussard, "Challenges in confirmation testing for drugs of abuse," "Accurate Results in the Clinical Laboratory," 243–256, Elsevier, Amsterdam, Netherlands, 2019.

[12] S. Graziano, L. Anzillotti, G. Mannocchi, S. Pichini, and F. P. Busardò, "Screening methods for rapid determination of new psychoactive substances (nps) in conventional and non-conventional biological matrices," *Journal of Pharmaceutical and Biomedical Analysis* 2019, 163, 170–179.

[13] R. Clark, *Bath Salt-type Aminoketone Designer Drugs: Analytical and Synthetic Studies on Substituted Cathinones*, National Institute of Justice, Washington, 2016.

[14] D. A. Skoog, F. J. Holler, and S. R. Crouch, *Principles of instrumental analysis*, Cengage learning, Boston, MA, 2017.

[15] G. A. Matzkanin, *Nondestructive characterization of materials*, Springer, New York, 1989.

[16] A. W. A. Rahman, M. Choudhary, *Solving problems with NMR spectroscopy*, Academic Press, Cambridge, Massachusetts, 2015.

[17] I. Rabi, "The discovery of nmr," .

[18] Basic, "Nmr, nuclear magnetic resonance spectroscopy." 1989.

[19] R. M. Silverstein and G. C. Bassler, "Spectrometric identification of organic compounds," *Journal of Chemical Education* 1962, 39, 11, 546.

[20] Y. Zhong, K. Huang, Q. Luo, S. Yao, X. Liu, N. Yang, C. Lin, and X. Luo, "The application of a desktop nmr spectrometer in drug analysis," *International Journal of Analytical Chemistry* 2018, 2018.

[21] J. C. Chatham and S. J. Blackband, "Nuclear magnetic resonance spectroscopy and imaging in animal research," *IlAR Journal* 2001, 42, 3, 189–208.

[22] F. Augusto, L. W. Hantao, N. G. Mogollón, and S. C. Braga, "New materials and trends in sorbents for solid-phase extraction," *TrAC Trends in Analytical Chemistry* 2013, 43, 14–23.

[23] I. Halász and P. Vogtel, "Some problems in quantitative analysis with concentration-sensitive detectors in high-performance liquid chromatography," *Journal of Chromatography A* 1977, 142, 241–259.

REFERENCES

[24] V. Camel et al., "Solid phase extraction of trace elements," *Spectrochimica acta Part B, Atomic Spectroscopy* 2003, 58, 7, 1177–1233.

[25] I. D. Wilson and J. Nicholson, "Solid phase extraction chromatography and nmr spectroscopy (spec-nmr) for the rapid identification of drug metabolites in urine," *Journal of Pharmaceutical and Biomedical Analysis* 1988, 6, 2, 151–165.

[26] S. Rodriguez-Mozaz, M. J. L. de Alda, and D. Barceló, "Advantages and limitations of on-line solid phase extraction coupled to liquid chromatography–mass spectrometry technologies versus biosensors for monitoring of emerging contaminants in water," *Journal of Chromatography A* 2007, 1152, 1-2, 97–115.

[27] N. Abd-Talib, S. H. Mohd-Setapar, and A. K. Khamis, "The benefits and limitations of methods development in solid phase extraction: Mini review," *Jurnal Teknologi* 2014, 69, 4.

[28] J. Ruzicka and G. D. Marshall, "Sequential injection: a new concept for chemical sensors, process analysis and laboratory assays," *Analytica Chimica Acta* 1990, 237, 329–343.

[29] J. Ruzicka, P. J. Baxter, O. Thastrup, and K. Scudder, "Flow injection microscopy: a novel tool for the study of cellular response and drug discovery," *Analyst* 1996, 121, 7, 945–950.

[30] C. H. Pollema, D. L. Campbell, and L. E. Moore, "Carrierless sequential injection analysis," 1998, uS Patent 5,849,592, Washington.

[31] O. B. Egorov, J. W. Grate, and L. A. Bray, "Method for sequential injection of liquid samples for radioisotope separations," 2000, uS Patent 6,153,154, Washington.

[32] A. Economou, P. Tzanavaras, and D. Themelis, "Sequential-injection analysis: Principles, instrument construction, and demonstration by a simple experiment," *Journal of chemical education* 2005, 82, 12, 1820.

[33] J. Ruscika, *Flow Injection Analysis*, 2019 (accessed March 11, 2020), URL `http://flowinjectiontutorial.com/index.html`.

[34] A. Pasamontes and M. Callao, "Determination of amoxicillin in pharmaceuticals using sequential injection analysis and multivariate curve resolution," *Analytica Chimica Acta* 2004, 515, 1, 159–165.

[35] Z.-L. Fang, Q. Fang, X.-Z. Liu, H.-W. Chen, and C.-L. Liu, "Continuous monitoring in drug dissolution testing using flow injection systems," *TrAC Trends in Analytical Chemistry* 1999, 18, 4, 261–271.

[36] H. Günther, *NMR spectroscopy: basic principles, concepts and applications in chemistry*, John Wiley & Sons, New Jersey, 2013.

REFERENCES

[37] A. Żwir-Ferenc and M. Biziuk, "Solid phase extraction technique–trends, opportunities and applications." *Polish Journal of Environmental Studies* 2006, 15, 5.

[38] A. M. Idris and A. O. Alnajjar, "Exploiting sequential injection analysis technique to automate on-line sample treatment and quantitative determination of morphine in human urine," *Talanta* 2008, 77, 2, 522–526.

[39] A. M. Idris, "On-line coupling of solid-phase extraction, derivatization reaction and spectrophotometry by sequential injection analysis: Application to trifluoperazine assay in human urine," *Journal of Pharmacological and Toxicological Methods* 2007, 56, 3, 330–335.

[40] K. Chaiyasing, B. Liawruangrath, S. Natakankitkul, S. Satienperakul, N. Rannurags, P. Norfun, and S. Liawruangrath, "Sequential injection analysis for the determination of fluoroquinolone antibacterial drug residues by using eosin y as complexing agent," *Spectrochimica Acta Part A: Molecular and Biomolecular Spectroscopy* 2018, 202, 107–114.

[41] J.-W. Luo, H.-W. Chen, and Q.-H. He, "Determination of cimetidine in human plasma by use of coupled-flow injection, solid-phase extraction, and capillary zone electrophoresis," *Chromatographia* 2001, 53, 5-6, 295–300.

[42] E. Şatana, N. Ertaş, and N. Göğer, "Determination of citalopram using

flow injection-solid phase extraction with spectrofluorometric detection," *Chromatographia* 2007, 66, 1, 75–79.

[43] Z.-Q. Zhang, J. Ma, Y. Lei, and Y.-M. Lu, "Flow-injection on-line oxidizing fluorimetry and solid phase extraction for determination of thioridazine hydrochloride in human plasma," *Talanta* 2007, 71, 5, 2056–2061.

[44] M. E. Salinas-Vargas and M. P. Cañizares-Macías, "On-line solid–phase extraction using a c18 minicolumn coupled to a flow injection system for determination of caffeine in green and roasted coffee beans," *Food Chemistry* 2014, 147, 182–188.

[45] Z. Legnerová, D. Šatınskỳ, and P. Solich, "Using on-line solid phase extraction for simultaneous determination of ascorbic acid and rutin trihydrate by sequential injection analysis," *Analytica chimica acta* 2003, 497, 1-2, 165–174.

[46] W. Boonjob, H. Sklenářová, L. Barron, P. Solich, and N. Smith, "Renewable sorbent material for solid phase extraction with direct coupling of sequential injection analysis-bead injection to liquid chromatography-electrospray ionization tandem mass spectrometry," *Analytical and Bioanalytical Chemistry* 2015, 407, 19, 5719–5728.

[47] J. Huclová, D. Šatínskỳ, O. Pavlíček, L. Vedralová, and R. Karlíček, "Using on-line solid phase extraction for determination of amiloride in human urine by sequential injection technique," *Analytica Chimica Acta* 2006, 573, 376–382.

Chapter 2

Experimental

2.1 Materials

2.1.1 Reagents

Analytical reagent grade (or higher) solvents were used without further purification.

(R)-(-) Phenylephrine hydrochloride (PEP), (1R,2S)-(-)-N-Methylephedrine (MEP) 99%

(w/w), DL-Norephedrine hydrochloride (PPA) ≥99% (w/w) and HPLC-grade methanol

≥99% (v/v) were purchased from Sigma Aldrich (Milwaukee, WI, USA). Authentic

samples used for testing the method were "confiscated samples" that were provided

by the Wisconsin State Crime Lab in Milwaukee. All the standards were prepared

in buffer solution. Buffer was prepared by using ACS-certified Sodium Phosphate

Monobasic and Sodium Phosphate Dibasic (Fisher Scientific, Pittsburgh, PA, USA).

Eluent used was prepared by using ACS-certified Sodium Chloride and trace metal

grade Hydrochloride Acid (Fischer Scientific). Strong cation-exchange, mixed mode

cation exchange column packing was purchased from Sigma Aldrich. CAPSTONE FS-

31 (Global FIA, Inc., Fox Island, WA, USA) was used as a surfactant for solid phase

extraction (SPE). A Barnstead Nanopure^{TM} water purification system (MA, USA) was used to prepare reagent water (18 MΩ-cm) from in-house deionized water.

2.1.2   Buffer Preparation

Buffer solution was prepared in a volumetric flask by mixing the acid and basic salt in a ratio that would yield the desired pH. For the project, Sodium phosphate monobasic and Sodium phosphate dibasic were mixed in reverse osmosis (RO) water to make buffer at pH 6.0. The solution was quantitatively transferred to a high-density polyethylene (HDPE) bottle and stored at room temperature.

2.1.3   Labware

Standards, samples, buffers, and eluents were typically prepared in Class A volumetric flasks. Eppendorf micropipettes were used for transferring small volumes. For the flow analysis instrument, solutions were placed in 20 mL glass vials. Buffer and waste solutions were placed in 500 mL glass vessels. A 1 mL glass syringe (Norm-ject, Hense-Sass Wolf, Tuttlingen, Germany) was used to inject sample into the NMR flow cell. Tapered mini-columns, narrow cylindrical columns, and wide cylindrical columns for SPE were obtained from Global FIA. All labware was cleaned using Citranox™ detergent (Alconox, White Plains, NY, USA).

2.2   Instrumentation

A FloPro-SPE system (GlobalFIA, Inc.) and 80 MHz picoSpin benchtop NMR (Thermo Fischer, Madison, USA) was used for the project. Instrument control and data acquisition were performed on a Dell personal laptop using FLO-ZF version 5.2 (GlobalFIA). NMR spectra were collected on Dell personal computer using picoSpin^{TM} 80 version 1.0 and MestReNova x64. A Delta Model 320 pH meter (Mettler-Toledo Instruments, Shanghai) was used for pH measurement and an analytical balance (Denver, CO, USA) was used for weighing purposes.

2.3   Flow Studies using Sequential Injection Analysis

2.3.1   Flow cell design

Sequential Injection Analysis (SIA) is a microscale approach to continuous flow analysis. The FloPro instrument (Figure 2.1) was equipped with two bi-directional ("milli-GAT") pumps and a hybrid multi-position selection valve (Valcon M Valco, Houston, TX) that was modified to allow SPE column in the flow manifold. The second milli-GAT pump was used for loading large samples. A 1.0 cm UV-VIS absorbance flow cell was coupled by optical fibers to a multi lamp light source (Hydrogen/Deuterium)

which could be used individually or in combination and multi wavelength spectrometer (without optical slits).

2.3.2   Flow manifold

The carrier was drawn by the first pump (P1) from a 500 mL glass reservoir. A pressure release valve was present to provide protection to both of the pumps in the event of blockage. The holding coil had a 1.2 mL volume and was located between the hybrid selection valve (HSV) and P1. A second pump (P2) was present between the holding coil and HSV to load sample onto the column. The HSV is similar to a standard multi-position selection valve but it has two additional ports and a custom rotor (Figure 2.3). The column was plumbed to the additional ports in the HSV, as shown in Figure 2.2. The system was operated by FloZF software, which is Global FIA's instrument control and data acquisition software.

Hybrid multi-position selection valve

The hybrid multi-position valve (Figure 2.3) combines the features of a multi-port selection valve and a two-position injection valve. Port descriptions are given below in Table 1.1. To use this hybrid valve for SPE, the column was installed between positions 1b and 6b. Thus, when port 6 was selected, fluid flowed through the column to waste (port 1) and the column was in the sample loading position. When port 1 was selected,

fluid flowed through the column to the detector flow cell (port 6) and the column was in the elution position. The first step (Figure 2.4) is the sample loading at which port 6 is selected. In this step the sample flows through the column. The second step is the washing in which buffer is loaded in the column which will elute adulterant, if present. The third step (Figure 2.5) is the aspiration of eluent in the holding coil. And the final step is the elution in which port 1 is selected. At this step the eluent flows through the column to the detector .

Detector Flow cell

The detector flow cell (Figure 2.6) was a modified Z-type design with a 1.00 cm path length. The two optical cables are positioned so that the quartz fiber protrudes beyond the end of the fluorinated ethylene propylene (FEP) sheath so that the tip of the cable reaches the fluid in and out the junctions (Figure 2.7). The internal diameters of the conduits in the flow cell were 1.00 mm and the total volume was approximately 8 μL.

2.3.3 picoSpin 80 series NMR Spectrometer

The picoSpin 80 (Figure 2.8) is a pulsed Fourier transform liquid-phase proton NMR spectrometer [1]. The instrument's fluid capillary system is contained within a replaceable cartridge which can hold approximately 40 μL of a liquid sample (Figure 2.9). It

has temperature controlled permanent magnet (2 Tesla) which does not require cryo-gens.

2.3.4 Quantitation method

The method used for analysis of synthetic cathinones is Solid Phase Extraction (SPE) which involves four general steps (Figure 2.10). SPE is an extractive technique in which compounds are dissolved in liquid mixture and separation occurs in stationary phase based on its chemical and physical properties. Compared to conventional liquid-liquid extraction, SPE is easy to use, consumes less time and requires small amount of sol-vents with much cleaner extract [2]. Initially, each fluid conduit was primed with the respective solution. The first step was the loading step, in which a specific volume of sample was loaded onto the column at a given flowrate. The second step was the wash-ing step, in which the column was washed with buffer of to prepare it in the proper ionization state for ion-exchange. The third step was the loading of eluent, in which a specific volume of the eluent was loaded at a given flowrate onto the column. The last step was the elution step, in which the eluent was passed through the column to elute the analyte to the NMR flow cell.

2.4 Figures and Tables

FIGURE 2.1: Flo Pro-SPE (taken from [3]).
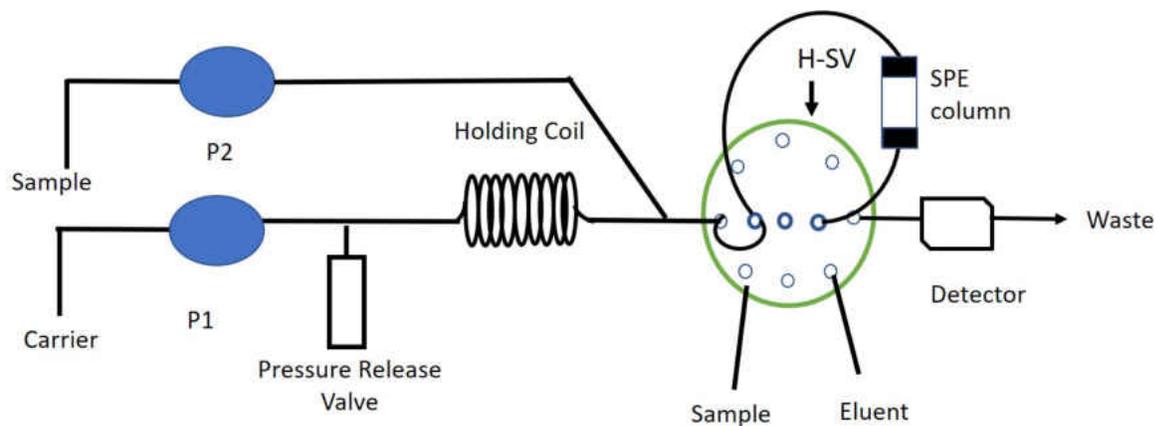
FIGURE 2.2: Schematic diagram of SIA system.

FIGURE 2.3: Schematic diagram of hybrid selection valve. The rotor (A) and stator (B) are shown.
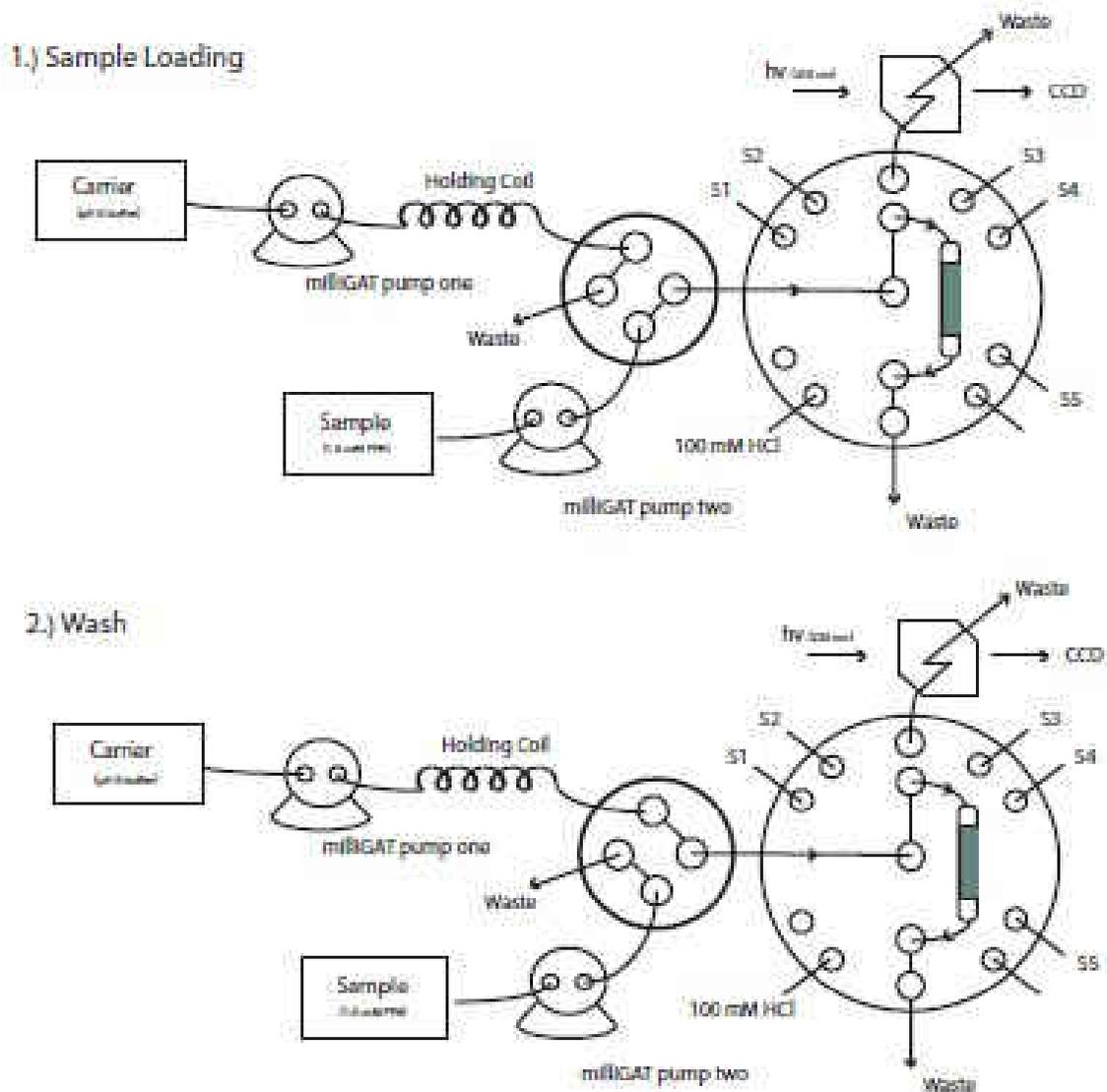
FIGURE 2.4: FloPro valves with Elution Scheme-1 (Adapted from [3]).
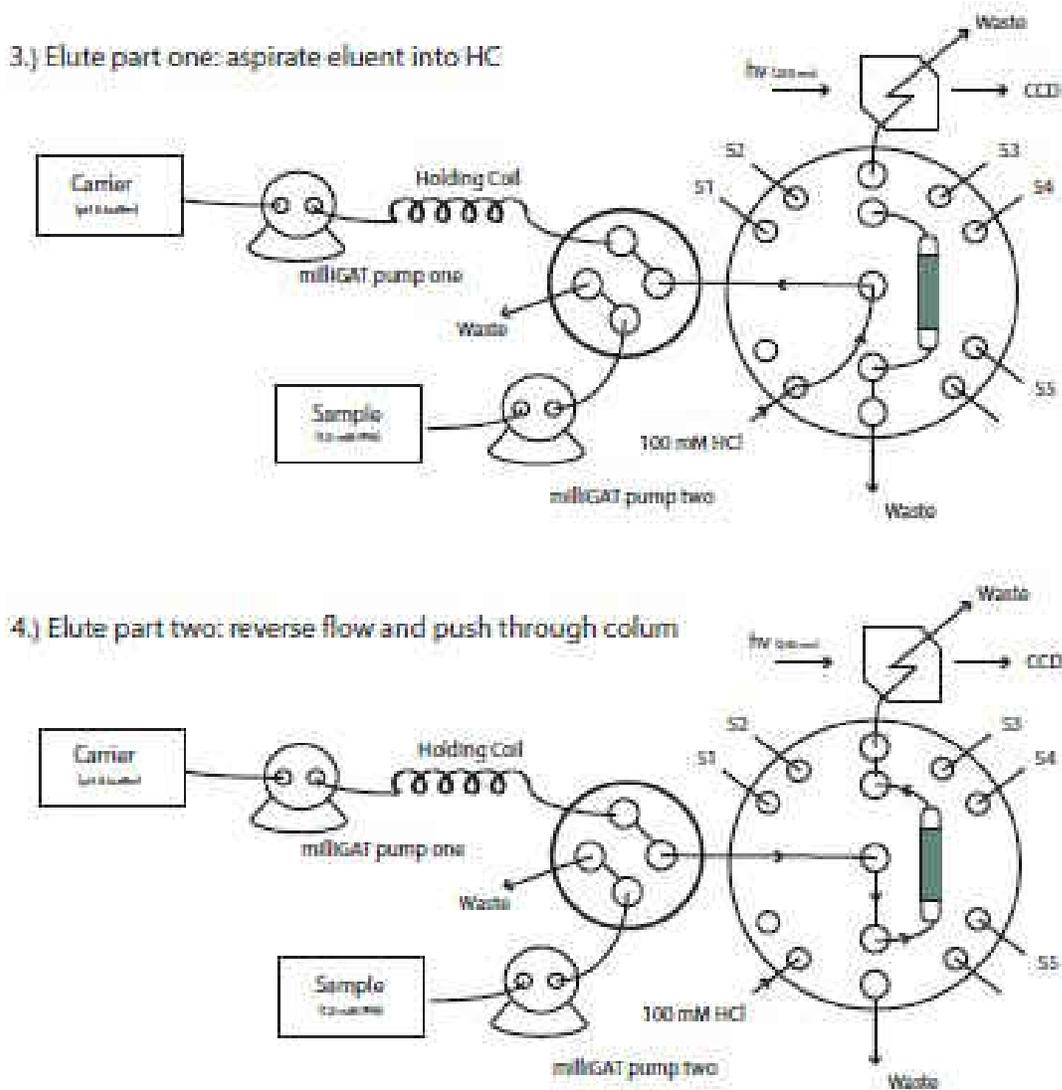
FIGURE 2.5: FloPro valves with Elution Scheme-2 (Adapted from [3]).
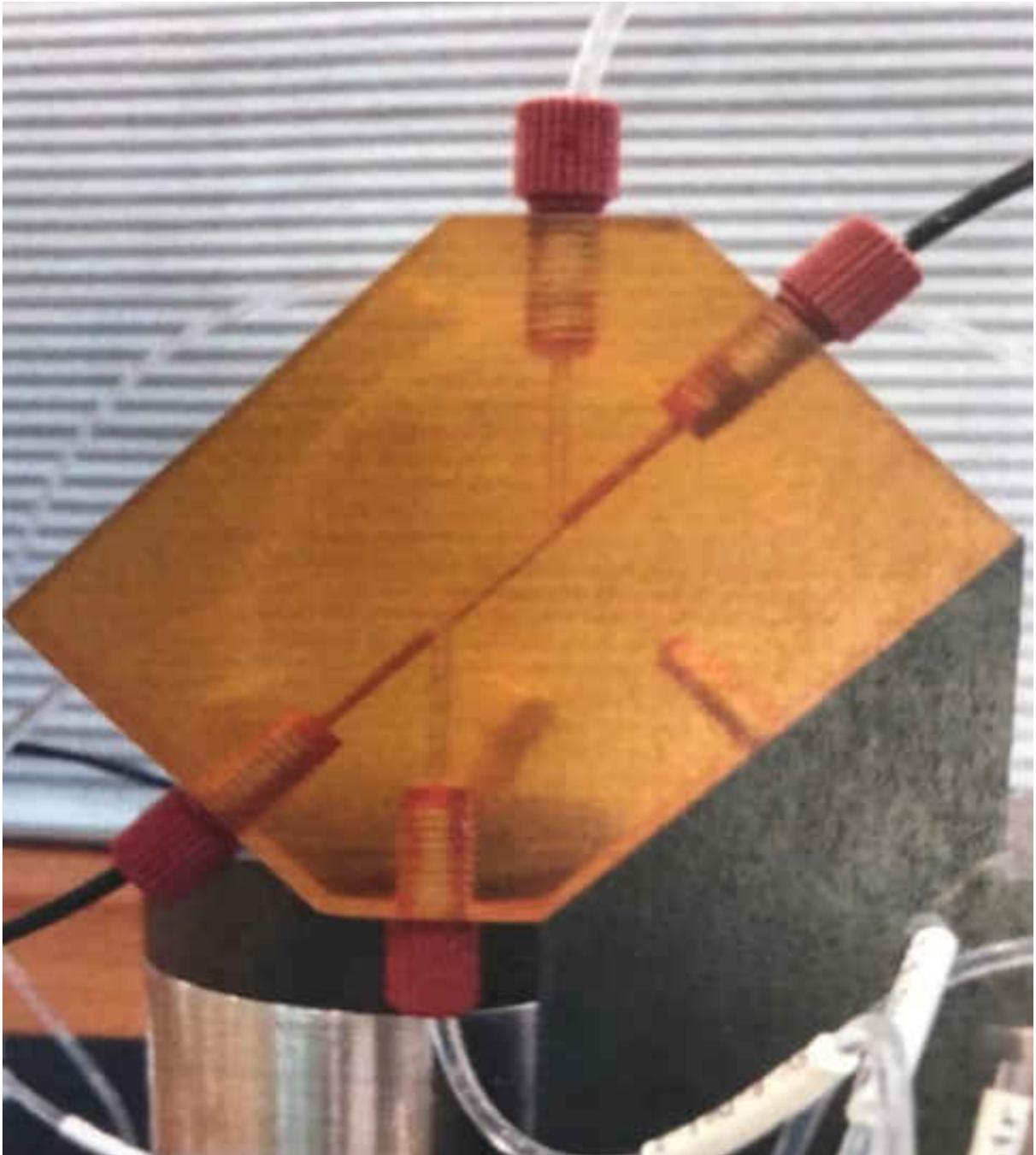
FIGURE 2.6: Bubble tolerant flow cell (taken from [3]).
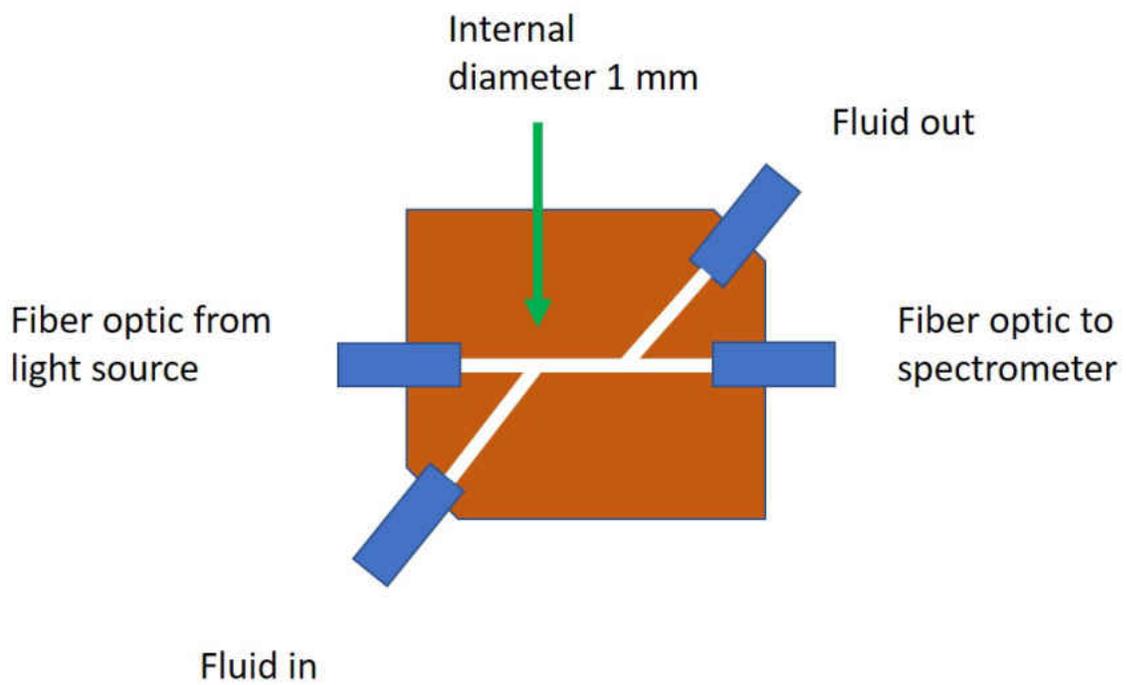
FIGURE 2.7: Schematic diagram of Flow cell.

FIGURE 2.8: picoSpin 80 mHz NMR Spectometer (Adapted from [1]).
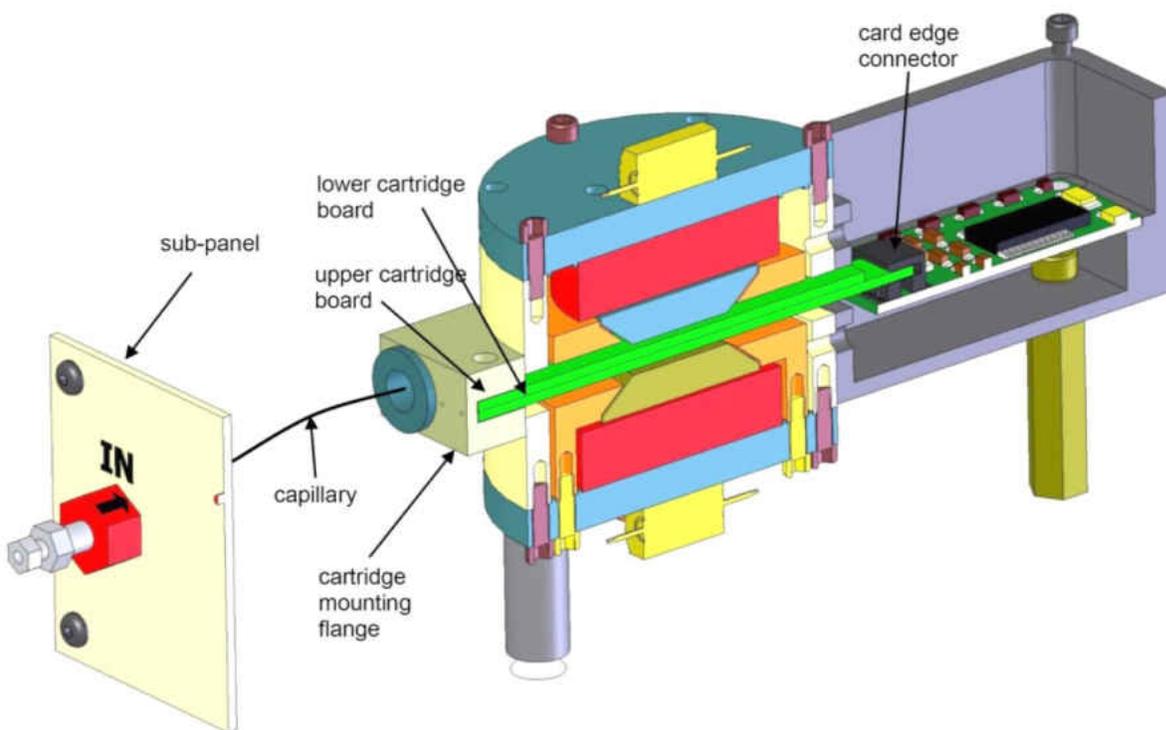
FIGURE 2.9: Internal Structure of picoSpin 80 mHz NMR Spectometer (Adapted from [4]).
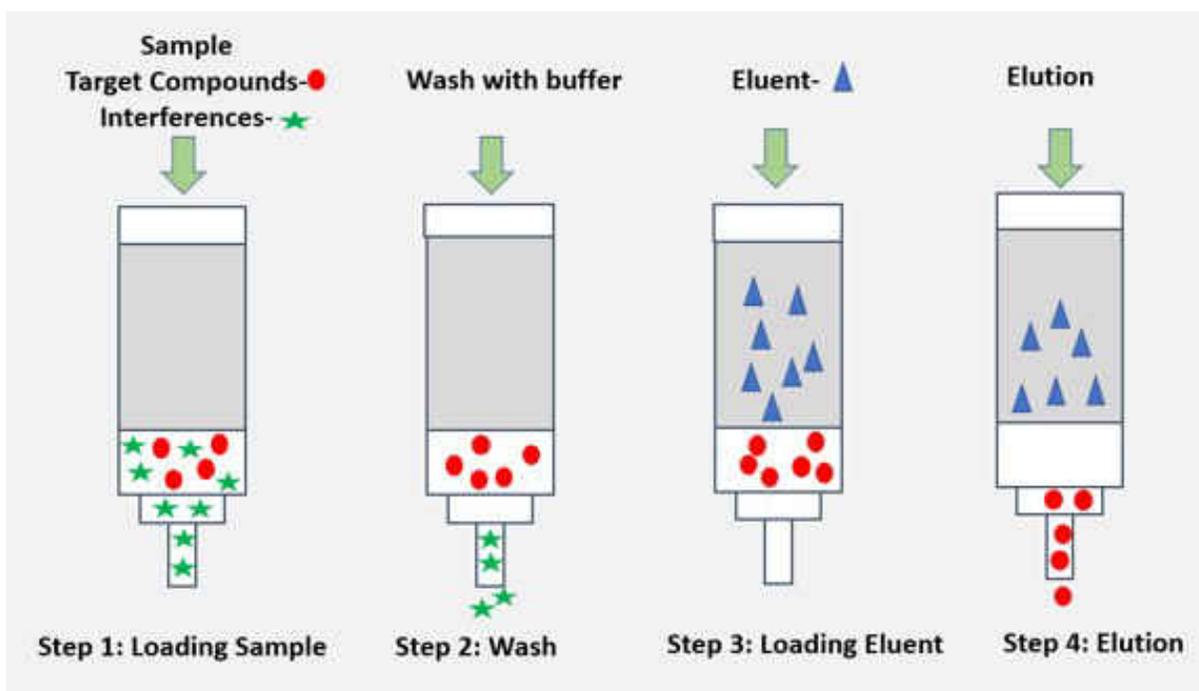
FIGURE 2.10: SPE extraction general procedure.

Port Number	Description
1	Waste
2	Reservoir 1
3	Reservoir 2
4	Reservoir 3
5	Reservoir 4
6	Detector
7	Reservoir 5
8	Reservoir 6
9	Waste
10	Air
1b	Column in
6b	Column out
11	Central Port

TABLE 2.1: Port description of HMV

References

[1] P. Dean Antic, "Illicit drug analysis using benchtop nmr: Amphetamines," *Thermo Fisher Scientific, Boulder, CO, USA* Accessed March 24 2020.

[2] I. Halász and P. Vogtel, "Some problems in quantitative analysis with concentration-sensitive detectors in high-performance liquid chromatography," *Journal of Chromatography A* 1977, 142, 241–259.

[3] G. Marshall, "Flopro analyser for solid phase extraction user manual," *Global FIA, Inc, Fox Island, WA, USA* 2017.

[4] T. F. Scientific, "picospin 80-installation and setup," *Thermo Fisher Scientific, Boulder, CO, USA* Accessed March 24 2020.

Chapter 3

Result and Discussion

3.1 Preface

This chapter will focus on the work done on the development of a novel method for the determination of Cathinones in forensic samples by using Sequential Injection Analysis-Proton Nuclear Magnetic Resonance Spectroscopy (SIA-NMR). The proton NMR spectra of the samples were collected in two ways. One way was by directly injecting the analyte to the NMR and the other way was by pre-treating the sample by SIA before introducing it to the NMR. Phenylpropanolamine (PPA), Phenylephrine (PEP), and Methylephedrine (MEP), whose structure is shown in Figures 3.1, 3.2, and 3.3, were used as primary, secondary, and tertiary amines for the development of method, respectively. The SIA-NMR method was then validated by applying it to confiscated samples which were provided by the Wisconsin State Crime Lab (WSCL) in Milwaukee.

3.2   Solid Phase Extraction.

Solid phase extraction (SPE) is a type of displacement chromatography which has rapidly established itself as one of the premier sample preparation techniques for either trace enrichment or matrix simplification [1]. In SPE, the sample is loaded onto the column as a discrete plug. High affinity analytes will be better retained in the column while others will be unretained and transported through the column. A substance known as the eluent is then introduced to the SPE column which will cause the analyte to be released from the stationary phase. Thus unlike elution chromatography in which solutes are continuously released from the stationary phase over time, in displacement chromatography a single "elution event" typically takes place [2].

Chromatography can be performed in three developmental modes, namely elution, displacement, and frontal (Figure 3.4) [3]. In frontal mode (Figure 3.4, top), A and B are continuously swept onto the column by eluent. When the stationary phase becomes saturated with respect to a particular analyte, the analyte is eluted followed by the next analyte. In elution mode (Figure 3.4, middle), analytes (A and B) are loaded on the column in the mobile phase (C). The individual analytes are differentially retained in the form of separate zones. In displacement mode (Figure 3.4, bottom), the mixture containing A and B are initially loaded onto the stationary phase followed by eluent (C). Although the latter two modes look similar in mechanism, there is a difference

45

between them. In elution, the mobile phase has higher affinity for stationary phase than any analytes in the sample. But, in case of displacement, a substance called a "displacer", which has higher affinity for the stationary phase than retained analytes, is added in the mobile phase [2]. The displacer elutes the analytes from the column in a single event.

SPE is popular as a sample pre-treatment method and has been widely applied in all types of drugs testing laboratories [4]. The recovery of analyte is dependent upon the type of sorbent used and experimental factors including column geometry, column capacity, and elution conditions [5]. An important consequence is that a basic functional group such as NH_2 can simultaneously exist in two different forms with different properties (i.e., R-NH_2 and R-NH_3^+). Each of these two forms can be the dominant form in aqueous solution depending upon the pH of that solution. For PPA, because it has a pK_a value of 9.4, the carrier was buffered at pH 6.00 [6]. At this pH, the analyte was positively charged (Figure 3.5). For the retention of the analyte, four different types of resins were studied, namely reversed-phase (octadecyl, C18), strong cation-exchange (SCX), mixed-mode cation exchange/reversed-phase (MCAX), and hydrophilic-lipophilic balanced (HLB) [7–9]. The wide cylindrical column was used with 10 mM PPA for the experiment. The breakthrough volume for the four resins was studied (Figure 3.6) and was found to be higher for SCX and MCAX. This result was expected because of their chemical compositions, however, it was surprising to observe

that MCAX had double the capacity compared to SCX. The SCX resin, used for the experiment, was several years old. So, the reason behind the observed capacity could be the degraded quality of the SCX resin. These two types of resins were therefore chosen for further method optimization.

Stationary phase (either SCX or MCAX) was made into a slurry (500 mg) by using methanol as the solvent. The slurry was then slowly poured into the column. Before using the column for experiments, it was flushed with approximately 10.0 mL of buffer. For the eluent, initially 0.10 M HCl was studied. Because the protonated amine at pH 6.00 will bind to the negatively charged sulphonic acid groups on the stationary phase, it can then be competitively displaced by the addition of an eluent with higher z^2/r (where z is the ionic charge and r is the ionic radius) which in this case was the hydrated proton (represented as H_3O^+). This elution mechanism works rather well, however increasing the acid concentration much beyond 0.10 M can cause the degradation of the stationary phase. Therefore, NaCl was added to the HCl solution not only to increase the ionic strength but also to play an important role for MCAX resins by blocking ionized silanol groups (-Si-O^-), which can be a cause of severe peak tailing in reversed-phase retention mechanism [10]. PPA (1 mM) was prepared in buffer of pH 6.00. It was then loaded onto the wide cylindrical column and washed with 1.00 mL of 100 mM NaCl / 100 mM HCl. The concentration of NaCl was then increased to see its effect on the displacement of PPA, as measured by absorbance spectroscopy.

An increase in absorbance was expected with an increase in the concentration of NaCl because it has a higher z^2/r which would displace the analyte more efficiently (Figure 3.7). Thus the observed result was found to be as expected.

The geometry of the chromatography column was studied for three different types of column (Figures 3.8, 3.9, and 3.10). The column capacity of the three column geometries was determined for the simulants (PPA, PEP, and MEP). PPA (10 mM) was prepared in phosphate buffer at pH 6.00. It was then loaded onto the column. As expected, the continuous aspiration of PPA yielded a sigmoidal response (Figure 3.11). The break-through time is the time at which the capacity of the column has been exceeded. Time units are then changed into volume units based upon the flowrate. All samples were determined in triplicate. The process was repeated for the remaining two simulants using the three column types.

a. Wide Cylindrical column : bed volume of 2.7 mL

b. Tapered column : bed volume of 27 μL

c. Narrow Cylindrical column : bed volume of 2.4 mL

Higher capacities were of course expected for the two cylindrical columns, and their capacities were found to be similar, and 14 times greater than observed for the small tapered column (Figure 3.12). In case of the wide cylindrical column and small tapered column, the SCX resin had a greater capacity towards the amphetamines (Figures 3.13

48

and 3.14) in comparison to MCAX. Because the SCX resin has negatively-charged sulphonic acid groups, the positively-charged amines are attached strongly, whereas in MCAX, along with sulphonic acid groups, the hydrocarbon chain can bind to the more hydrophobic regions of the analyte molecules. Surprisingly, for the narrow cylindrical column, SCX and MCAX had almost equal capacities for the three amphetamines (Figure 3.15). Also, for the narrow cylindrical column, when the flowrate was increased above 20 μL/s, leakage in the pressure release valve of the SIA was observed because of the narrower internal diameter of the column compared to the other large column.

In addition to sorbent and column, the performance of other organic modifier like benzoic acid and methanol were also studied in mobile phases. These modifiers were chosen because they were soluble in water. Methanol has small alkyl group which could help in the retention of amphetamine in the tether of the resin. The pk_a value of benzoic acid is 4.20. So, it would be in anion form and help in retention of amphetamine. The problem with benzoic acid was its strong absorbance at 250 nm which interfered with the molecular absorbance spectrum of PPA. For methanol, the methanol peaks overlapped with the primary amine protons in the NMR spectrum. So, the research was continued with unmodified phosphate buffer.

3.3   Testing at WSCL (Part 1)

To measure the performance of the SIA-NMR method, testing with authentic samples was conducted over a three-day period in June 2018 at the Wisconsin State Crime Lab (WSCL) in Milwaukee by Dr. Joseph Aldstadt and Mr. Tim Trinklein. Ms. Sandra Koresch, Controlled Substances Technical Unit Leader at WSCL provided the samples for analysis and assisted in the testing.

The SIA-NMR system was initially set up, shimmed with reagent water, and calibrated with PPA standards. Shimming is the process carried out to correct any inhomogeneities in the applied magnetic field during the NMR experiment. A test sample of 50 mM PPA was determined by SIA with UV molecular absorbance detection, and appeared normal (i.e., within QC control chart limits). Three case samples were provided by WSCL:

   a. Methylone (white powder, ~300 mg)

   b. Methcathinone (white powder, ~100 mg)

   c. N-Ethylpentylone (yellow powder, ~30 mg)

3.3.1 Methylone

Methylone, whose structure is shown in Figure 3.16, is a primary amine. A 50 mM sample solution of Methylone was prepared using D_2O and 50 mM TMSP-d_4, assuming 100% purity of the Cathinone. TMSP-d_4, whose structure is shown in Figure 3.17, is a standard that is used to calibrate the x-axis (chemical shift, ppm). The sample was injected directly into the NMR (bypassing the SIA, and 64 scans were averaged. All the peaks expected for methylone were clearly visible as shown in Figure 3.18. A more concentrated sample was prepared (~500 mM), and 256 scans were averaged, resulting in a high-resolution NMR spectrum (Figure 3.19).

A 50 mM methylone sample was then determined by SIA-NMR using the wide cylindrical column packed with 400 mg of SCX sorbent. A 2.00 mL wash cycle of buffer (10 mM phosphate, pH 6.00) was followed by elution with a 1.45 mL of 100 mM HCl / 200 mM NaCl. The resultant NMR spectrum showed peaks at 7.5 ppm (aromatic) and 1.0 ppm (alpha methyl) but was very noisy. When elution began, the UV absorbance was greater than 3 AU. After the SIA-NMR run, a separate eluent wash was performed three times to regenerate the column.

3.3.2   Methcathinone

Methcathinone, whose structure is shown in Figure 3.20, is a secondary amine. A 500 mM sample (containing Mannitol as a potential interference) was prepared using D_2O and 50 mM TMSP-d_4, assuming 100% sample purity. The sample was injected directly into the NMR, and 256 scans were averaged. A characteristic signal for Mannitol was observed in the spectrum at 3.0 ppm (Figure 3.21). A 175 mM sample of Methcathinone was then loaded onto the SPE column packed with the SCX sorbent. A 2.00 mL wash cycle of buffer was followed by 1.45 mL of eluent. The NMR spectra were collected with 512 scans which clearly showed Methcathinone (aromatic, N-methyl, and alpha methyl shifts). After SIA-NMR, Mannitol was absent indicating that the SIA had efficiently removed Mannitol during the wash cycle (Figure 3.22).

3.3.3   N-Ethylpentylone

N-Ethylpentylone, whose structure is shown in Figure 3.23, is a secondary amine. A 500 mM solution of N-Ethylpentylone was prepared using D_2O and 50 mM TMSP-d_4. The solution did not dissolve readily, and it became rather coagulated. A 100 μL aliquot of D_2O was added to the remaining dark yellow solution. The solution was injected directly into the NMR, and 256 scans were averaged. The peaks expected for N-Ethylpentylone as well as a characteristic peak from Caffeine (at 3-4 ppm and 8 ppm)

was visible (Figure 3.24). The WSCL analyst confirmed from previous GC-MS analysis that the sample had been found to contain a high concentration of Caffeine.

3.4 Retention of primary, secondary and tertiary amine for two different sorbents.

There was a difference in the retention of the Simplex depending upon whether they were primary, secondary, or tertiary amines. Our previous results from testing at WSCL showed that tertiary amines were more difficult to quantitatively elute than primary and secondary amines. Previous results were examined and was found that the cylindrical column with the SCX resin had the highest capacity for MEP. This agrees with the fact that MEP required a larger volume, and/or a stronger eluent to quantitatively recover it from the column.

3.5 Elution of tertiary amines.

The effect of different concentrations of HCl in the elution behavior of a tertiary amine (MEP) was studied. MEP (250 μL of a 50 mM solution) was injected at flow rate of 20 μL/s in the wide cylindrical column packed with the SCX resin. The column was then washed with 2.0 mL of 10 mM phosphate buffer at pH 6.00 and eluted with 1450 μL of 200 mM of NaCl / 100 mM HCl. Then the concentration of HCl was increased,

and its effect on a second elution of MEP was studied. As expected, the absorbance of the analyte in the second elution was found to decrease with the increase in HCl concentration as shown in Figure 3.25. However, the cause of the large error bar in the 150 mM HCl experiment was unknown. After studying different concentrations of HCl (Figure 3.25), a concentration of approximately 350 mM HCl was found to be optimal to elute the analyte with an average absorbance of 0.0753, which is essentially the background signal.

The effect of NaCl concentration on the efficiency of elution of the three amines was also examined. As predicted, the absorbance of MEP increased as the concentration of NaCl increased (Figure 3.26). Experimentally, a concentration of approximately 200 mM NaCl was found to efficiently elute the MEP in the first elution step. On further increasing the concentration, there was not much (<0.0596%) increase in absorbance of MEP. The increase in the elution of MEP in the first wash is because to the increase in z^2/r which makes displacement of the analyte easier. The elution behavior of the three simulants was compared using the original eluent solution (100 mM HCl / 200 mM NaCl), and the optimized eluent solution (350 mM HCl / 200 mM NaCl). When the original eluent solution (100 mM HCl / 200 mM NaCl) was used, 24.0% of MEP was still on column after the first wash as shown in Figure 3.27. When the optimized eluent was used for the method, >97.0% of the MEP was eluted in first wash.

For PPA and PEP, the original eluent was effective in eluting them quantitatively

in the first wash cycle (>97.0% for PPA and >94.0% for PEP). But for MEP, which is a tertiary amine, a third wash cycle was required for quantitative (>93.0%) elution with the original eluent. MEP was thus retained on the SCX resin much more strongly than PPA and PEP. It might be because of the chemical structure of MEP which contains more hydrocarbon group. The tether in the SCX might attach with the hydrocarbon group of MEP resulting in secondary interaction. Thus in addition to cation-exchange, there might be reverse phase interaction in the process.

3.6   Optimization of the SIA method.

Optimization is an essential step when developing a new method in analytical chemistry. The main purpose of optimization is to find the proper conditions to most efficiently operate a method to achieve better figures of merit, e.g., improved accuracy, precision, and sensitivity [11]. To optimize the SIA-NMR system, the strategy was to apply a (P-B) screening design, and then a Simplex multi-variate optimization approach to determine the optimal values of the most significant factors for maximizing the response. The common method to optimize an analytical method is uni-variate, i.e., to study one factor at a time while keeping the rest of the factors constant. This is both time-consuming, inefficient, and ignores the effects of "interacting factors" which can produce a "synergistic" effect on the response [12].

3.6.1 Plackett-Burman Screening Design

The Plackett-Burman (P-B) design is an example of a "saturated" design, i.e., a design in which every experiment is associated with a model term [13]. It was developed in 1986 by statisticians R.L. Plackett and J.P. Burman [13]. P-B designs are used to investigate the dependence of different factors with the assumption that the interactions between factors are negligible. The screening designs are highly recommended for early stages of investigations to identify active factors that influence the response. P-B designs allow the experimenter to study "main" and "interaction" effects [14]. The main effect is the difference in expected average response, that is, when a certain factor is at its highest level and at its lowest level [15]. Interaction effects are the differences of one factor on the response compared to the other factors.

The protocol used in P-B screening design experiments is straightforward [16]. In this type of design, the number of experiments is an integral multiple of four. The number of factors that can be studied is 4n-1, thus for eight experiments the PB design can study seven factors. Experiments are performed with high and low values of factors, and their effect on the response is analyzed [17]. For example, suppose one wants to study four factors, but four experiments will be insufficient. Therefore, one should choose a seven factor design, and then conduct eight experiments, as shown in Table 3.1. Thus three of the factors were "dummy factors" which would not have any effect

on the experiment. Dummy factors could be things like the current phase of the Moon or whether the elevators are working. PB designs utilize two levels for each factor, the higher being denoted as "+" and the lower denoted as "−". Individual experiments are assigned in a cyclical manner which means that the first row is sequentially rotated to the right to generate each succeeding row [18]. For example, for eight experiments with seven factors labelled 1-7, the levels for the first experiment will be as shown in Table 3.2. The levels for the second experiment are obtained by moving the last sign for the first experiment to be the beginning of the line as shown in Table 3.3. The cyclical process is repeated for the first seven experiments. This will lead to the eighth experiment with all of the factors at their low level, as shown in Table 3.1. The effect of each factor is then calculated by using Equation 3.1:

$$2[\Sigma(y+) - \Sigma(y-)]/N \qquad\qquad (3.1)$$

where N is the total number of experiments; in this example, N is eight. The response when a given factor is at its higher level is denoted as y+ and y- is the response when the given factor is at its lower level [18]. One major drawback with PB designs is that the main effects are confounded with interactions, especially with two-factor interaction, as there are not enough degrees of freedom [19]. To eliminate this drawback, fold-over or a "reflection design" is used [20]. The fold-over design for the previous

design is shown in Table 3.4. Thus the final PB design with fold-over is shown in Table 3.5.

For this work, 20 factors (Table 3.6) were considered for the SIA method. It was decided that eight factors were considered much more important than the others, but eight experiments will be insufficient. Therefore, an 11 factor (4n-1 where n=3) design was chosen and 24 experiments were conducted. The 11 factors are shown in Table 3.7. Three of the factors were dummy factors. Based on results from 24 experiments (Table 3.8), the factors that had the greatest impact (optimized absorbance with highest precision) on the system were the sample volume (V_S, factor 1), the loading flowrate of carrier (F_L, factor 2), the volume of eluent (V_E, factor 6), the concentration of NaCl (C_{NaCl}, factor 7) used in the elution solution, the concentration of HCl (C_{HCl}, factor 8) used in the elution solution , the flowrate of the elution solution (F_E, factor 9), and the sample aspiration flowrate (F_S, factor 10). The significance of each of the factor is shown in Table 3.9. Those factors, having either positive or negative influence (greater than 0.2) on the response, were considered as active factors. As shown in Figure 3.28, seven factors were found to be active factors and rest of the four factors were found to have minimum effect on the response. Thus those seven factors were chosen to perform a Simplex optimization for the SIA system.

3.6.2   Simplex optimization.

Simplex optimization is a strategy that efficiently locates the region of optimal response by varying all factors simultaneously [21]. A Simplex is defined as"...a geometric figure with k + 1 corners, where k is equal to the number of variables in a k-dimensional experimental domain" [22]. In two-dimensional factor space, the Simplex is a triangle, while in a three-dimensional space, it is tetrahedron [23]. In this work, the response function that was chosen to possess both an optimized absorbance with high precision (i.e., minimum %RSD). The range for the seven factors was from the low to the high values that were used for the P-B screening design. The increment for each factor is displayed in Table 3.10. The step-size for flowrate of sample aspiration, carrier aspiration, and elution were 5 μL/s. The higher flowrate could cause leakage in the SIA system and slower flowrate could take longer time for the response. The step-size for sample volume was 70 μL. It was determined based on capacity of sorbent in wide cylindrical column. The step-size for volume of eluent was 150 μL which was approximately double the volume of sample. The step-size for concentration of NaCl and HCl was 50 mM. The higher concentration could degrade the quality of the SCX resin and lower concentration could be problem for efficient elution. Choosing the size of the initial Simplex is a crucial step for the optimization process because it depends on the experience or "intuition" of the researcher concerning the levels to be chosen [12]. Note

that the values for the remaining four factors were kept constant at their original values used in the screening design. This means that they were "dummy factors" which did not have much effect in the response.

The experiment was carried out by using 2.5 mM of PPA (n=3). The response function which the Simplex would optimize was the absorbance divided by the %RSD value as a mean to balance a high response with good precision (Figure 3.29). In typical Simplex optimization studies, a broad plateau is observed once the optimal state is reached which suggests that slight changes in the values of the factors will not drastically change the response. The response function surface for a typical Simplex would therefore resemble the contour plot as shown Figure 3.30(a). However, in the present study, a "sharp peak" at the optimal response was observed. This indicates that the contour plot for the response surface resembled that shown in Figure 3.30(b). Examination of the result for the series of Simplex experiments (Figure 3.29) shows that for experiments 16 and 17, the optimal response was observed but for experiments 18 and 19, a slight change in the levels of the factors yielded a severe drop in the response function.

3.7 Comparison of the optimized method.

For comparing the efficiency of the optimized method to the original method, several factors are worth noting. Calibration models were created using PPA with the values shown in Table 3.11 to find the LOD and %RSD (Figure 3.31). The Limit of Detection (LOD), the lowest quantity of substance that can be distinguished from the absence of that substance with a stated confidence level (generally 99%) [24], was improved significantly, as shown in Table 3.12. The LOD for the optimized method was 0.023 mM, which is 70% lower than observed for the original method (0.077 mM) (Table 3.12). The greatest improvement was realized for the precision. The precision improved from 1.47% to 0.10% RSD which is a 93% improvement (Figure 3.32).

3.8 Crime lab testing (Part 2).

To measure the performance of the optimized SIA-NMR method, a second round of testing with authentic samples was conducted over a two-day period in July 2019 in collaboration with WSCL. The author, Dr. Joseph Aldstadt, and Ms. Lexie Lanphere, and I worked with Ms. Sandra Koresch, Controlled Substances Technical Unit Leader at WSCL. The SI-NMR system set up, shimmed with reagent water, and calibrated with PPA. A test sample of 50 mM PPA was analyzed by SIA with UV molecular absorbance

detection, and appeared normal (i.e., within QC control chart limits). Two case samples were provided by WSCL:

a. N-Ehylpentylone (White powder, ~250 mg)

b. N-Ethylhexedrone (White powder, ~240 mg)

3.8.1 N-Ethylpentylone (NEP)

The structure of NEP, a secondary amine, is shown in Figure 3.23. A 50 mM of NEP was prepared in 10 mM phosphate buffer at pH 6.00, assuming 100% purity of the Cathinone. The sample was directly injected into the NMR, and 512 scans were averaged (Figure 3.33). All of the expected peaks were clearly visible which shows that there were not any adulterants (Table 3.13). A sharp singlet at 6.00 ppm for protons attached to the methylenedioxy group, which is the characteristic peak for most Cathinones. Two doublets were observed for benzene protons at 7.00 and 7.50 ppm. A quartet was observed for methylene protons at 3.00 ppm. Peaks from methyl protons were observed to be overlapped between 0.50 and 2.00 ppm.

The sample was then studied by the SIA-NMR method. NEP (800 μL) was loaded onto the SPE column packed with the SCX sorbent (500 mg). A 2.00 mL wash cycle of buffer was followed by 1.56 mL elution with 60 mM HCl / 215 mM NaCl. The NMR spectrum was collected with 512 scans (Figure 3.34). All the expected peaks

were clearly visible. SIA-NMR spectra were expected to be clearer, and sharper than spectra from direct NMR because the sample was not only pre-concentrated but also the matrix was removed. However, the peaks observed in the SIA-NMR spectrum were found to be less sharp with higher noise when compared to the direct NMR spectrum. It might be because of high salt concentration which reduces the efficiency of NMR probes leading to decreased sensitivity [25].

3.8.2 N-Ethylhexedrone (NEH)

N-Ethylhexedrone, whose structure is shown in Figure 3.35, is also a secondary amine. A 50 mM of NEH was prepared using 10 mM phosphate buffer at pH 6.00 assuming 100% sample purity. The sample was injected directly to the NMR and 512 scans were averaged (Figure 3.36). All the expected peaks were clearly visible which shows that there were not any adulterants (Table 3.14). A doublet and triplet were observed for benzene protons at 7.50 and 8.00 ppm and a quartet was observed for methylene protons at 2.50 ppm. The rest of the peaks from methyl protons were observed to be overlapped between 0.50 and 2.00 ppm. The SIA-NMR was performed using the wide cylindrical column packed with the SCX sorbent (500 mg). The NMR spectrum was collected with 512 scans (Figure 3.37).

After working on the optimization of SPE-SIA, the second part of the method was optimized, which was the SIA-NMR.

3.9 Optimization of elution volume.

The volume of eluent that is sent to the NMR flow cell from the SPE column is a crucial factor to optimize. A smaller volume may cause a concentration gradient to form in the flow cell. On the other hand, a larger volume may cause dilution of the analyte, and thereby yield a lower response. In both cases, the response of the analyte will not be optimal. For optimizing the eluent volume, a 50 mM PPA standard was prepared in 10 mM phosphate buffer at pH 6.00. For the SIA-NMR measurement, the peak area for the benzene hydrogen of PPA (64 scans, n=3) was used for quantitation over the range of 800 μL to 1000 μL (Figure 3.38). The optimized eluent volume was found to be 950 μL.

Larger error bars were observed at higher volumes as shown in Figure 3.38. The NMR flow cell volume of 5-10 μL (the exact volume is proprietary). The eluting zone from the column is in the shape of bolus. The change in the volume of eluent that is sent to the NMR flow cell corresponds to the change in time at which the flow of analyte is stopped. When the sample volume is optimal, the center of the bolus reside in the NMR flow cell as shown in Figure 3.39 (top). This part of zone will have a more homogeneous concentration gradient in the cell and thus a higher and more stable signal such that higher precision will be observed. When the sample volume is too low, the front part of the bolus will reside in the NMR flow cell as shown in Figure 3.39

(middle), and a lower signal with lower precision will be observed. When the sample volume is too large, the latter part of the bolus will reside in the NMR flow cell as shown in Figure 3.39 (bottom). This part of the bolus will have a more heterogeneous concentration gradient across the cell and a lower signal with low precision will be observed. Lower precision will of course result in the larger error bars in Figure 3.38.

3.10   NMR Interpretation.

NMR is arguably the most powerful tool available to the analytical chemist for the elucidation of molecular structures. Proton NMR was used for this project, and the proton NMR spectra is rich in qualitative information — factors such as chemical shift, spin multiplicity, coupling constants, and peak integration can be used [26]. Proton NMR spectra have the chemical shift in ppm along the x-axis, and signal intensity along the y-axis. Chemical shift is the frequency observed for a nucleus relative to a standard in the magnetic field. For this project, H_2O or D_2O were used as the calibration standard for the x-axis, where the chemical shift (δ) was 4.70 ppm. TMSP-d_4 was also used to calibrate the x-axis at 0.0 ppm. The proton NMR spectrum is affected by the different types of atoms that are found in the vicinity. Protons with chemical equivalence have the same chemical shift because of symmetry within the molecule. Spin-spin splitting, which occurs when the absorbing peak is spilt by more than one neighboring proton, is also qualitatively useful [27]. Splitting is very important to obtain information about

the number of neighboring protons. Spin multiplicity follows Pascal's triangle rule as shown in Table 3.15. [27]. For example, 1,1-dichloroethane (CH_2CHCl_2) contains two types of hydrogen atoms. Methine (-CH) proton is bonded to carbon having three protons. So, a quartet (3+1) will be observed for the methine proton. Similarly, methyl (-CH_3) protons is bonded to carbon having one hydrogen. Thus a doublet will be observed for the methyl protons.

Predicted NMR spectrum of a compound are seldom identical to the observed NMR spectrum. The purity of a compound, solvent used, and volume of the sample injected in the NMR are factors that may account for the differences. There might be some peaks in the predicted NMR spectrum which are not observed in the observed NMR spectrum and vice versa. For this project, a detailed analysis of the predicted vs. observed proton NMR spectra of the four "case " (i.e., confiscated) samples from WSCL was undertaken.

3.10.1   N-Ethylhexedrone

N-Ethylhexedrone (Figure 3.40) is a secondary amine with 21 protons. Five types of protons were of interest as shown in Table 3.16. In Figure 3.41 (top), for protons attached to carbon numbers 1, 2, and 3, (herafter denoted as "C-1, C-2, and C-3") the software predicted a triplet at 7.25 ppm with a peak intensity ratio of 1:2:1 because

three of those protons were attached to two carbon atoms (each having one hydrogen) on either side, as expected from application of Pascal's triangle, and those were observed (Figure 3.41, bottom). For protons attached to C-4 and C-6, the MNova software predicted an equivalent doublet at 7.75 ppm because both protons are attached to a carbon having one hydrogen, and those peaks were also observed. Note that C-5 and C-7 do not have any protons attached to them.

For protons attached to C-8, a quartet was expected at 4.00 ppm with a peak intensity ratio of 1:3:3:1 because it is attached to a carbon atom bonded to two protons, and a nitrogen atom bonded to one proton. The peak was not observed because it was obscured by the large water peak at 4.70 ppm. For protons attached to C-9, a quartet was expected at 3.25 ppm with a peak intensity ratio 1:3:3:1 because it is bonded to a carbon atom having two hydrogen atoms, and to a carbon atom attached to one hydrogen atom. This peak was also not observed because the aqueous buffer constantly exchanged this proton because it is acidic.

For proton attached to C-10, a quintet was expected at 2.50 ppm with a peak intensity ratio of 1:4:6:4:1 because it is bonded to a carbon atom which has three hydrogen atoms, and to a nitrogen atom with one hydrogen. A quartet was observed rather than a quintet because of over-lapping signals from protons C-11, 12, 13, 14, and 15, which reside on the alkyl group.

3.10.2   N-Ethylpentylone

N-Ethylpentylone (Figure 3.42) is a secondary amine with 19 protons. Seven types of protons were of interest as shown in Table 3.17. C-1 and C-2 do not have any protons. In Figure 3.43 (top), for protons attached to C-3, the Mnova software predicted an equivalent doublet at 6.75 ppm with peak intensity ratio 1:1 because it is bonded to a carbon having one hydrogen, and the peak was observed at 7.00 ppm (Figure 3.43, bottom). For protons attached to C-4, the software predicted an equivalent doublet at 7.50 ppm with peak intensity ratio 1:1 because it is bonded to a carbon having one hydrogen. In the predicted spectrum, one of the peaks of the doublet was under the singlet. A distorted peak was observed at 7.75 ppm because of coupling effect — it was four bonds away from the proton attached to C-6. Coupling effects are the process where the spin of the nucleus of one proton is close enough to affect the spin of another proton. Also, the peak was observed at higher ppm ("down-field") because it was near an oxygen atom. The electronegative nature of oxygen will lower the electron density around the proton, shifting its response down-field. As a result, proton will experience de-shielding effect i.e. higher magnetic field around it. Carbon number 5 do not have any proton. For proton attached to C-6, the Mnova software predicted a singlet at 7.50 ppm because it is bonded to a carbon having no protons. The singlet was observed at 7.50 ppm.

For protons attached to C-8, a sharp singlet was predicted at 6.00 ppm because the neighboring carbon does not have any protons. This peak is characteristic for many Cathinones. The peak was observed at 6.25 ppm. For proton attached to carbon 12, a quartet was expected at 4.00 ppm with peak intensity ratio 1:3:3:1 because it is bonded to a carbon having two protons and nitrogen having one proton. The peak was not observed because it was obscured by the water peak at 4.7 ppm. Note that Carbon 10 does not have any protons.

For proton attached to C-14, a quartet was expected at 3.25 ppm with peak intensity ratio 1:3:3:1 because it is bonded (on one side) to a carbon having two hydrogen atoms and (on other side) to a carbon having one hydrogen atom. The peak was not observed because the solvent was an aqueous buffer and there was constant exchange of protons with the buffer. For protons attached to C-15, an equivalent doublet and a quartet were expected at 2.50 ppm because it is bonded to nitrogen having one proton and carbon having three protons. One of the limitations of the coupling effect is that it does not occur between heteroatoms because of differences in electronegativity between carbon and another atom. Thus the quintet was not observed for protons attached to C-15 but rather a quartet was observed at 3.00 ppm. Overlapped signals for the rest of the alkyl protons attached to C-13, 16, 17, and 18 were observed at 0.50 ppm.

3.10.3 Methylone

Methylone (Figure 3.44) is a secondary amine with 17 protons. Eight types of protons were of interest as shown in Table 3.18. C-1 and C-2 do not have any protons. In Figure 3.45 (top), for protons attached to C-3, the Mnova software predicted an equivalent doublet at 7.00 ppm with peak intensity ratio 1:1 because it is attached to carbon bonded to one hydrogen atom. The peak was observed at 7.00 ppm (Figure 3.45, bottom). For protons attached to C-4, the software predicted an equivalent doublet at 7.50 ppm with peak intensity ratio 1:1 because it is attached to carbon bonded to one hydrogen atom. In the predicted spectrum, one of the peaks of the doublet is underneath the other, creating a singlet. A distorted peak was observed at 7.75 ppm because of coupling effect because it was four bonds away from proton attached to carbon 6. Coupling effect is the process where spin of nucleus of one proton is close enough to affect the spin of another proton. Also, the peak was at higher ppm. It is because it was near to carbonyl group. The electronegative nature of oxygen will lower the electron density around the proton. As a result, proton will experience de-shielding effect i.e. higher magnetic field around it.

For proton attached to carbon 6, the software predicted a singlet at 7.50 ppm because it is bonded to carbon with no hydrogen atom. The singlet was observed at 7.50 ppm. For protons attached to carbon 8, a sharp singlet was predicted at 6.00 ppm

because it is bonded to carbon with no hydrogen atom. The peak is a characteristic peak for many Cathinones. The peak was observed. For proton attached to carbon 12, a quintet was expected at 5.00 ppm with peak intensity ratio 1:4:6:4:1 because it is bonded to nitrogen having one proton and to a carbon having three protons. The peak was not observed because is was overlapped with the water peak. For protons attached to C-14, a quintet was expected at 4.00 ppm with peak intensity ratio 1:4:6:4:1 because it is bonded to carbon having three hydrogen atoms and to carbon having one hydrogen atom. The peak was not observed because the aqueous buffer constantly exchanged this proton. For protons attached to C-13, an equivalent doublet was expected at 1.25 ppm with peak intensity ratio 1:1 because it is bonded to carbon having one proton and was observed at 1.50 ppm. For protons attached to C-15, an equivalent doublet was expected at 2.25 ppm with peak intensity ratio 1:1 because it is attached to a nitrogen having one proton. The peak was not observed because the aqueous buffer also constantly exchanged this proton.

3.10.4 Methcathinone

Methcathinone (Figure 3.46) is a secondary amine with 13 protons. Six types of protons were of interest as shown in Table 3.19. In Figure 3.47 (top), for protons attached to C-1, 2, and 3, the Mnova software predicted a triplet at 7.50 ppm with peak intensity ratio 1:2:1 because they were bonded to two carbons each with one hydrogen atom. Faint

peaks were observed at 7.75 ppm (Figure 3.47, bottom). For protons attached to C-4 and C-6, the software predicted an equivalent doublet at 8.00 pm because both protons are bonded to a carbon having one hydrogen atom. Faint peaks are observed at 8.00 ppm. For proton attached to C-8, a quintet was expected at 4.00 ppm with peak intensity ratio 1:4:6:4:1 because it is bonded to carbon having three protons and nitrogen having one proton. The peak was not observed because it is obscured by the large water peak at 4.70 ppm.

For protons attached to C-9, an equivalent doublet was expected at 1.25 ppm with peak intensity ratio 1:1 because it is bonded to a carbon having one hydrogen atom, and those peaks were observed at 1.50 ppm. For protons attached to C-10, a quintet was expected at 5.00 ppm with peak intensity ratio 1:4:6:4:1 because it is bonded to a carbon having one hydrogen atom and to a carbon having three hydrogen atoms. The peak was not observed because the aqueous buffer constantly exchanged this proton. For protons attached to C-11, an equivalent doublet was expected at 2.25 ppm with peak intensity ratio 1:1 because it is bonded to nitrogen having one hydrogen atom. A singlet was observed because the proton on the nitrogen was in constant exchange with D2O. Thus splitting was not observed for protons attached to C-11. A giant peak at 3.50 ppm was also observed from Mannitol in the sample.

3.11   Figures and Tables
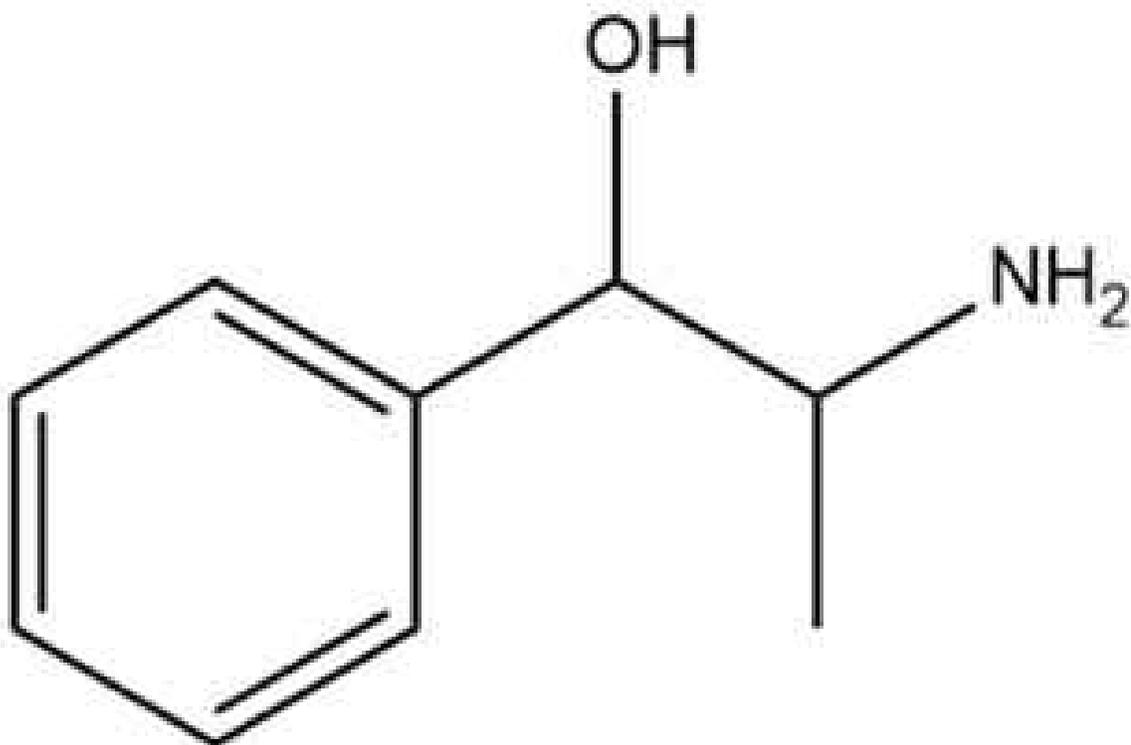
FIGURE 3.1: The structure of Phenylpropanolamine (PPA).
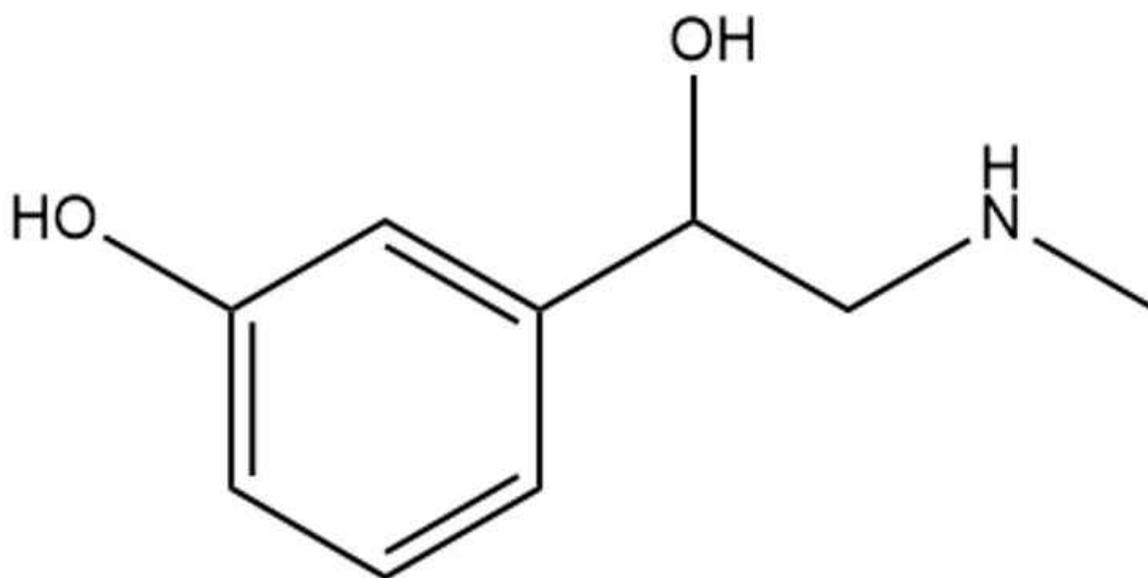
FIGURE 3.2: The structure of Phenylephrine (PEP).
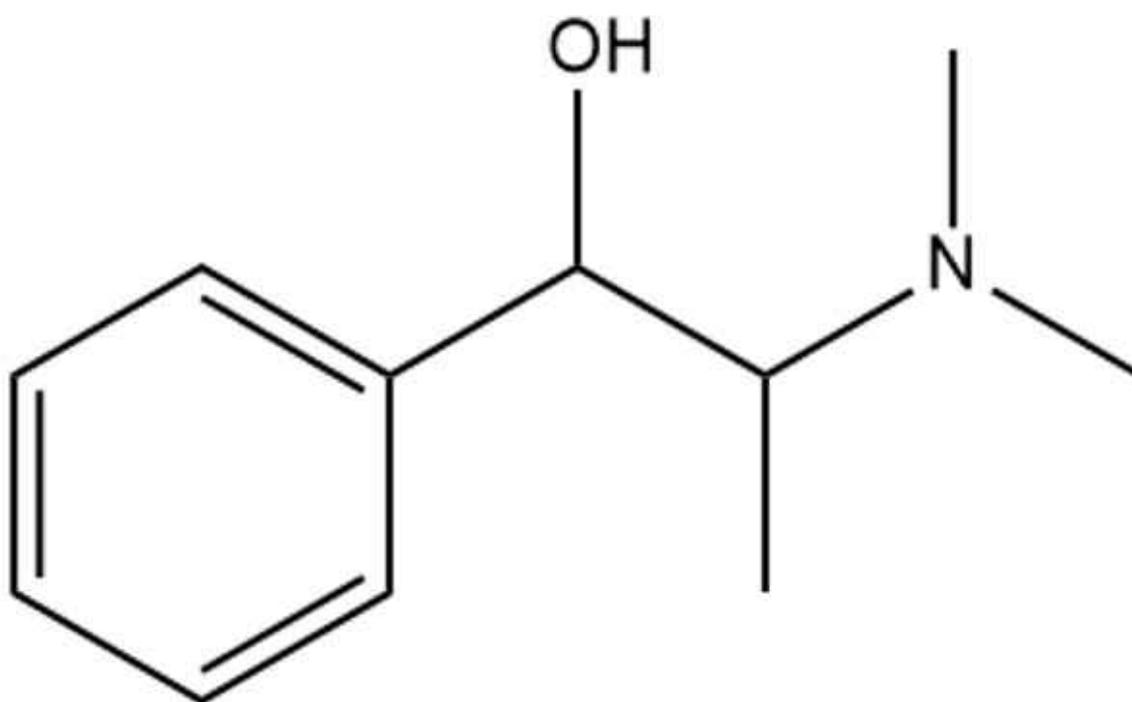
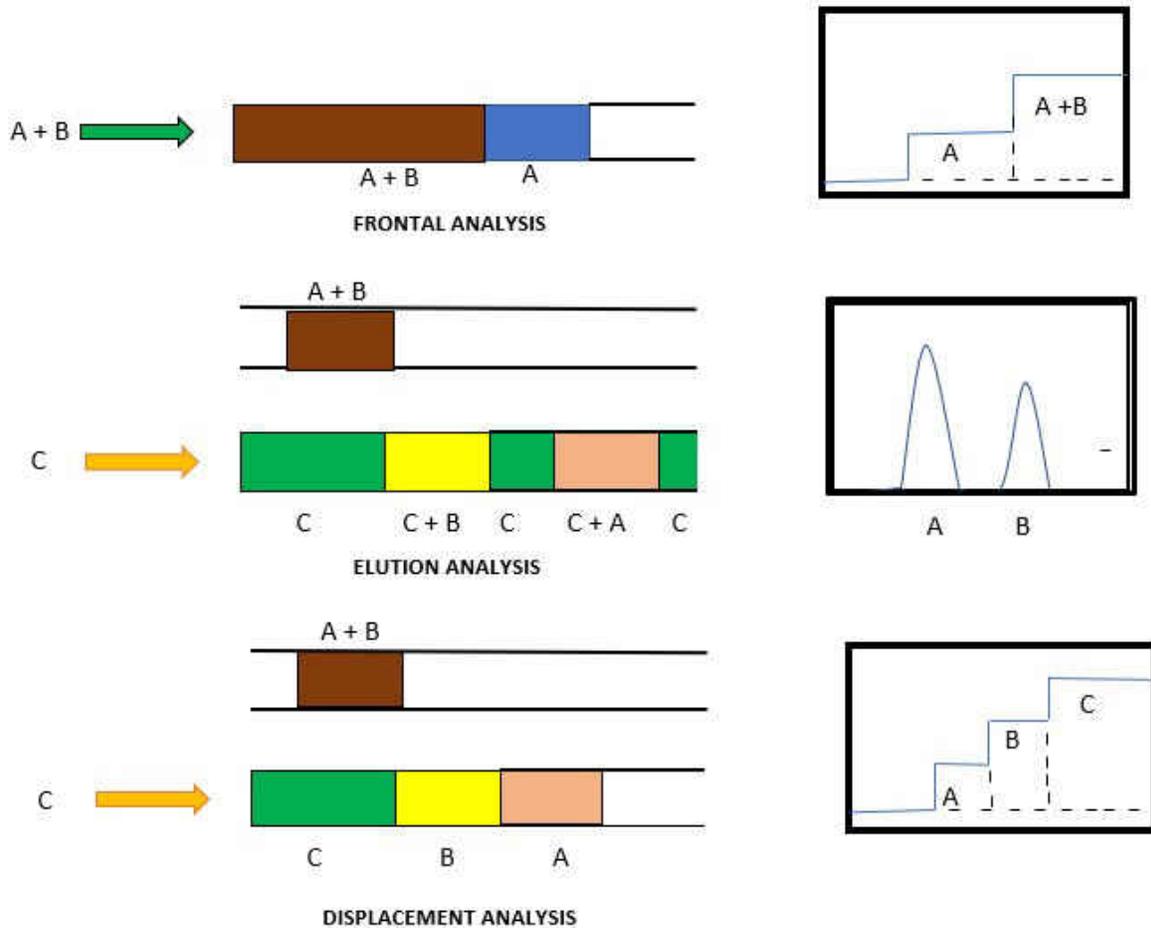FIGURE 3.3: The structure of Methylephedrine (MEP).

FIGURE 3.4: Schematic representation of the different development modes. The displacement mode of chromatographic development (bottom). The mixture containing the analytes (A and B) are initially loaded onto the column, followed by the eluent (C). In this case, A is eluted first because it is more easily displaced than B by C. Adapted from [2].
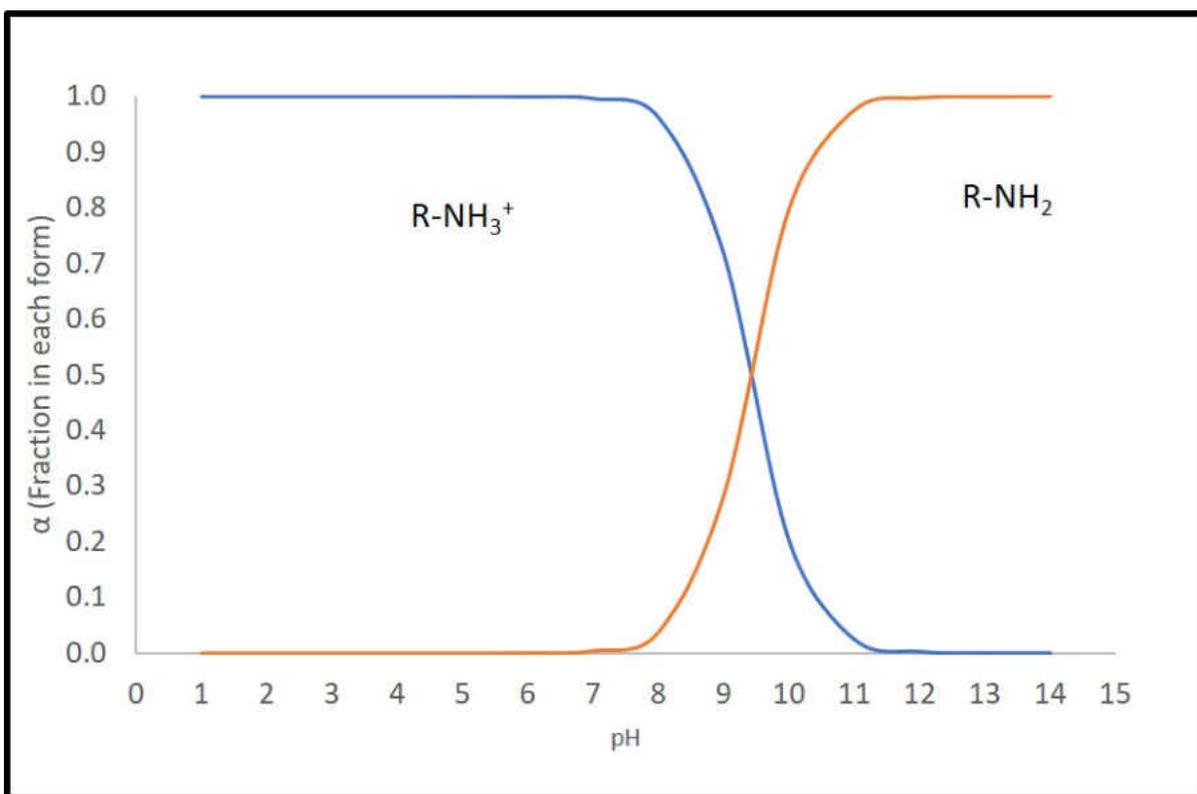
FIGURE 3.5: Fractional composition diagram of PPA.
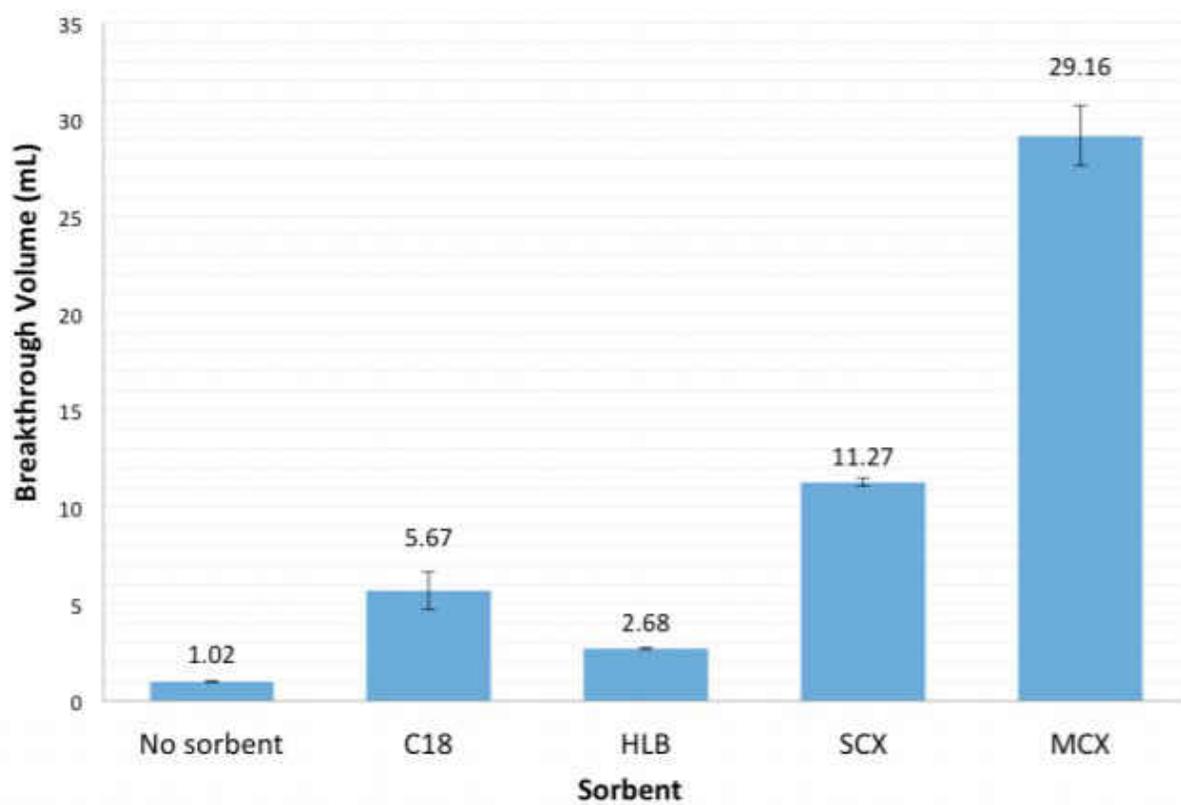
FIGURE 3.6: A higher breakthrough volume for PPA was observed on SCX and MCX for PPA. Error bars correspond to the 95% confidence interval (n=3).
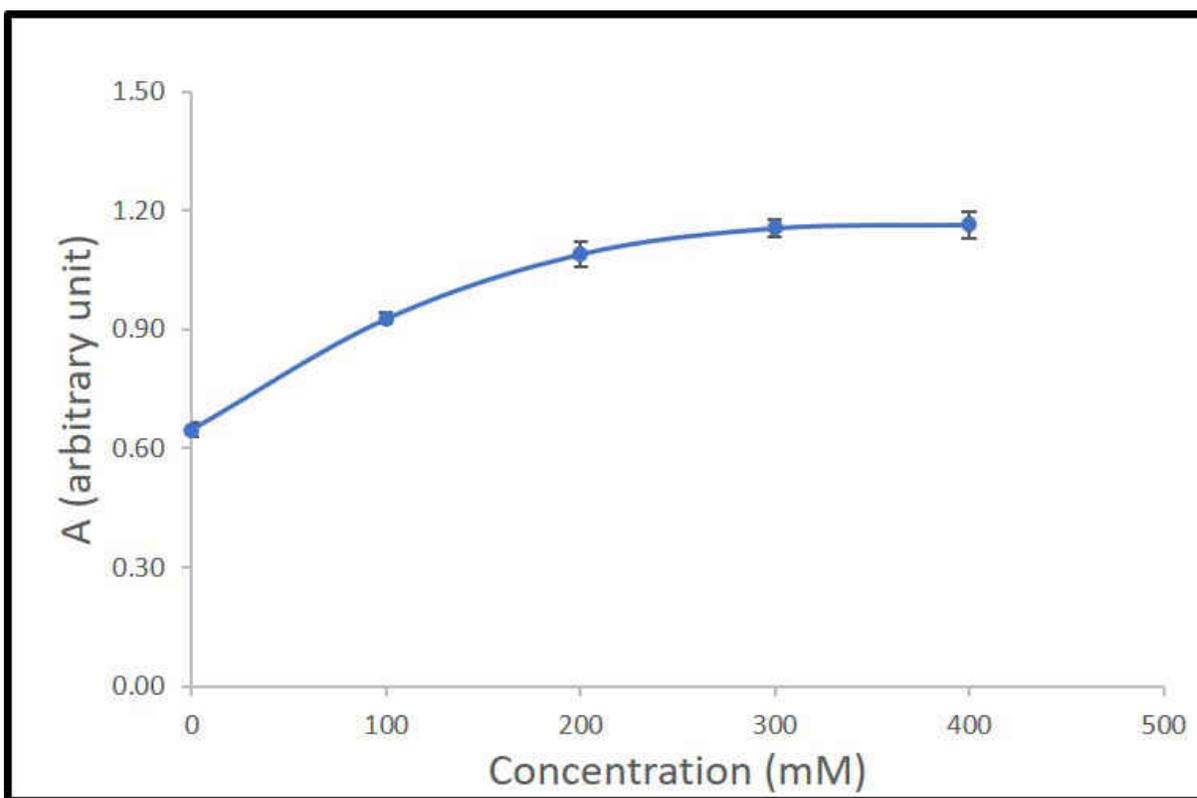
FIGURE 3.7: Optimal concentration for PPA elution was 200 mM.
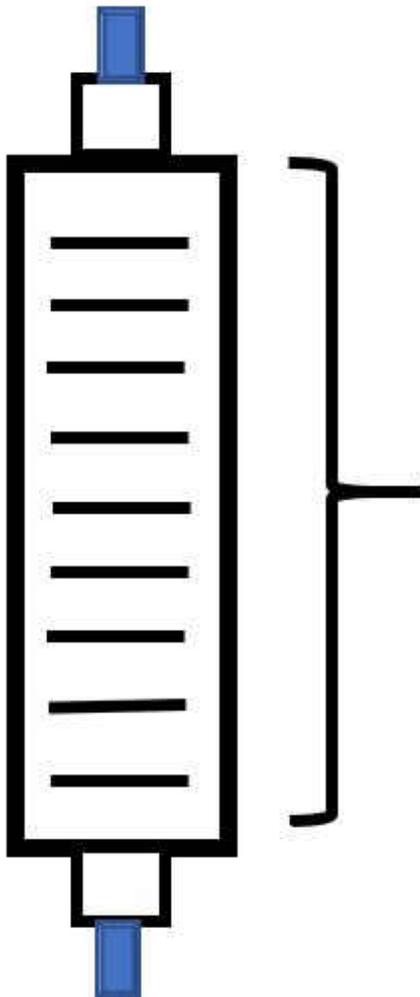
FIGURE 3.8: Wide Cylindrical column.
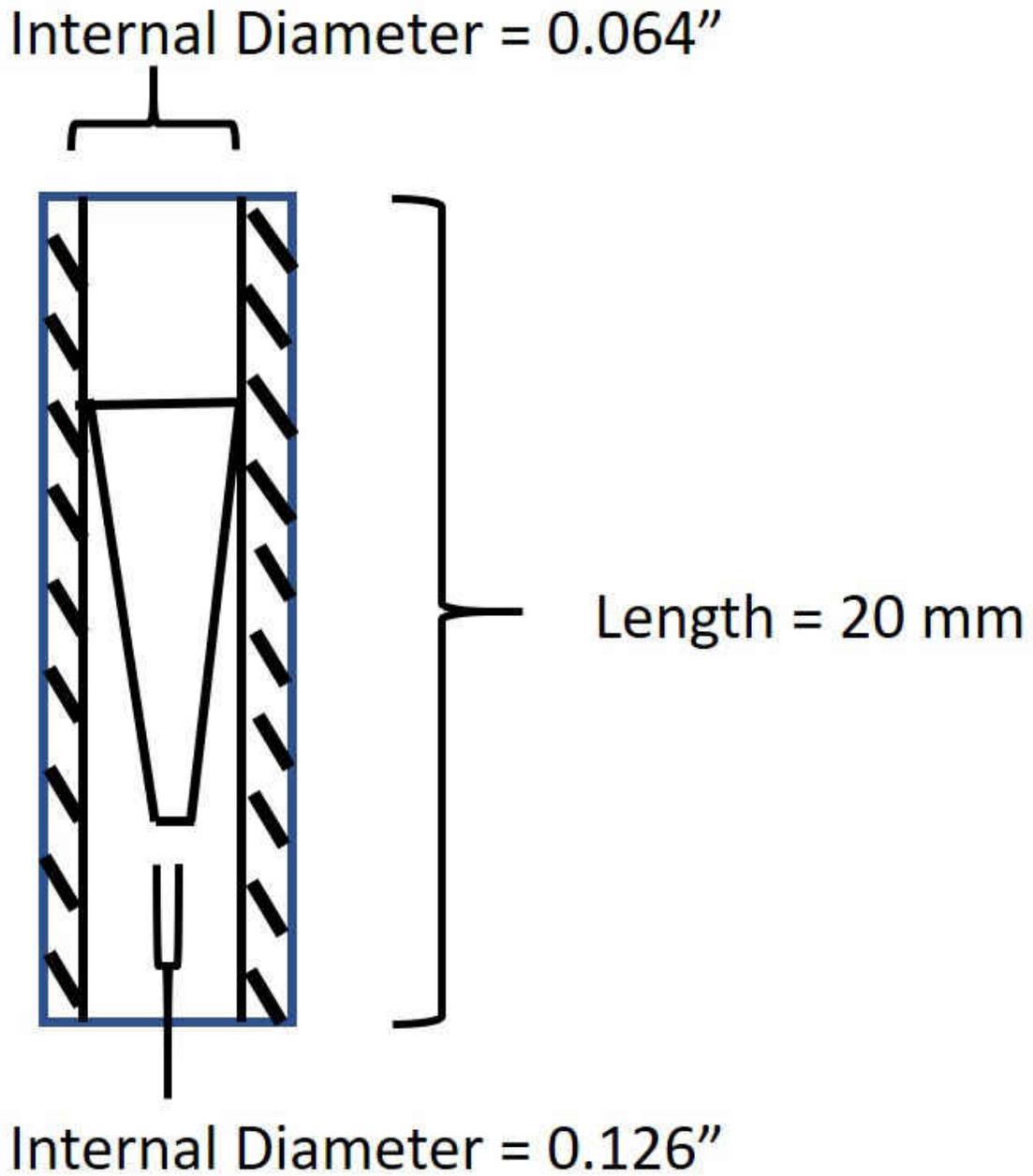
FIGURE 3.9: Tapered column.

Internal Diameter = 4.8 mm

Length = 33 mm
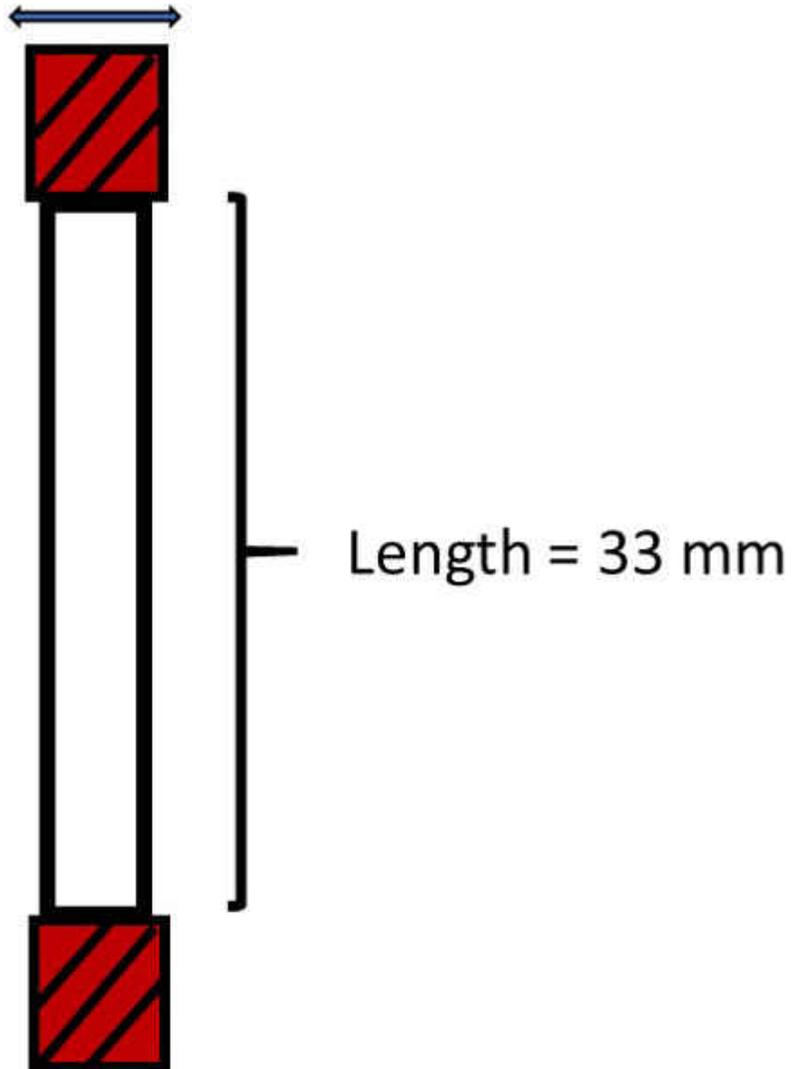
FIGURE 3.10: Narrow Cylindrical column.
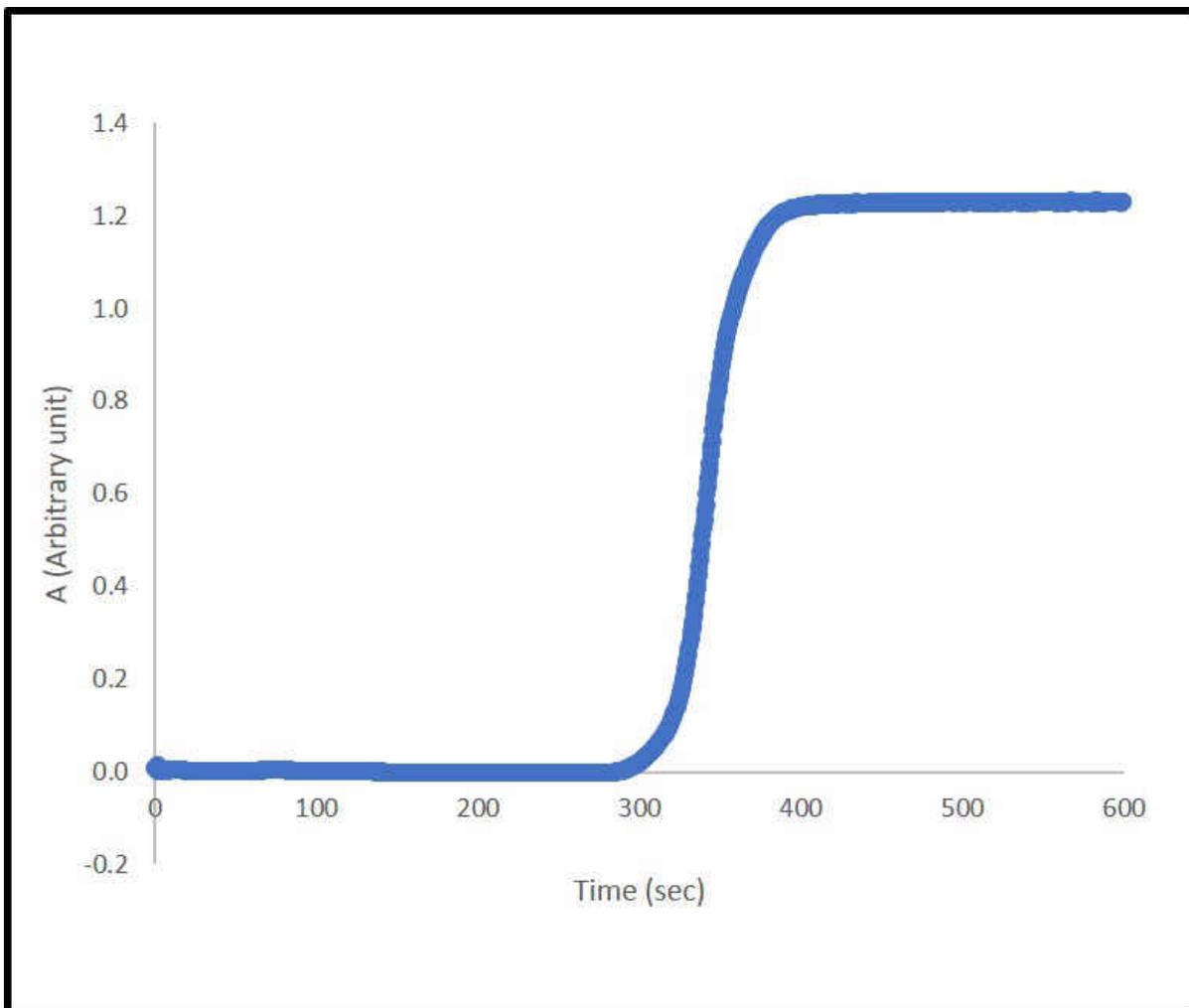
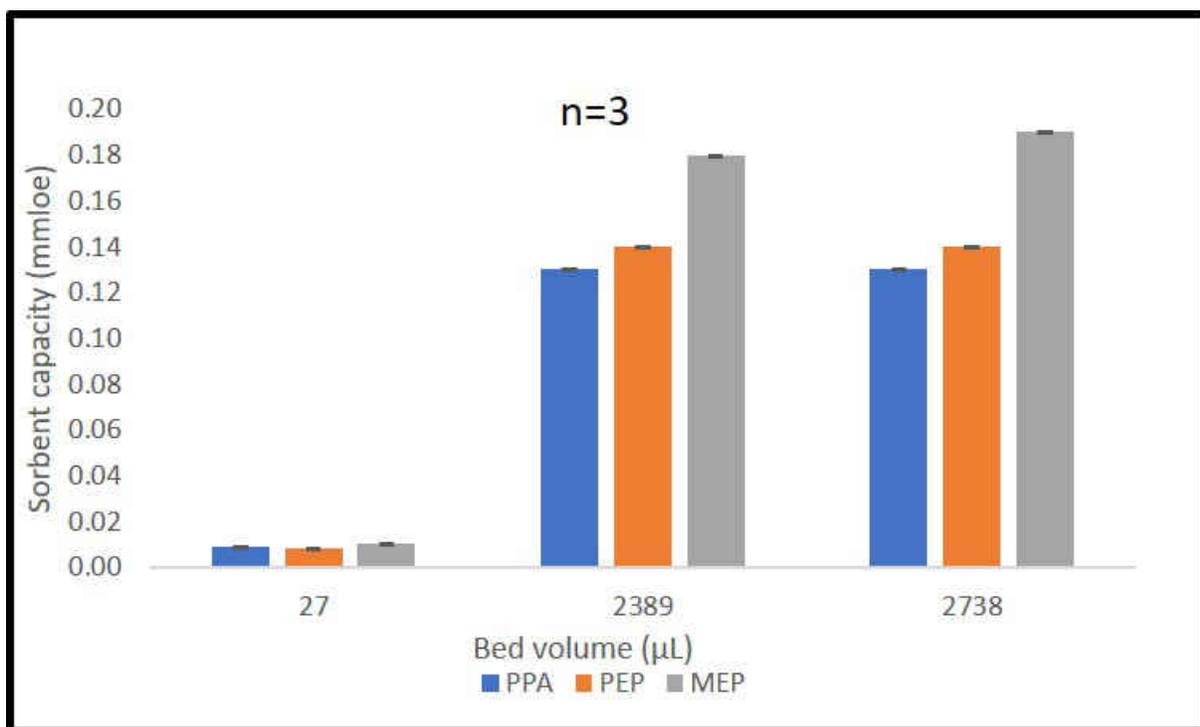FIGURE 3.11: Breakthrough value of PPA on the SCX resin.

FIGURE 3.12: Capacity of sorbent (SCX) in three different columns with different volumes. Error bars correspond to the 95% confidence interval (n=3).
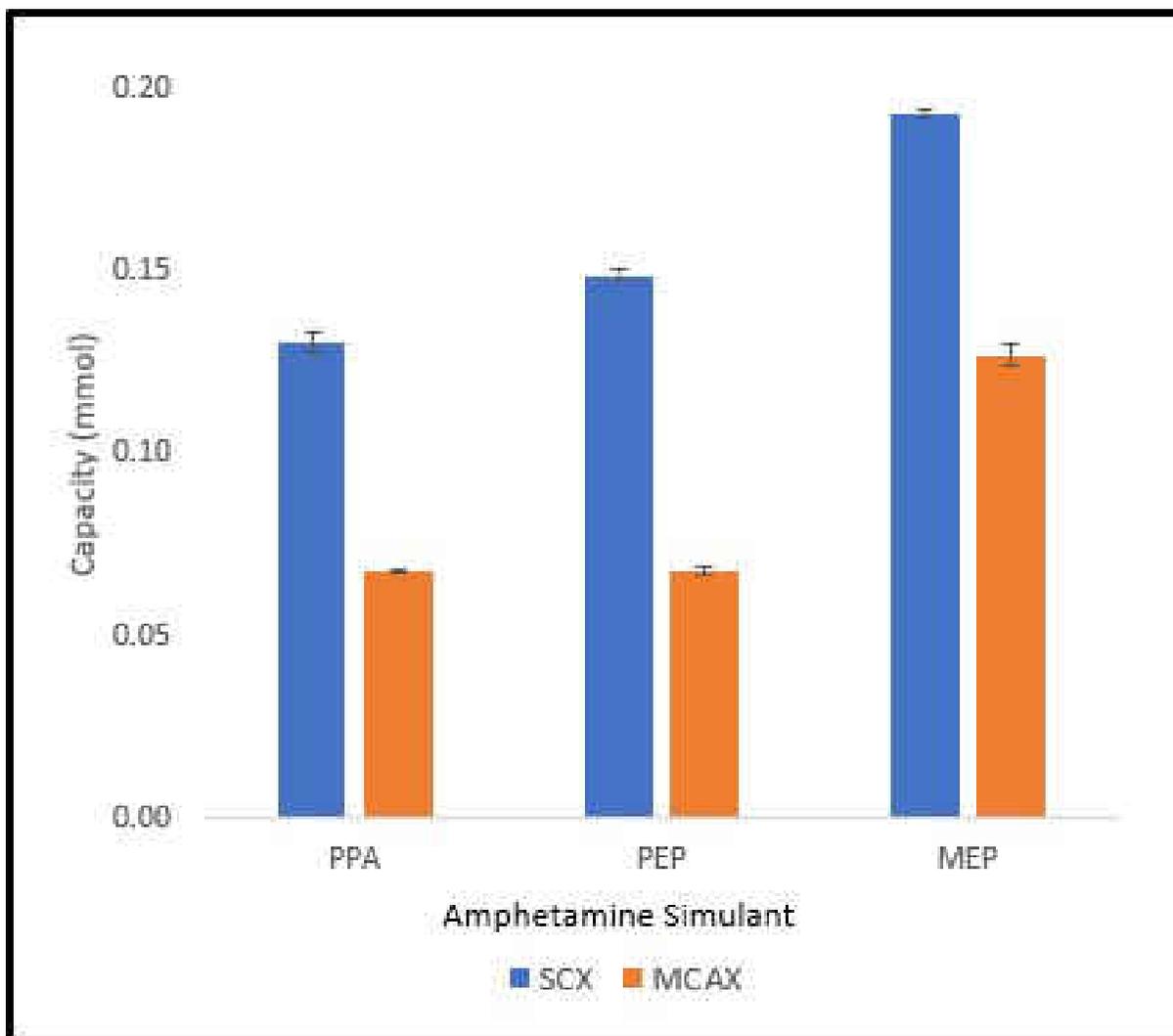
FIGURE 3.13: Wide cylindrical column capacity. Error bars correspond to the 95% confidence interval (n=3).
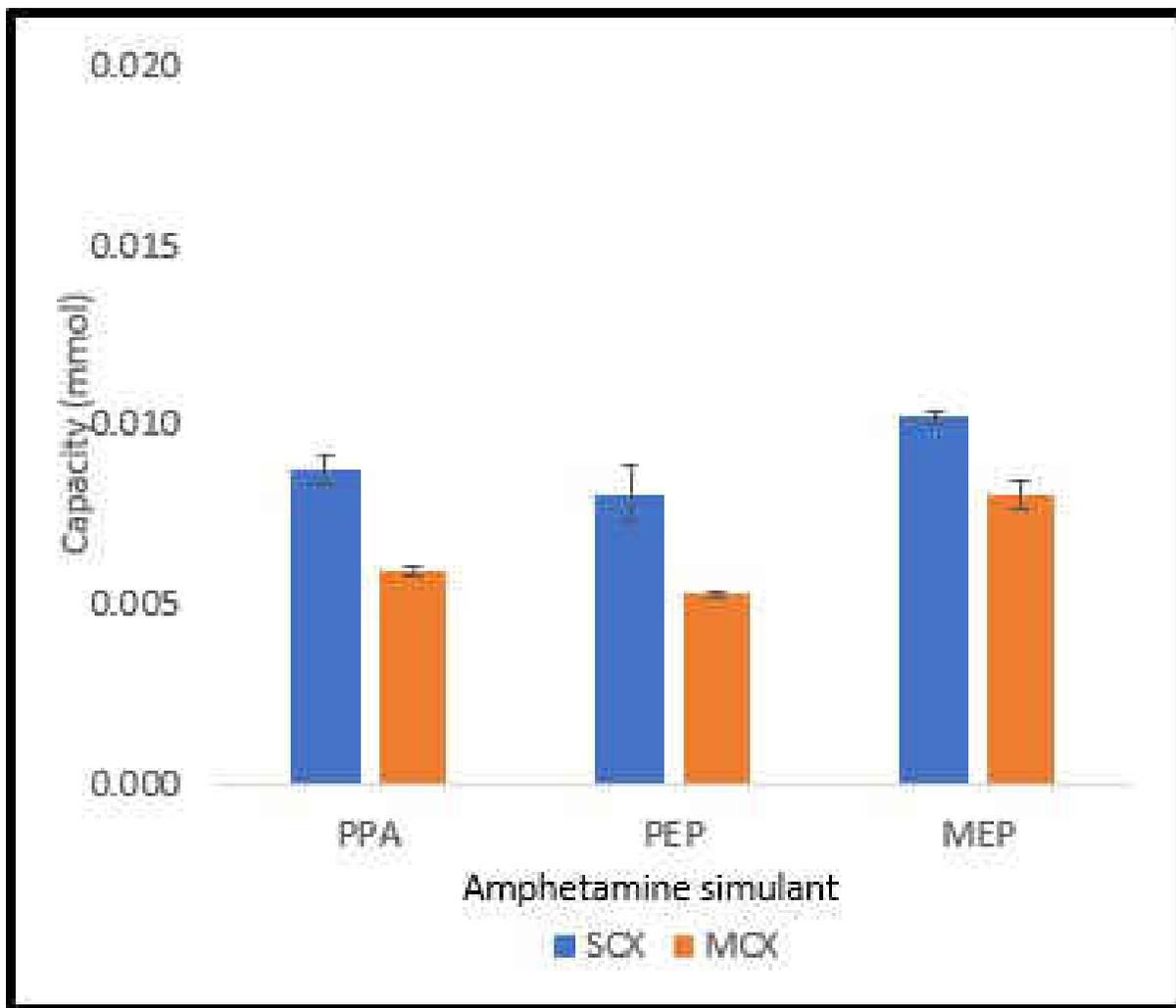
FIGURE 3.14: Small tapered column capacity. Error bars correspond to the 95% confidence interval (n=3).
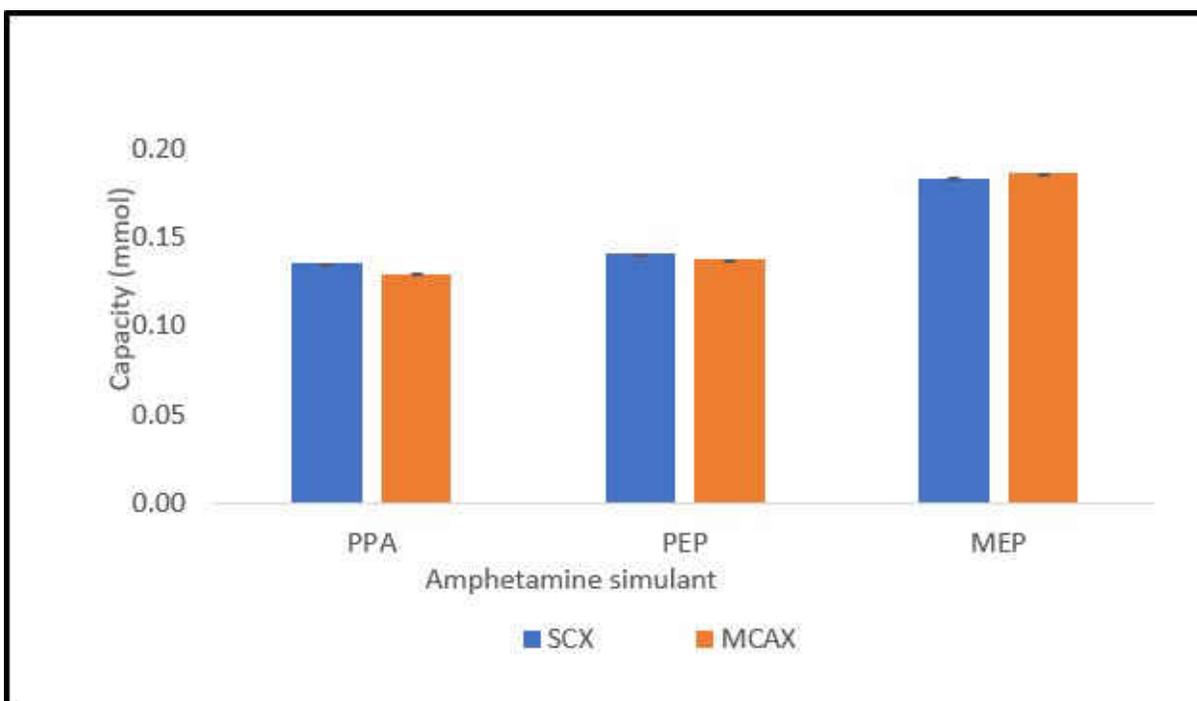
FIGURE 3.15: Narrow cylindrical column capacity. Error bars correspond to the 95% confidence interval (n=3).
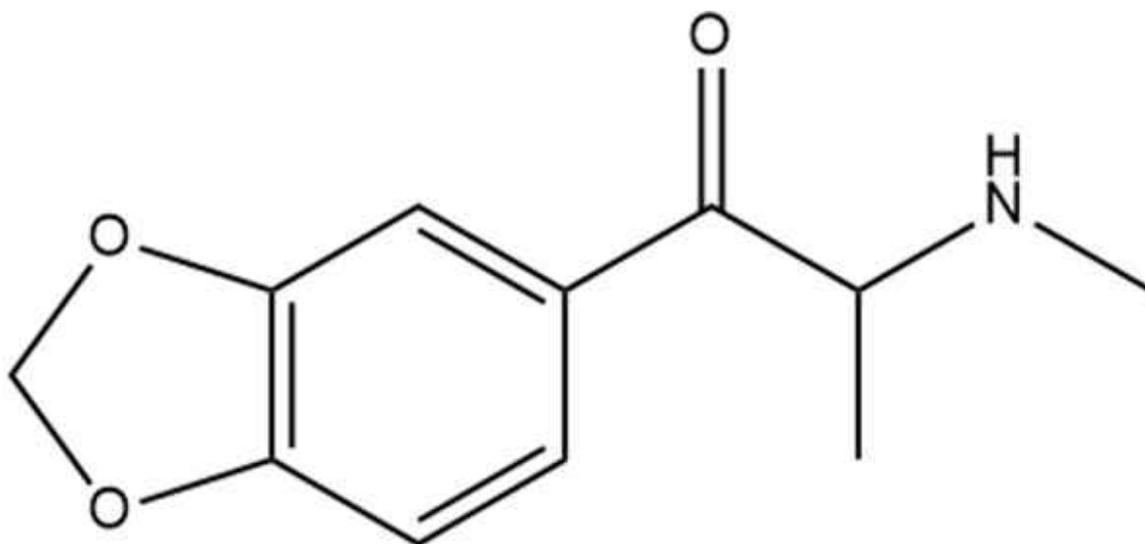
FIGURE 3.16: The structure of Methylone.

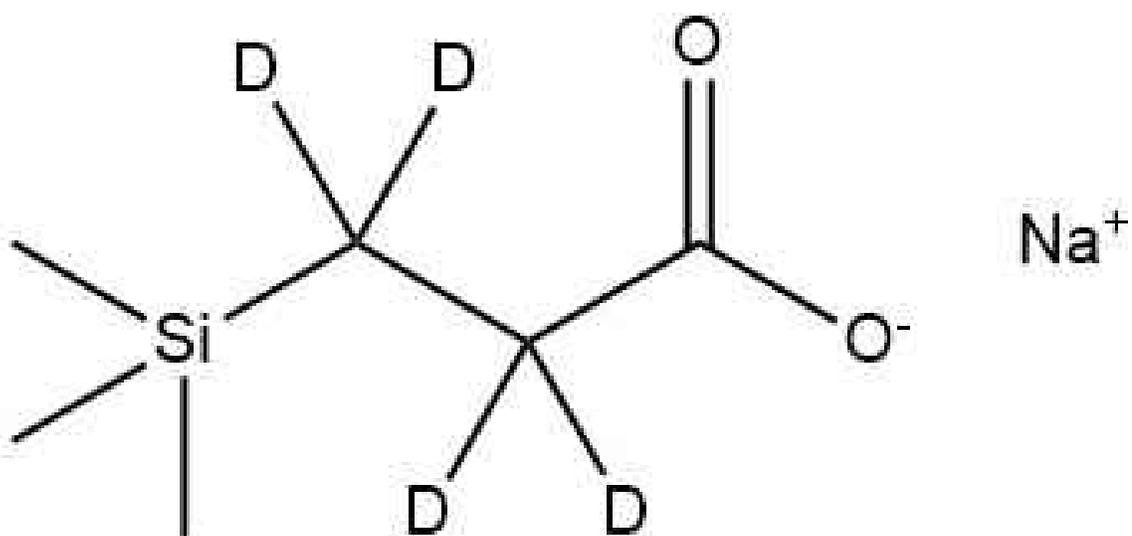FIGURE 3.17: The structure of TMSP-d_4.
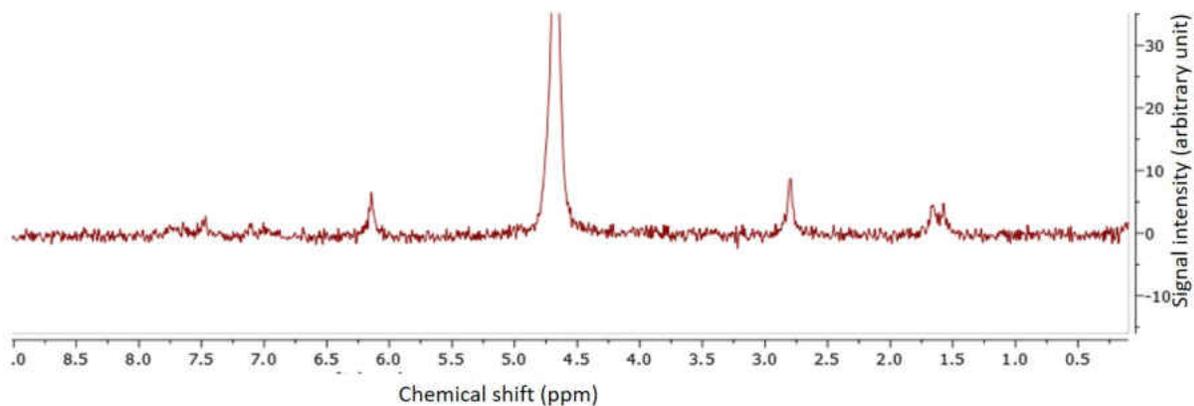
FIGURE 3.18: Response for 50 mM Methylone by NMR (64 scans).
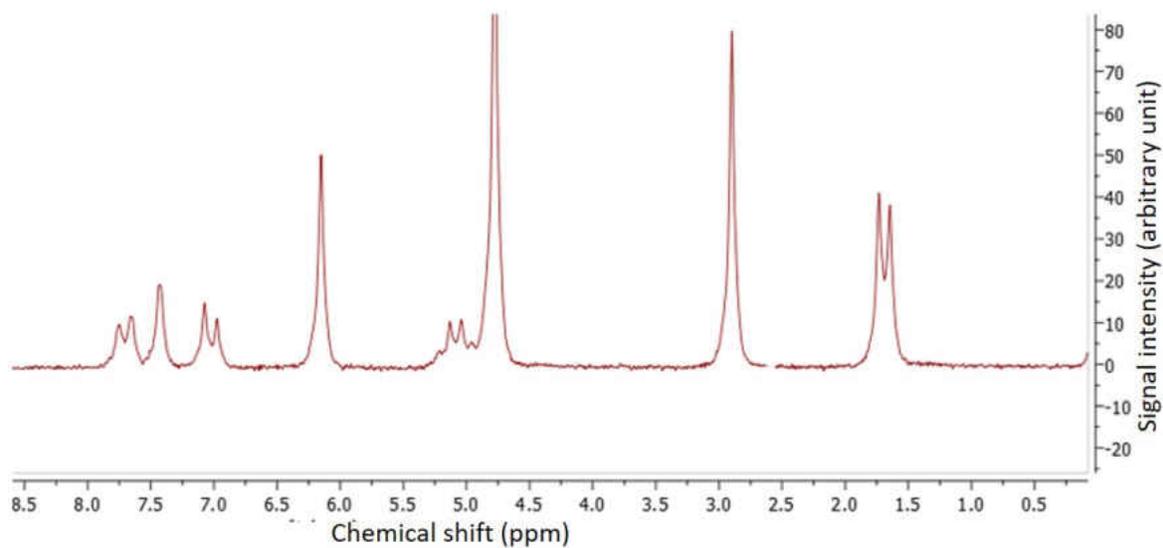
FIGURE 3.19: Response for 500 mM Methylone by NMR (256 scans).
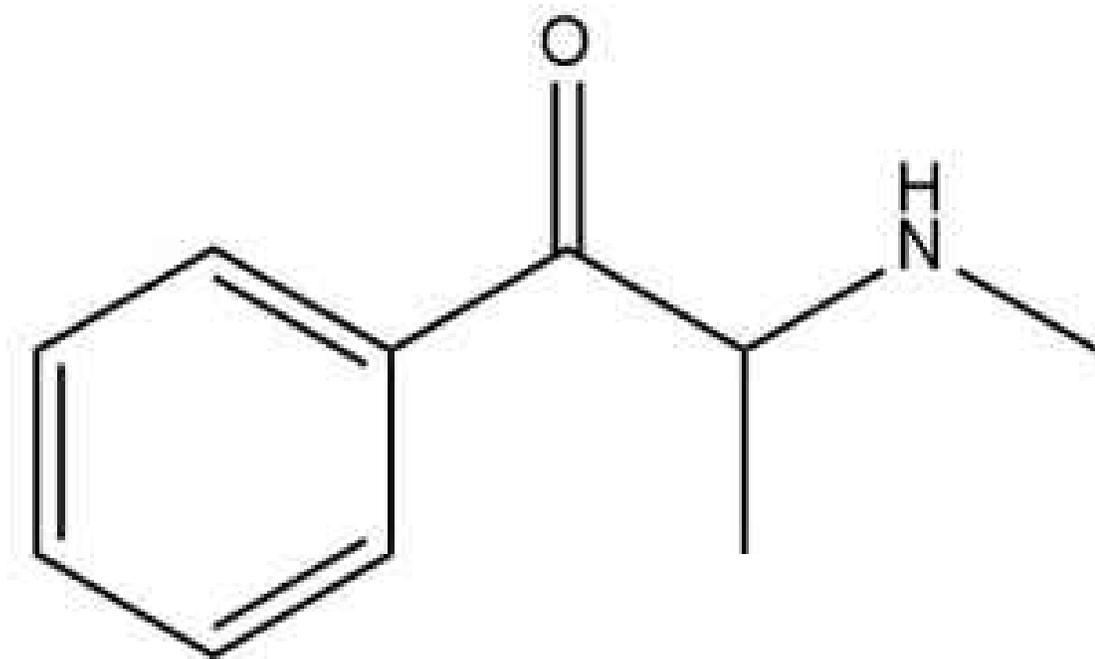
FIGURE 3.20: The structure of Methcathinone.
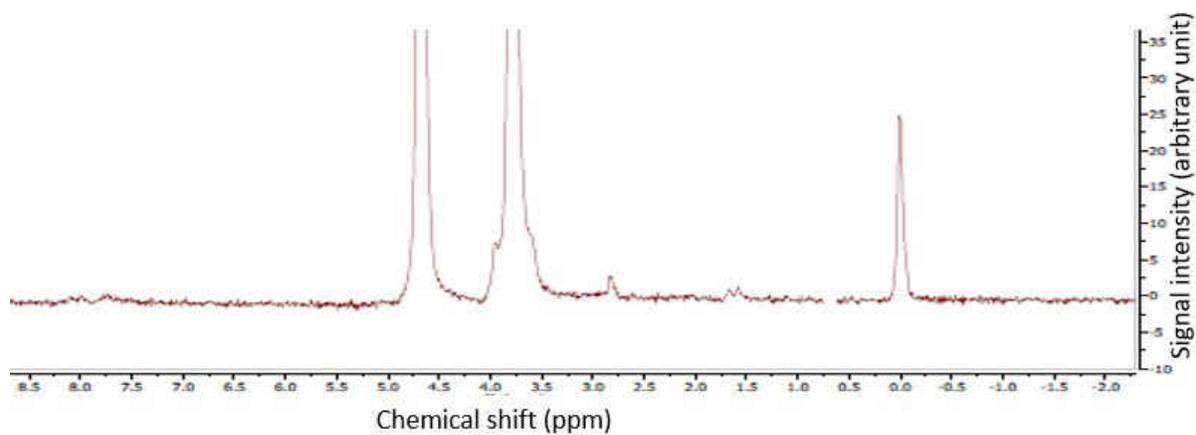
FIGURE 3.21: Response for 500 mM Methcathinone by NMR (256 scans).

FIGURE 3.22: Response for 175 mM Methcathinone by SIA-NMR (512 scans).
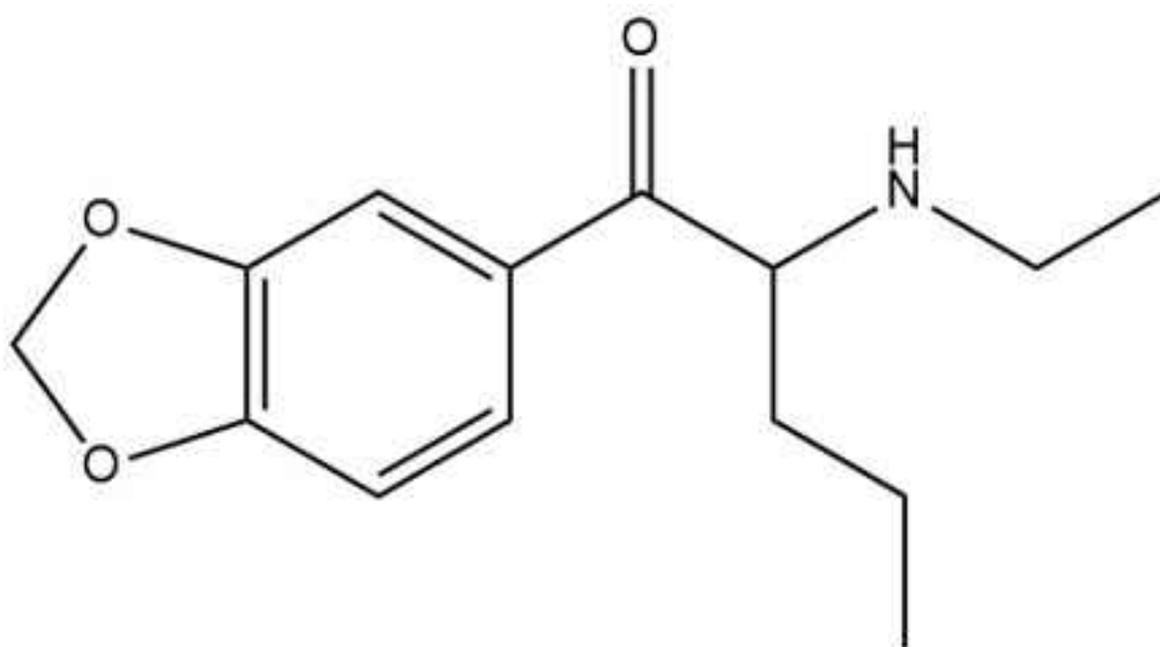
FIGURE 3.23: The structure of N-Ethylpentylone.
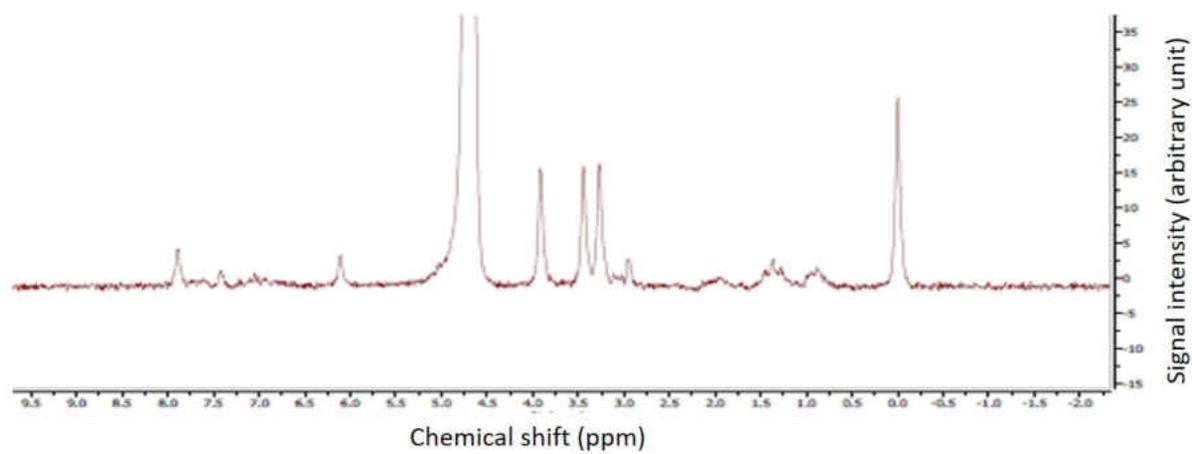
FIGURE 3.24: Response for 500 mM N-Ethylpentylone NMR (256 scans).
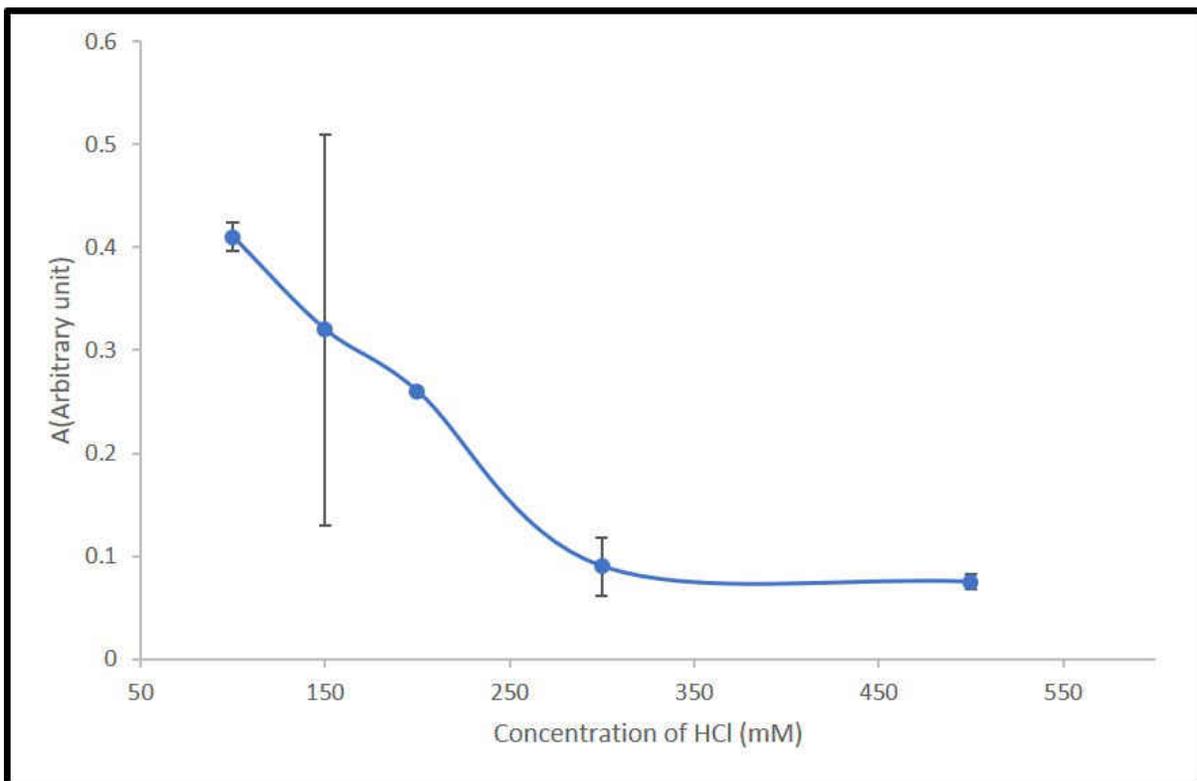
FIGURE 3.25: Optimal concentration of HCl for elution of MEP was 350 mM. Error bars correspond to the 95% confidence interval (n=3).
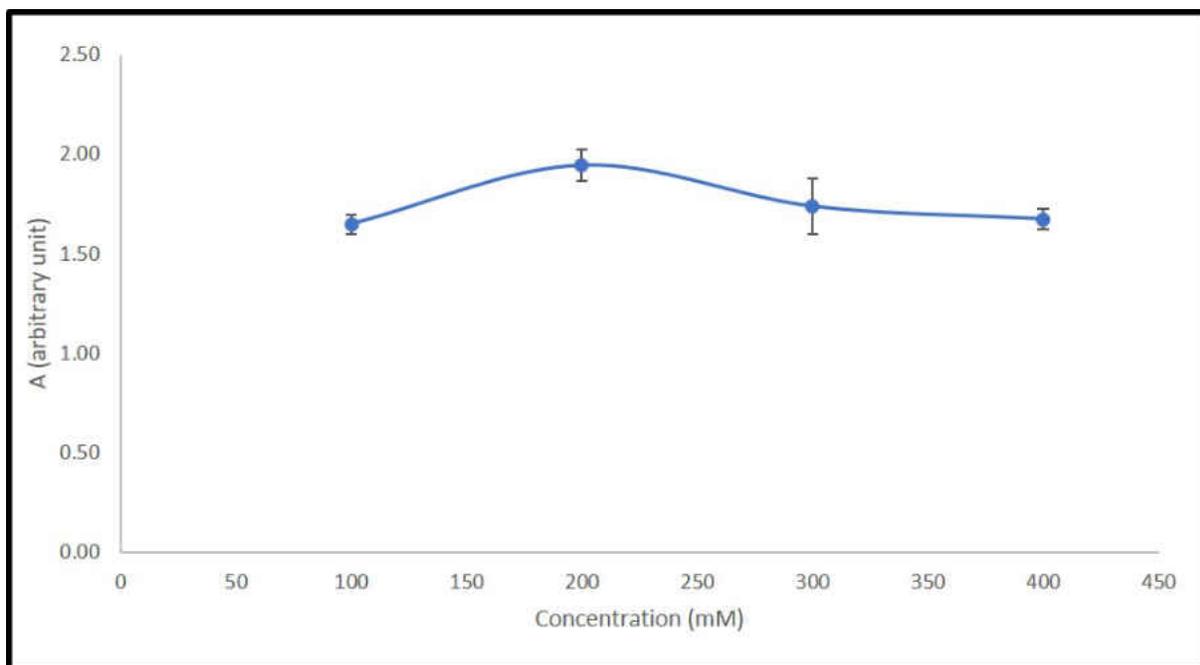
FIGURE 3.26: Optimal concentration of NaCl for the elution of MEP was 200 mM. Error bars correspond to the 95% confidence interval (n=3).
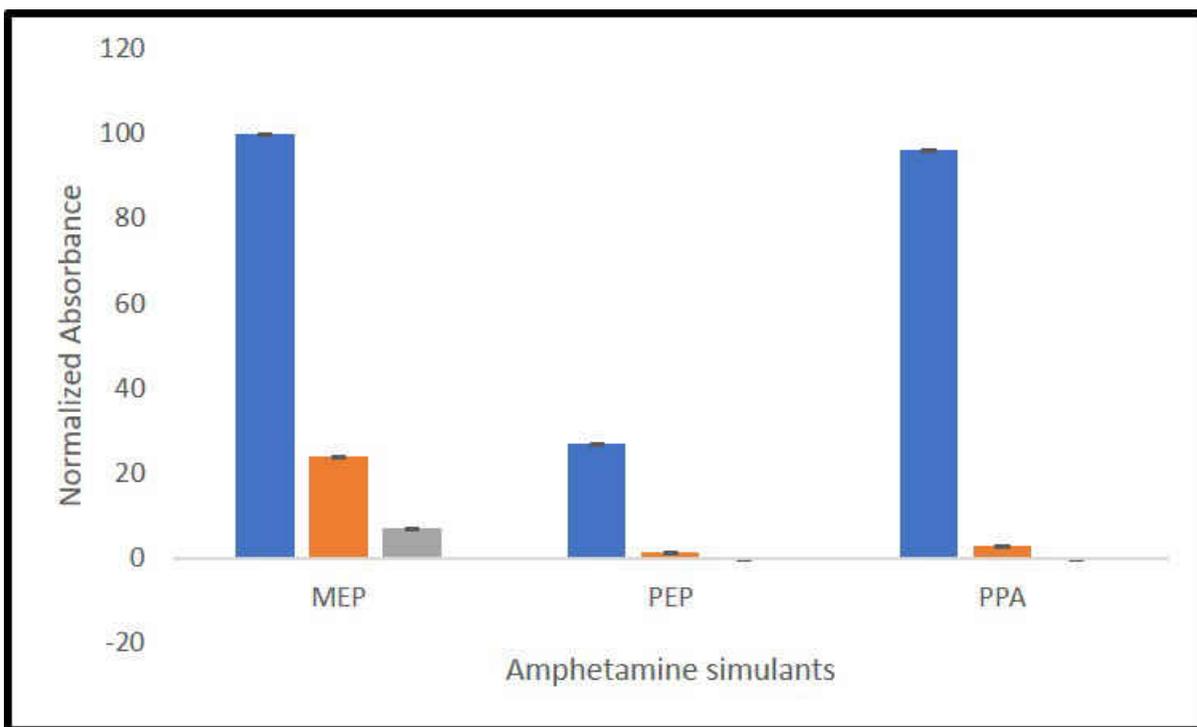
FIGURE 3.27: Elution behavior of three simulants with original eluent solution. First (blue), second (orange), third (gray) elution cycles. Error bars correspond to the 95% confidence interval (n=3).
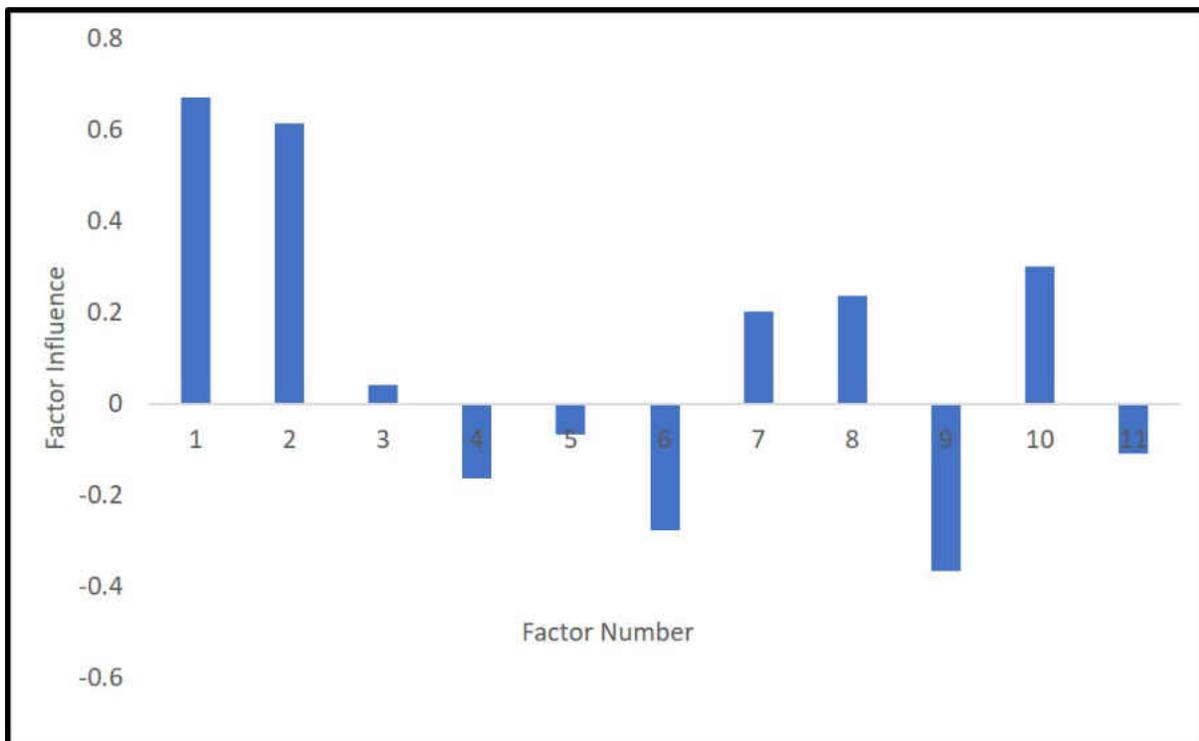
FIGURE 3.28: The degree to which factors 1 through 11 influenced the response.
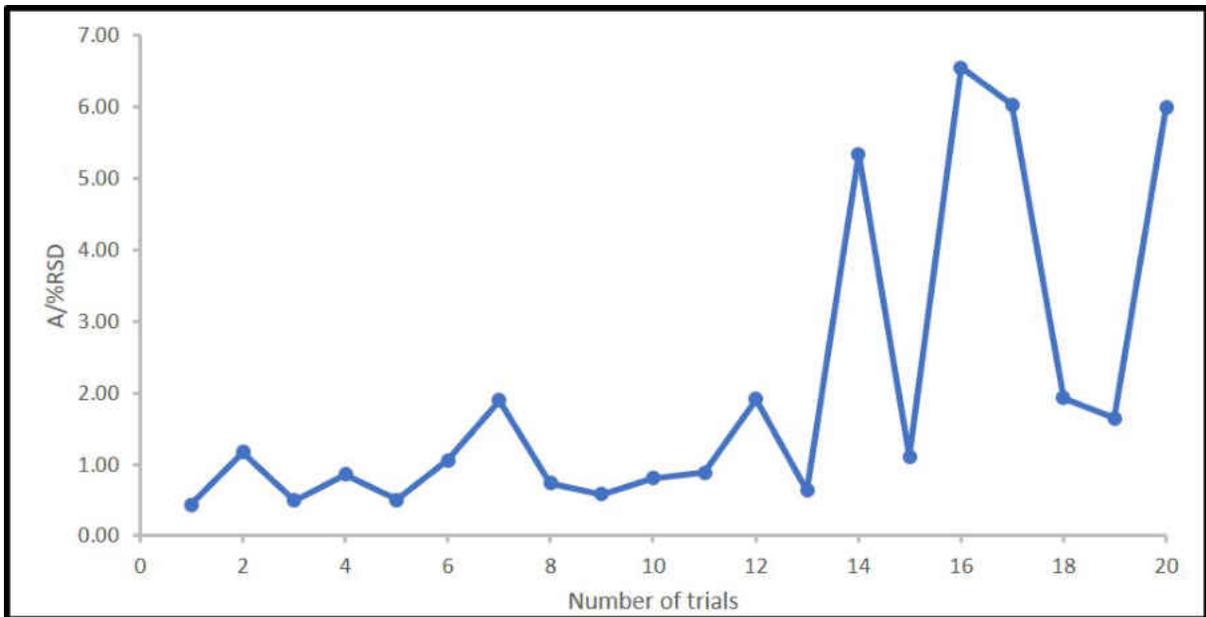
FIGURE 3.29: Variation of response function (A divided by %RSD) during Simplex optimization.
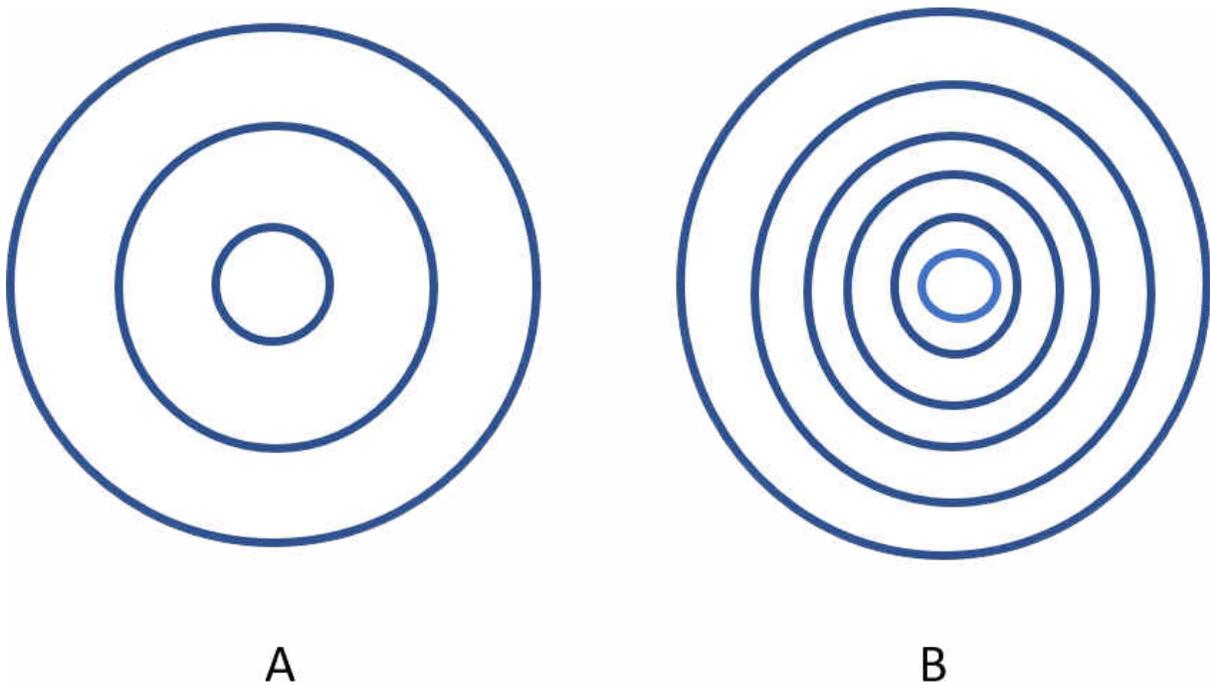
FIGURE 3.30: Schematic of contour plots of response surfaces. In "A", a broad "mountain top" will have a gentle decrease in the response value if there is a slight change in the values of the factors, whereas in "B" a narrow "mountain top" will have a sharp fall in the response value with only slight changes in the values of the factor.
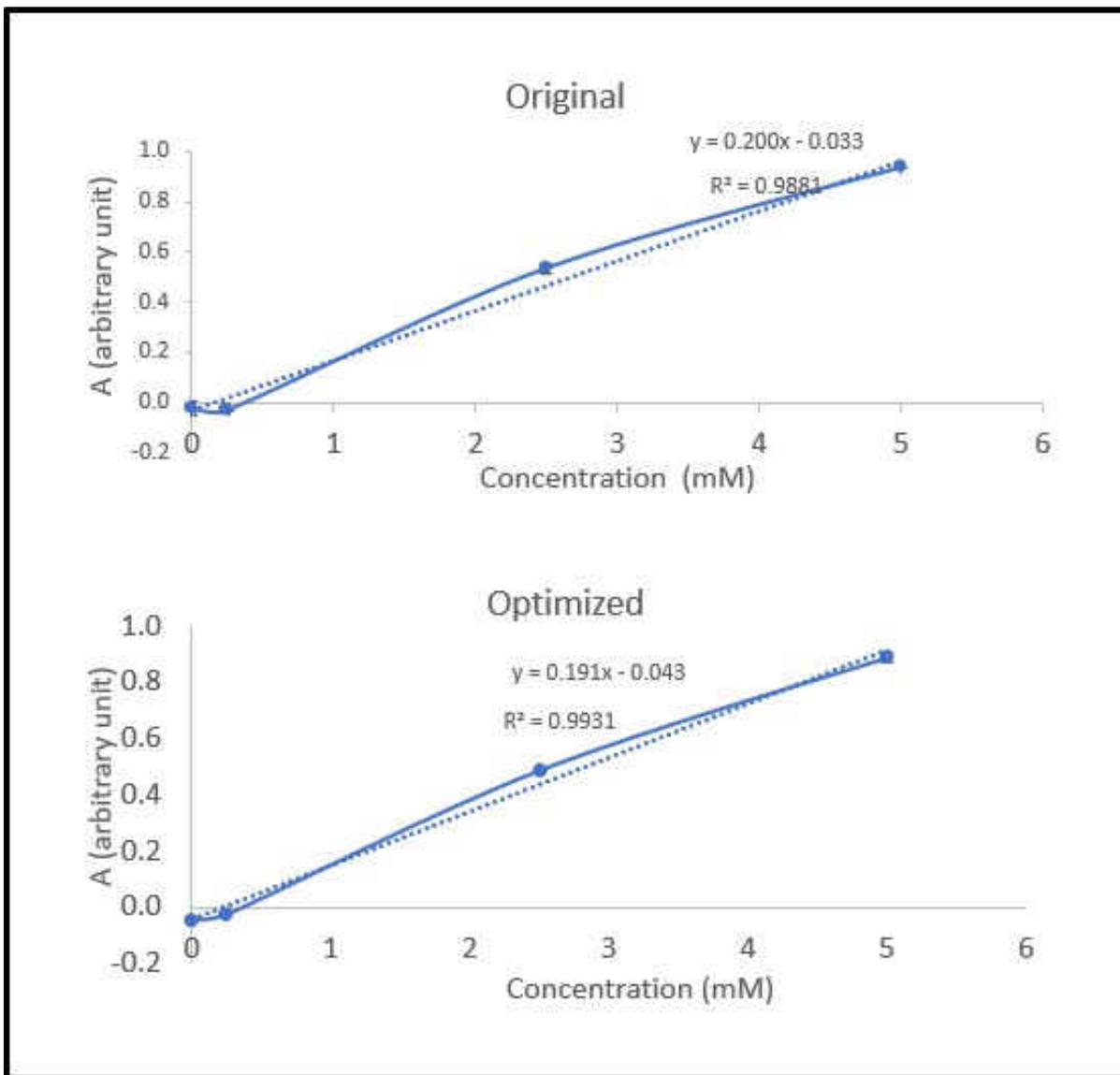
FIGURE 3.31: Calibration models using PPA for the two SIA-NMR methods.
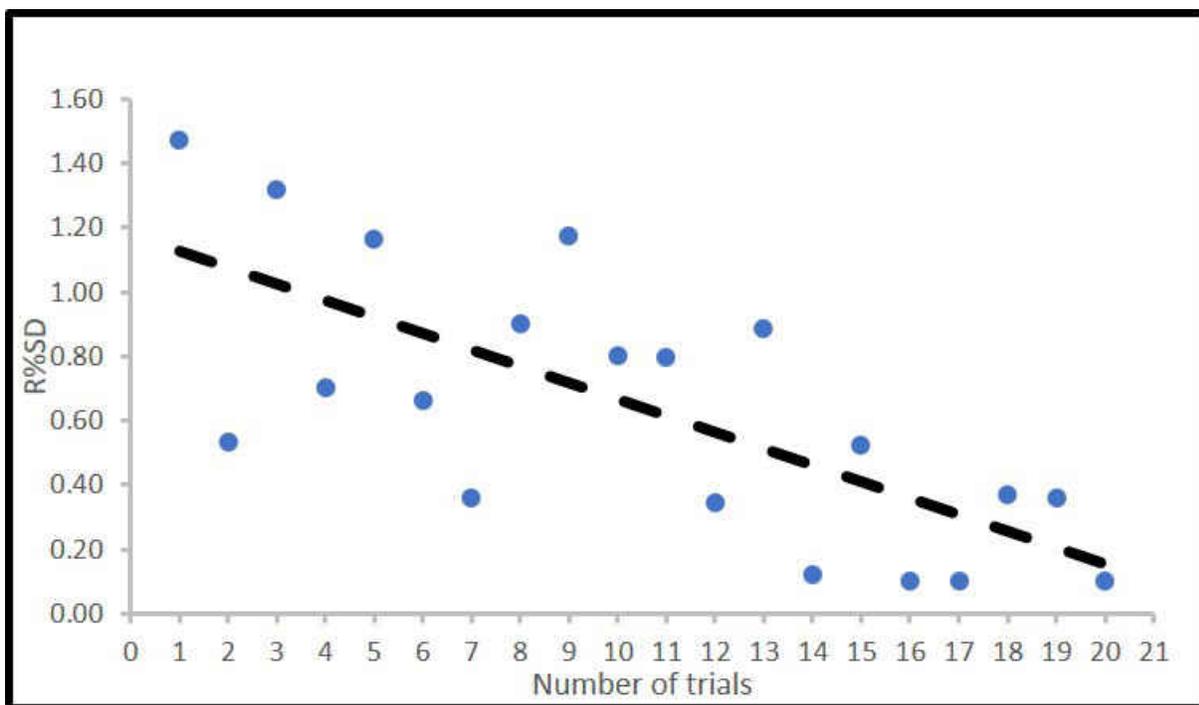
FIGURE 3.32: Variation of %RSD with the number of trials suggested by Simplex.

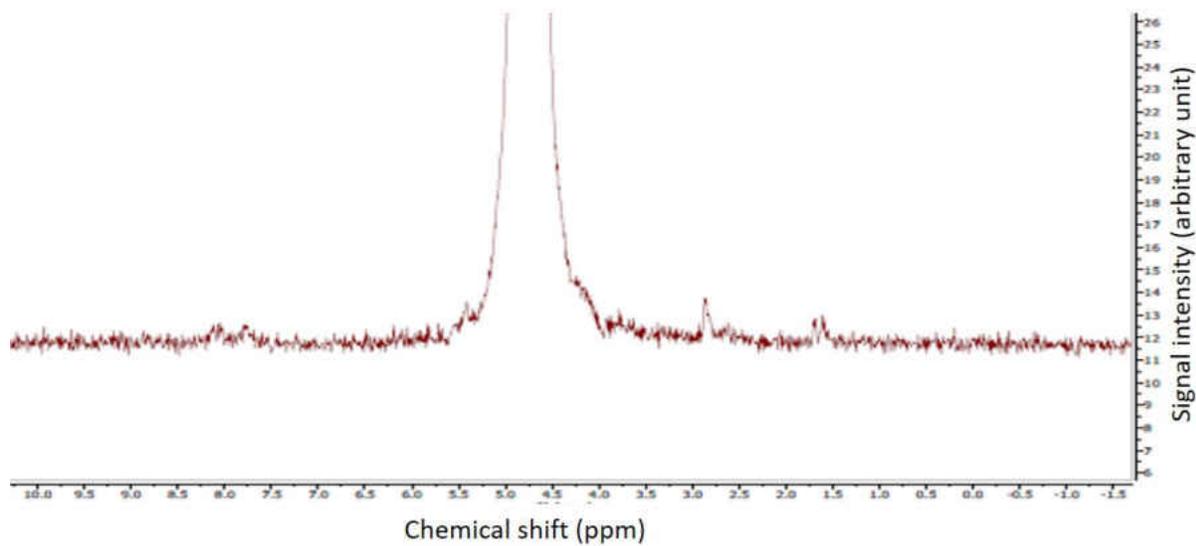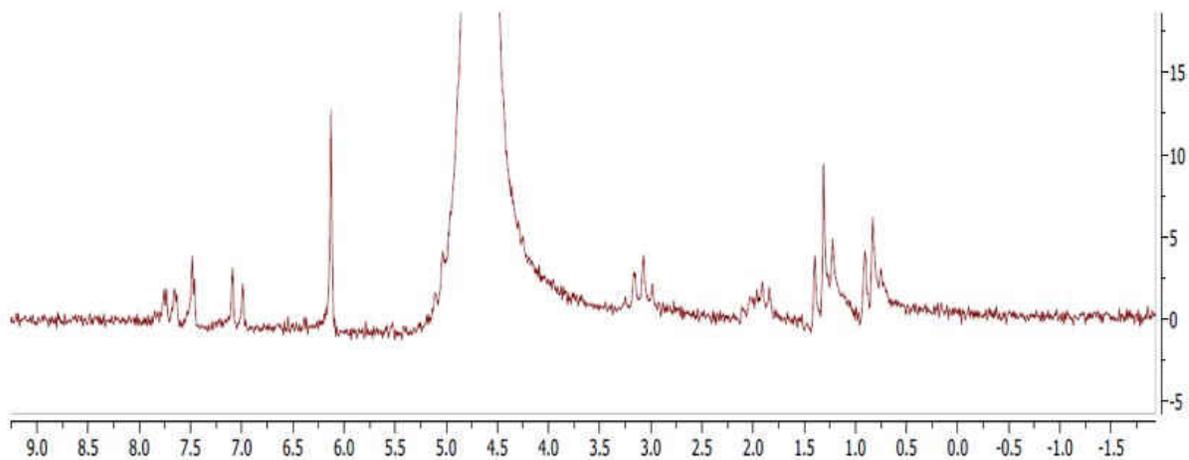FIGURE 3.33: Response for 50 mM N-Ethylpentylone by NMR (512 scans).
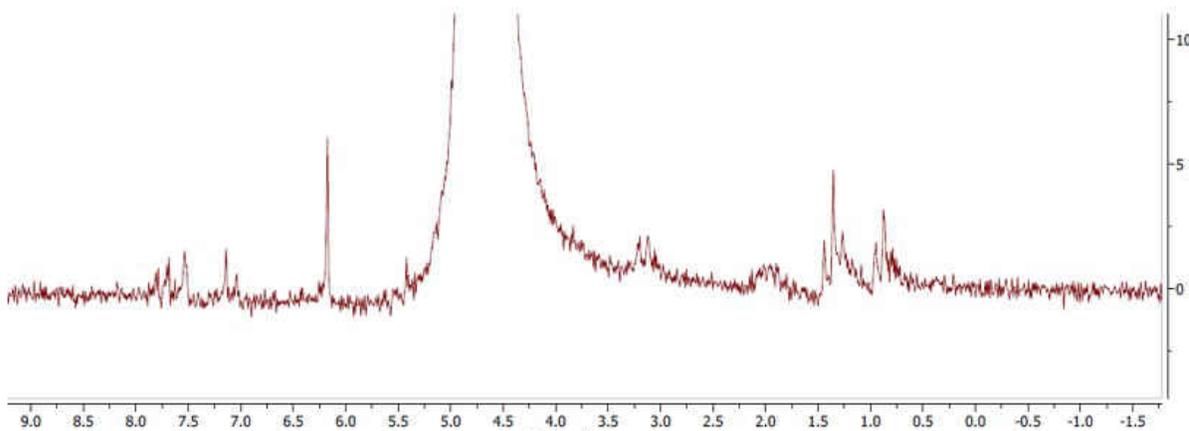
FIGURE 3.34: Response for 50 mM N-Ethylpentylone by SIA-NMR (512 scans).
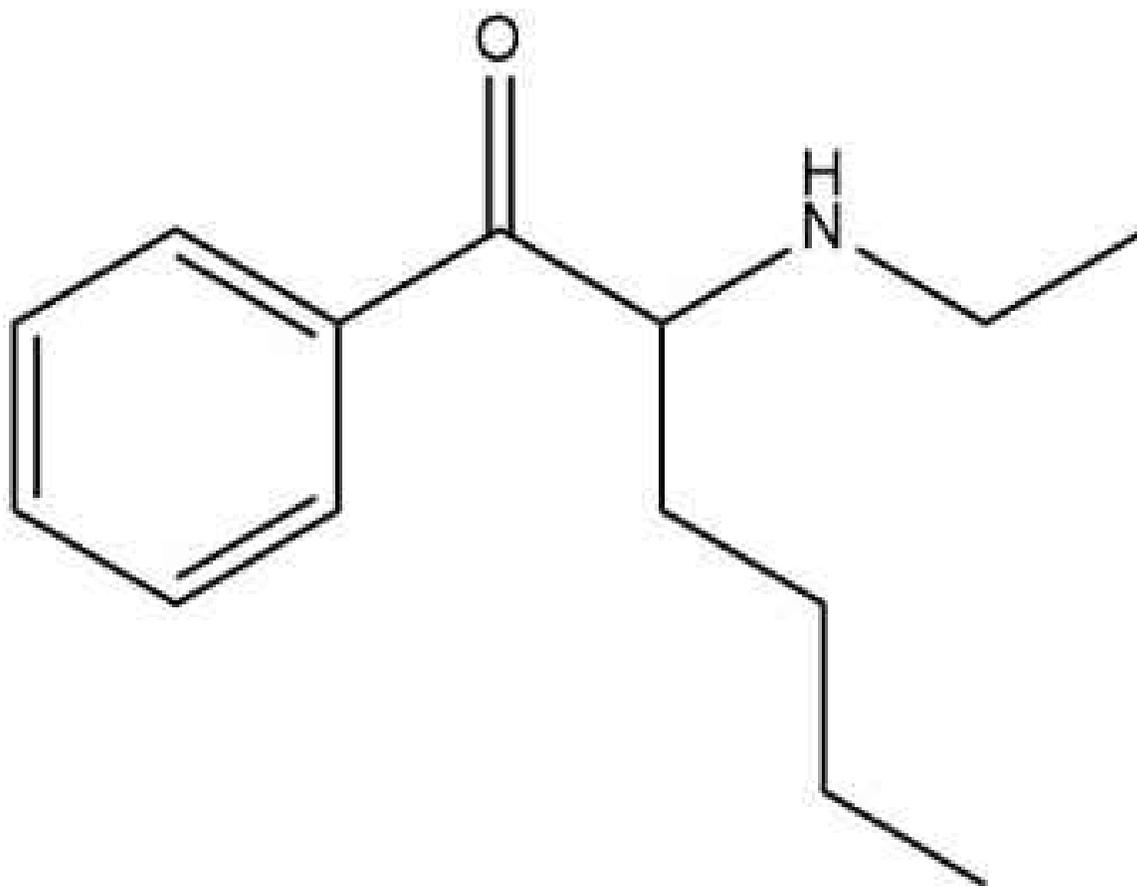
FIGURE 3.35: The structure of N-Ethylhexedrone.
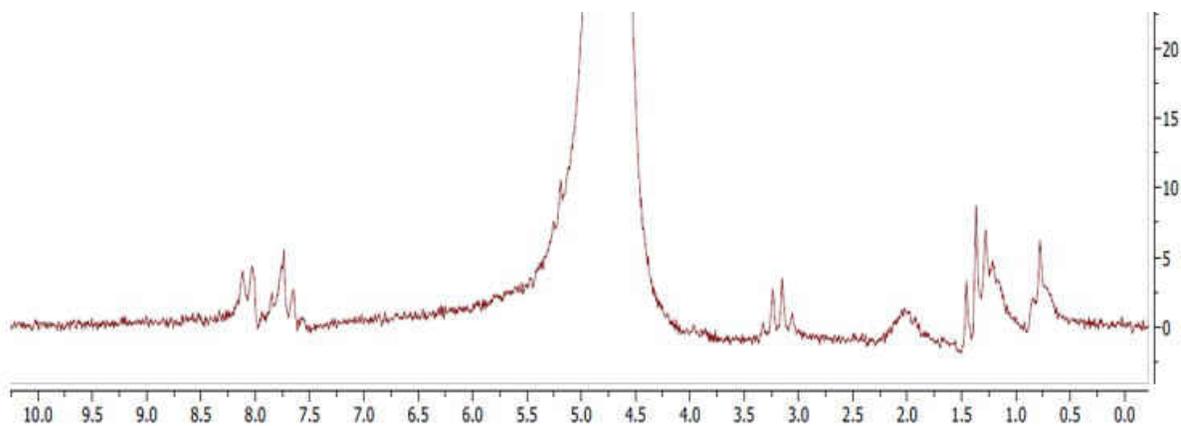
FIGURE 3.36: Response for 50 mM N-Ethylhexedrone by NMR (512 scans).
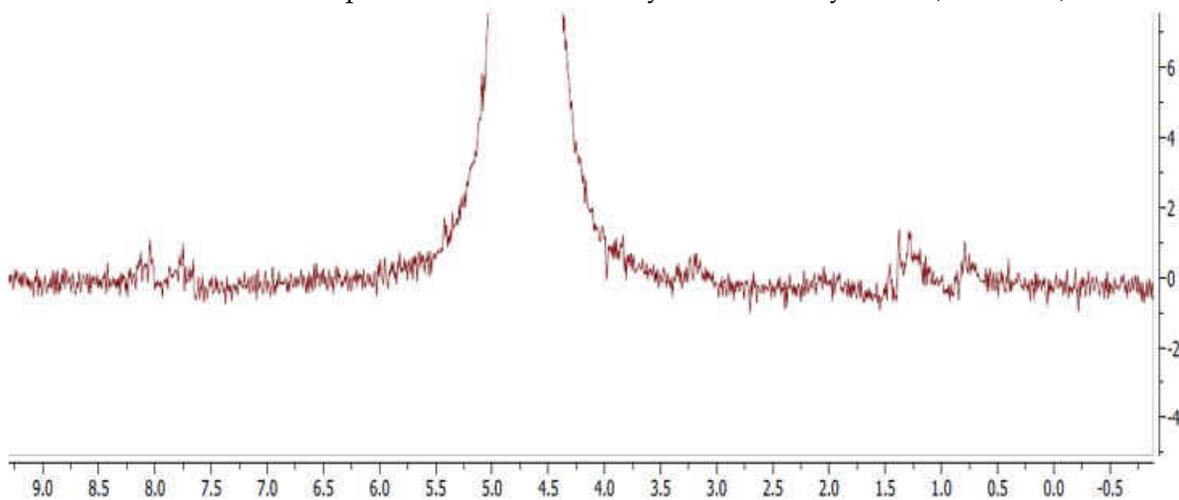
FIGURE 3.37: Response for 50 mM N-Ethylhexedrone by SIA-NMR (512 scans).
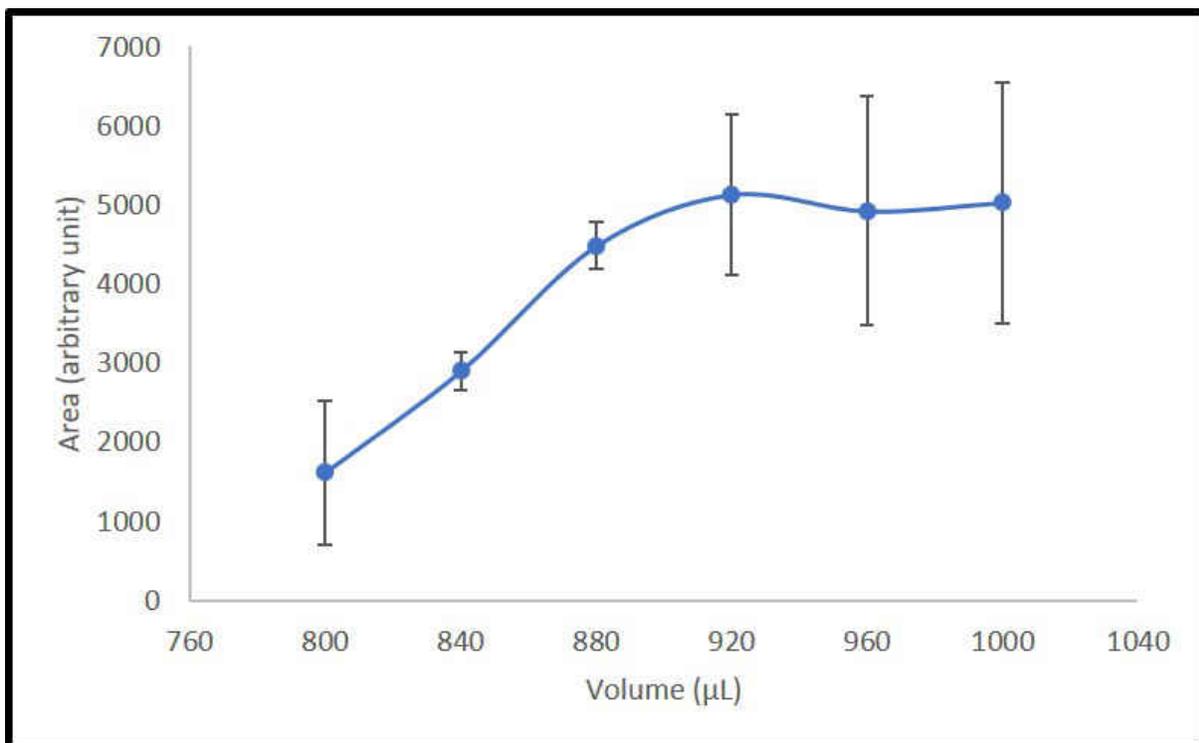
FIGURE 3.38: Response in change in area with respect to change in volume of analyte.
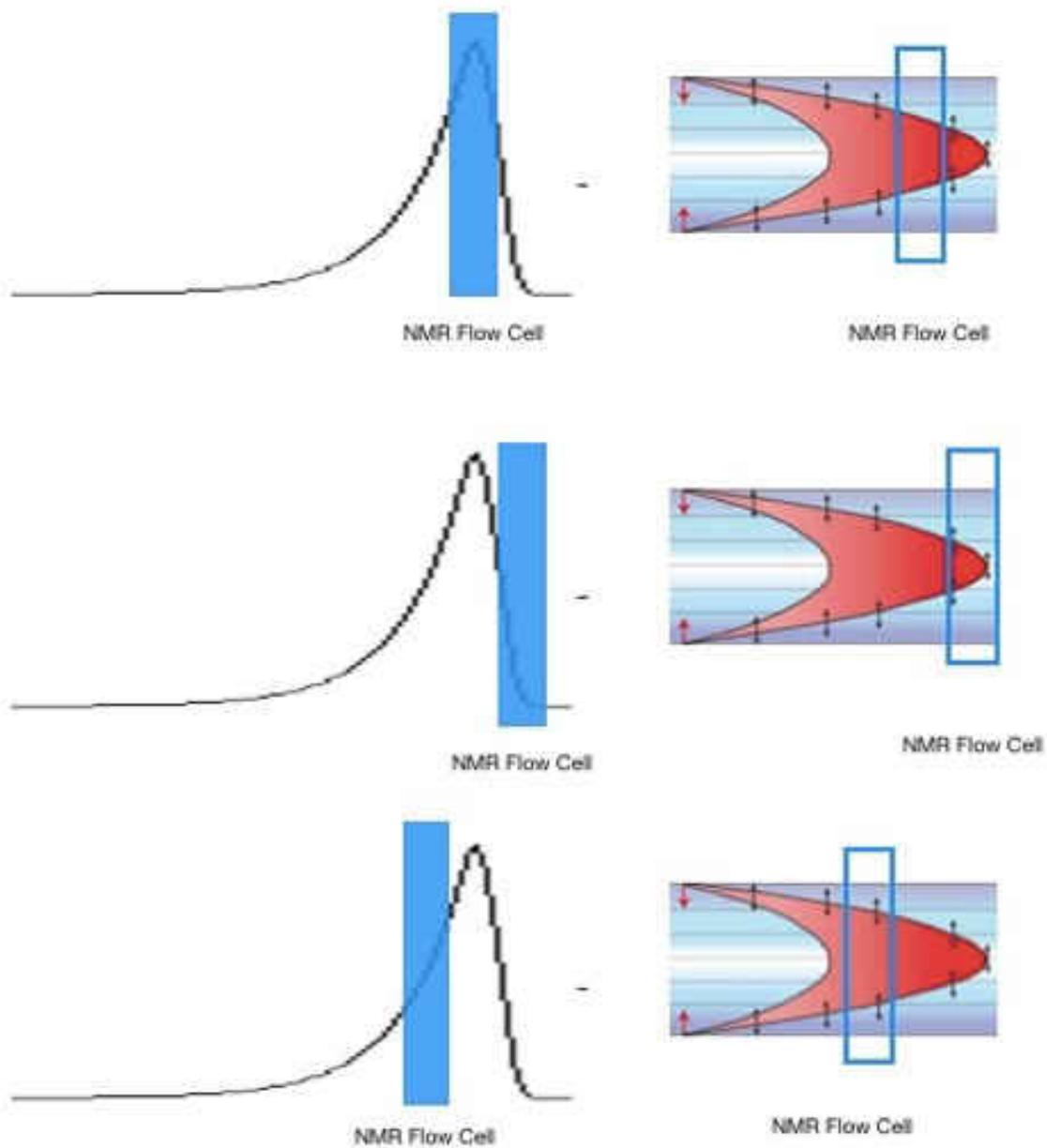
FIGURE 3.39: Response of sample zone for optimal volume (top), for small volume (middle) and for large volume (bottom) [28].
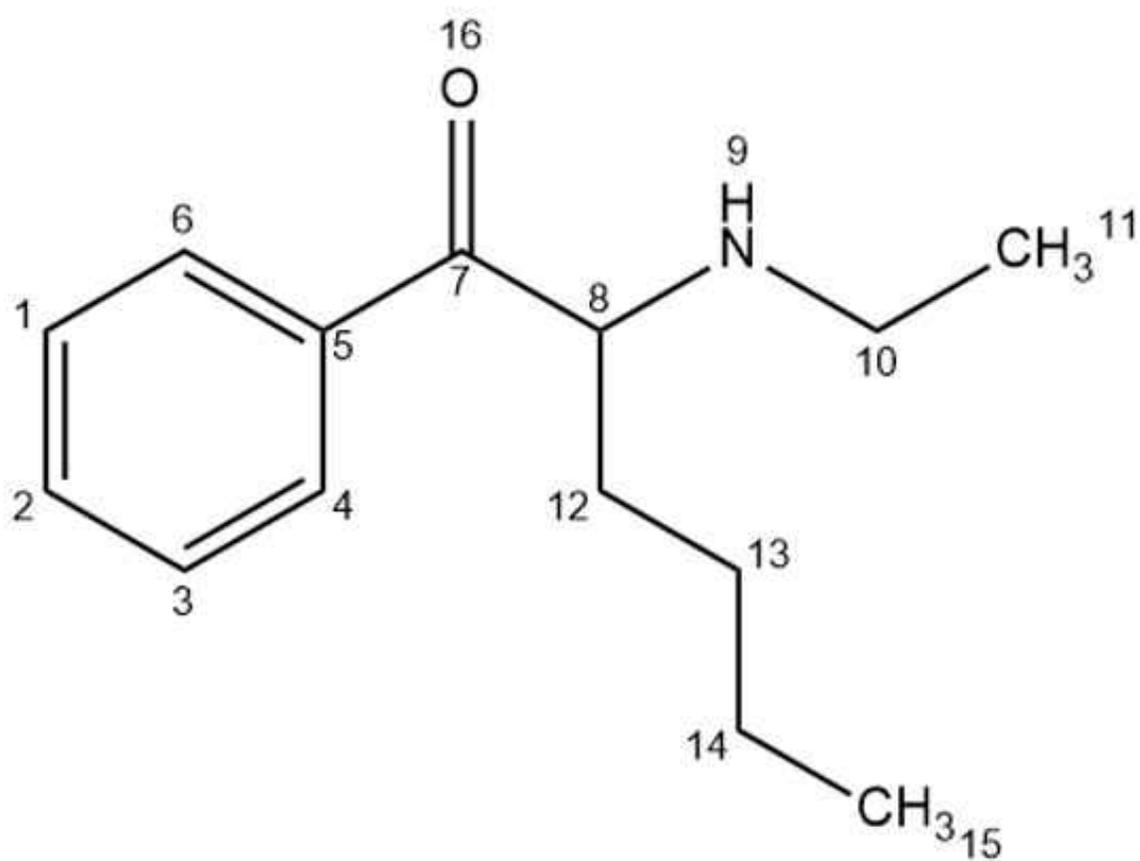
FIGURE 3.40: The structure of N-Ethylhexedrone.
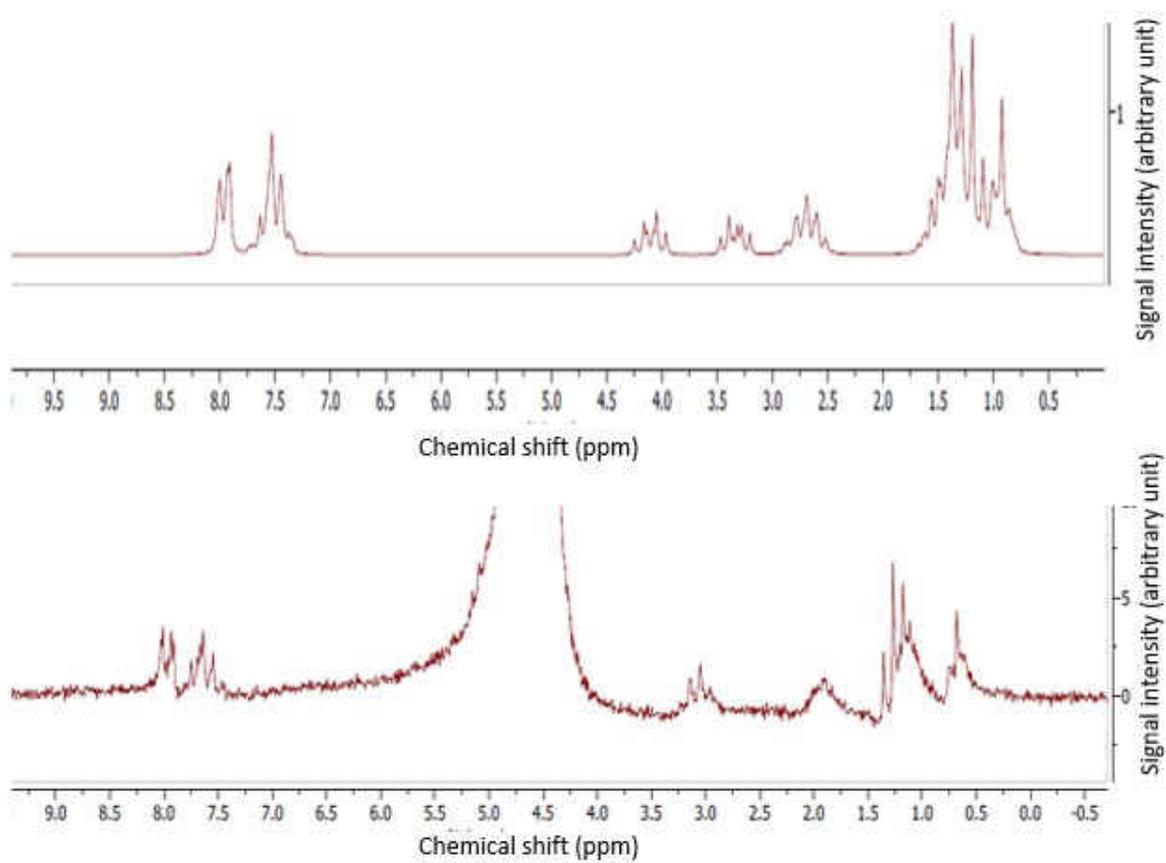
FIGURE 3.41: Predicted (top) and observed (bottom) 1H NMR spectrum of N-Ethylhexedrone
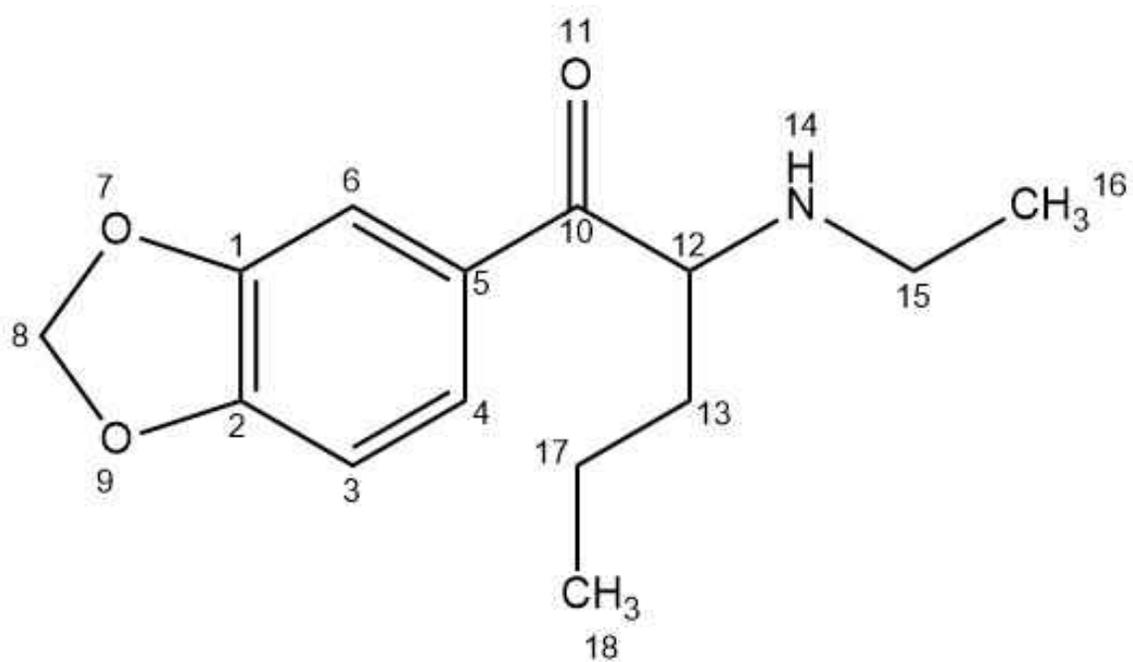
FIGURE 3.42: The structure of N-Ethylpentylone.
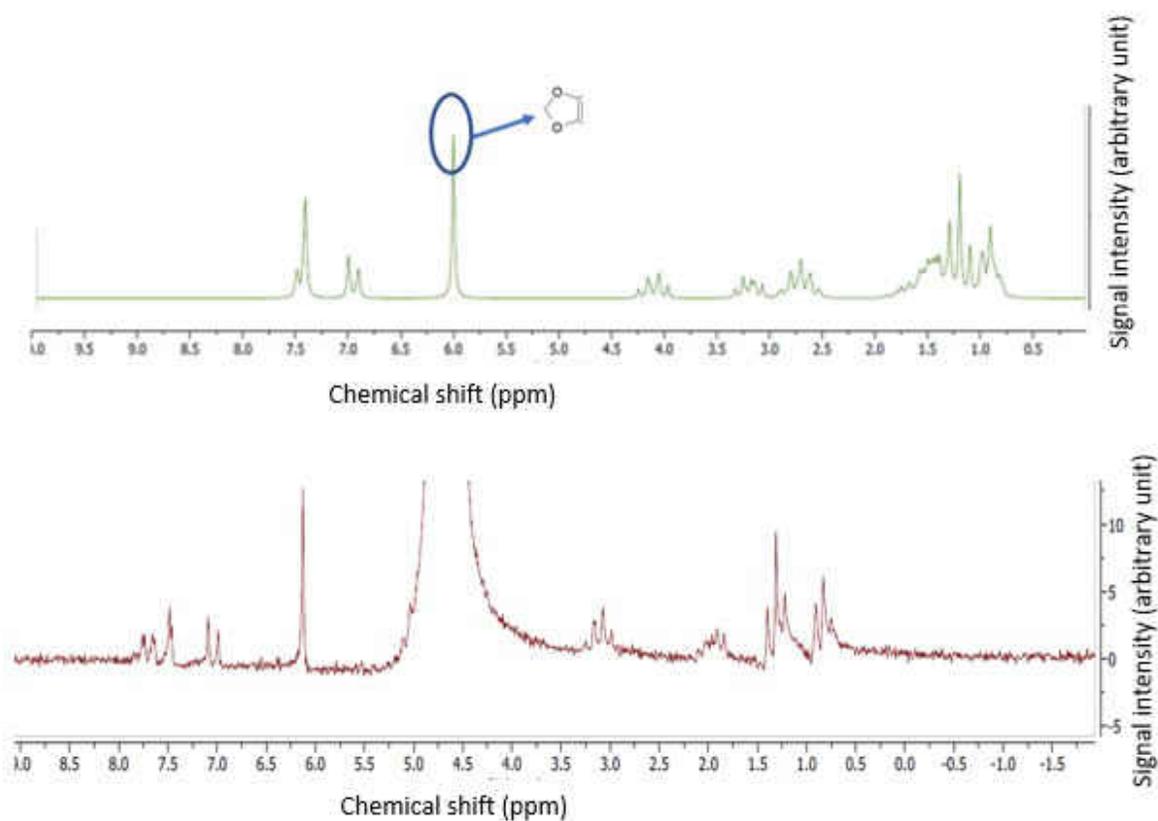
FIGURE 3.43: Predicted (top) and observed (bottom) 1H NMR spectrum of N-Ethylpentylone.
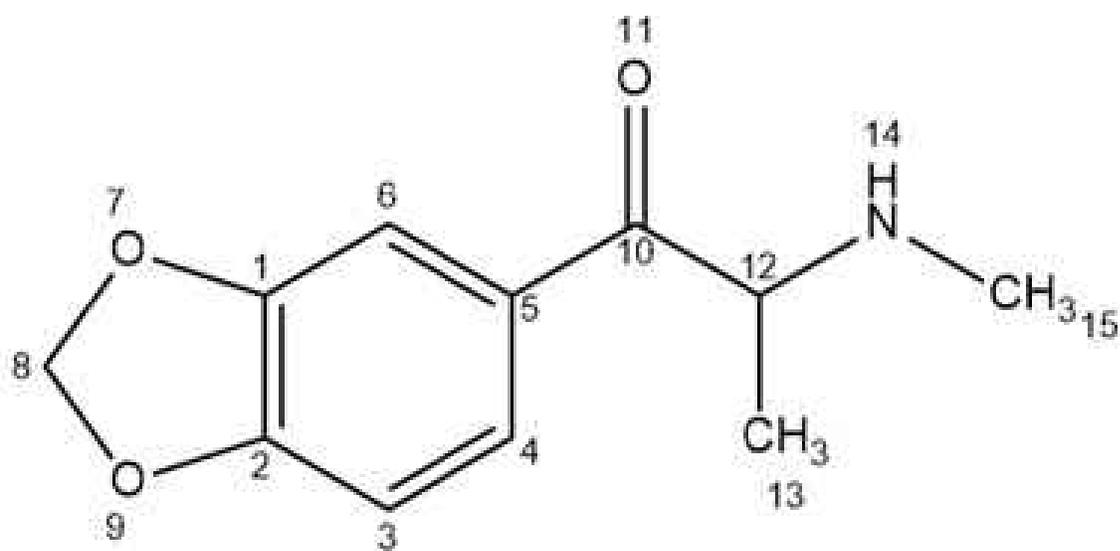
FIGURE 3.44: The structure of Methylone.
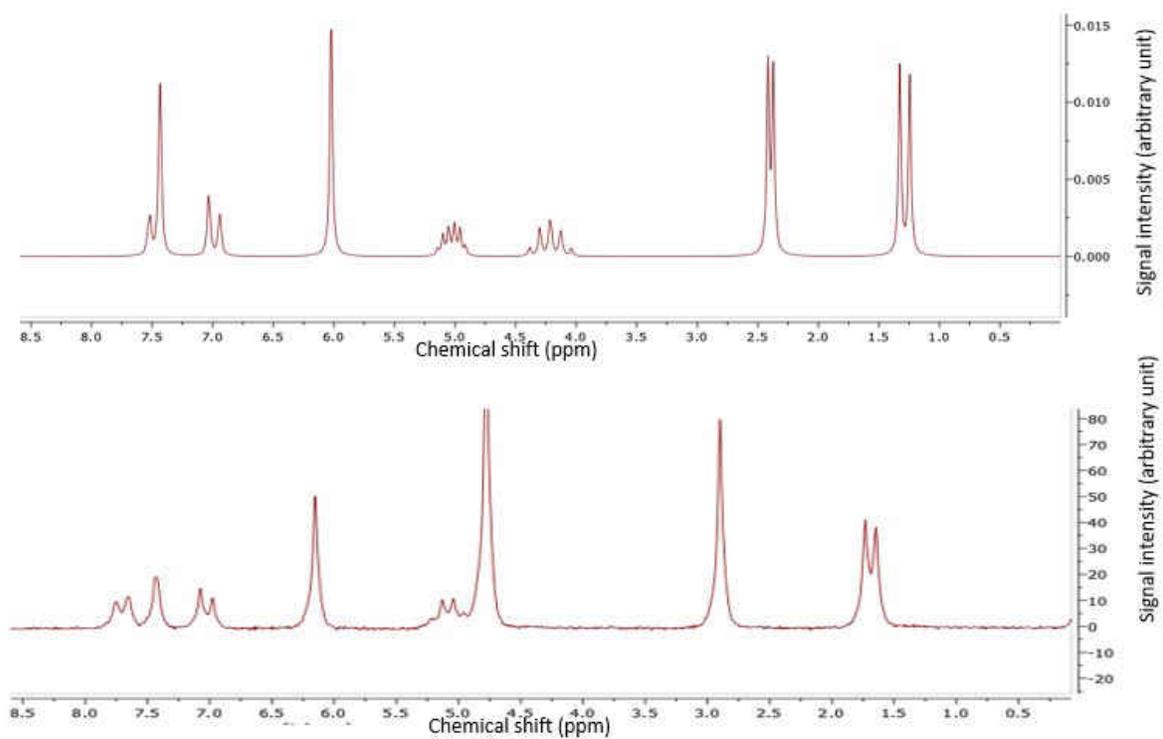
FIGURE 3.45: Predicted (top) and observed (bottom) 1H NMR spectrum of Methylone.
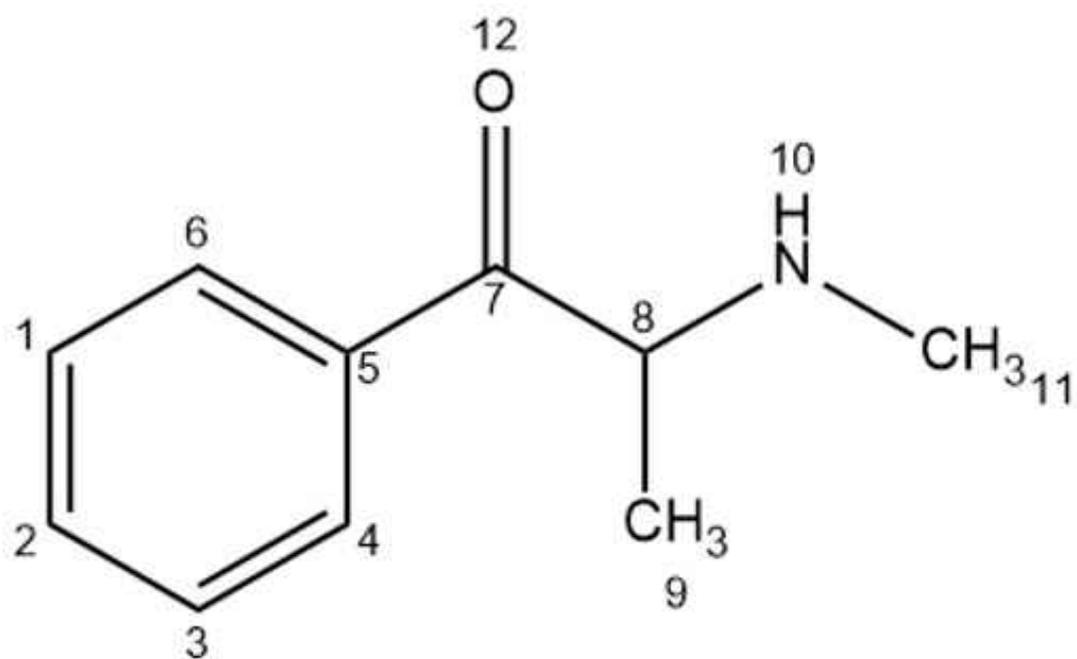
FIGURE 3.46: The structure of Methcathinone.
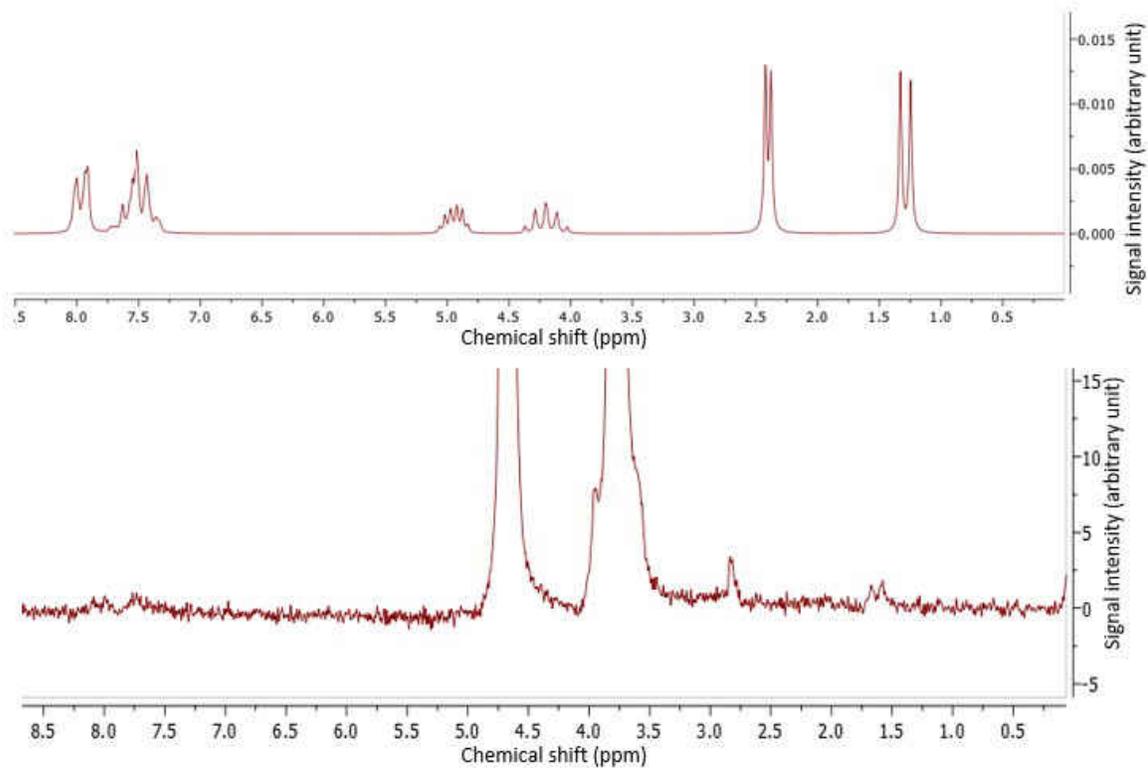
FIGURE 3.47: Predicted (top) and observed (bottom) 1H NMR spectrum of Methcathinone.

Run	1	2	3	4	5	6	7
1	+	-	-	+	-	+	+
2	+	+	-	-	+	-	+
3	+	+	+	-	-	+	-
4	-	+	+	+	-	-	+
5	+	-	+	+	+	-	-
6	-	+	-	+	+	+	-
7	-	-	+	-	+	+	+
8	-	-	-	-	-	-	-

TABLE 3.1: Plackett-Burman design for seven factors.

1	2	3	4	5	6	7
+	-	-	+	-	+	+

TABLE 3.2: Levels for first experiment with seven factors.

1	2	3	4	5	6	7
+	+	-	-	+	-	+

TABLE 3.3: Levels for second experiment with seven factors.

Run	1	2	3	4	5	6	7
1	-	+	+	-	+	-	-
2	-	-	+	+	-	+	-
3	-	-	-	+	+	-	+
4	+	-	-	-	+	+	-
5	-	+	-	-	-	+	+
6	+	-	+	-	-	-	+
7	+	+	-	+	-	-	-
8	+	+	+	+	+	+	+

TABLE 3.4: The foldover design for seven factors.

Run	1	2	3	4	5	6	7
1	+	-	-	+	-	+	+
2	+	+	-	-	+	-	+
3	+	+	+	-	-	+	-
4	-	+	+	+	-	-	+
5	+	-	+	+	+	-	-
6	-	+	-	+	+	+	-
7	-	-	+	-	+	+	+
8	-	-	-	-	-	-	-
9	-	+	+	-	+	-	-
10	-	-	+	+	-	+	-
11	-	-	-	+	+	-	+
12	+	-	-	-	+	+	-
13	-	+	-	-	-	+	+
14	+	-	+	-	-	-	+
15	+	+	-	+	-	-	-
16	+	+	+	+	+	+	+

TABLE 3.5: Plackett-Burman design with foldover for seven factors.

Serial Number	Factor
1	Volume of sample
2	Volume of eluent
3	Volume of carrier
4	Concentration of NaCl
5	Concentration of HCl
6	Concentration of Sample
7	Flowrate of sample aspiration
8	Flowrate of eluent aspiration)
9	Flowrate of elution
10	Flowrate of washcycle
11	pH of carrier
12	Purity of SCX
13	Purity of NaCl
14	Purity of amphetamine
15	Purity of phosphate salt
16	Temperature
17	Diameter of the tubing
18	Material of the tubing
19	Age of the tubing
20	Length of the tubing

TABLE 3.6: Twenty factors were chosen for the Plankett-Burman screening experiments.

Serial Number	Factor
1	Sample volume (V_S)
2	Concentration of sample (V_S)
3	Volume of carrier (V_L)
4	Sample aspiration flowrate (F_L)
5	pH
6	Volume of eluent (V_E)
7	Concentration of NaCl (C_{NaCl})
8	Concentration of HCl (C_{HCl})
9	Elution flowrate (F_E)
10	Sample aspiration flowrate (F_S)
11	Eluent aspiration flowrate (F_A)

TABLE 3.7: Eleven interacting factors identified by the Plackett-Burman screening design.

Run	V_S (μL)	C_S (mM)	V_L (μL)	F_L (μL/s	pH	C_{NaCl} (mM)	C_{HCl} (mM)	F_E (μL/s)	F_S (μL/s)	F_L (μL/s)	F_A (μL/s)
1	800	5	5000	5	4.0	500	500	500	30	5	30
2	800	50	1000	30	4.0	500	50	500	30	30	5
3	100	50	5000	5	6.0	500	50	25	30	30	30
4	800	5	5000	30	4.0	2000	50	25	5	30	30
5	800	50	1000	30	6.0	500	50	25	5	5	30
6	800	50	5000	5	6.0	2000	500	500	5	5	5
7	100	50	5000	30	4.0	2000	50	250	30	5	5
8	100	5	5000	30	6.0	500	500	500	30	5	30
9	100	5	1000	30	6.0	2000	50	500	30	5	30
10	800	5	1000	5	6.0	2000	500	25	30	30	5
11	100	50	1000	5	4.0	2000	500	500	5	30	30
12	100	5	1000	5	4.0	500	50	25	5	5	5
13	100	50	1000	30	6.0	2000	50	25	5	30	5
14	100	5	5000	5	6.0	2000	500	500	5	5	30
15	800	5	1000	30	4.0	2000	500	500	5	5	5
16	100	50	1000	5	6.0	500	500	500	30	5	5
17	100	5	5000	5	4.0	2000	50	25	30	30	5
18	100	5	1000	30	4.0	500	500	500	30	30	30
19	800	5	1000	5	6.0	500	50	25	5	30	30
20	800	50	1000	5	4.0	2000	500	25	30	5	30
21	800	50	5000	5	4.0	500	500	500	5	30	5
22	100	50	5000	30	4.0	500	50	25	5	5	30
23	800	5	5000	30	6.0	500	50	25	30	5	5
24	800	50	5000	30	6.0	2000	500	500	30	30	30

TABLE 3.8: Plackett-Burman design with fold-over for the 11 interacting factors.

Factor	Factor name	Significance
1	Sample Volume	0.672
2	Concentration of sample	0.614
3	Volume of carrier	0.042
4	Sample aspiration flowrate	-0.164
5	pH	-0.069
6	Volume of eluent	-0.279
7	Concentration of NaCl	0.201
8	Concentration of HCl	0.237
9	Elution flowrate	-0.367
10	Sample aspiration flowrate	0.300
11	Elution aspirartion flowrate	-0.110

TABLE 3.9: Results of Plackett-Burman study.

Factor	Initial value	Step-size
Sample volume (V_S)	800 μL	70 μL
Carrier aspiration flowrate (F_L)	20 μL/s	5 μL
Volume of eluent (V_E)	1425 μL	150 μL
Concn of NaCl (C_{NaCl})	200 mM	50 MM
Concn of HCl (C_{HCl})	100 mM	50 mM
Elution flowrate (F_E)	20 μL/s	5 μL
Sample aspiration flowrate (F_S)	20 μL/s	5 μL

TABLE 3.10: Seven interacting factors with their values and step-size.

Factor	Optimized	Original
Sample volume (μL)	800	800
Volume of eluent (μL)	1565	1425
Conc of NaCl (mM)	215	200
Concn of HCl (mM)	60	100
Sample aspiration flowrate (μL/s)	21	20
Carrier aspiration flowrate (μL/s)	18	20
Elution flowrate (μL/s)	25	20

TABLE 3.11: Factors with their optimized and original values.

Figures of Merit	Original	Optimized
LOD (mM)	0.077	0.023
%RSD	1.495	0.104

TABLE 3.12: LOD, %RSD and sensitivity of the original and optimized methods.

Serial Number	Types of proton	Observed shift (ppm)
1	Methyl protons	1.20 and 1.00
2	Methylene protons	3.00
3	Protons attached to methylenedioxy group	6.00
4	Benzene protons	7.00 and 7.50

TABLE 3.13: Major peaks of N-Ethylpentylone.

Serial Number	Types of proton	Observed shift (ppm)
1	Methyl protons	1.20 and 1.00
2	Methylene protons	2.50
3	Benzene protons	7.50 and 8.00

TABLE 3.14: Major peaks of N-Ethyhexedrone.

No. of neighbors	Relative intensities	Pattern
0	1	Singlet
1	1:1	Doublet
2	1:2:1	Triplet
3	1:3:3:1	Quartet
4	1:4:6:4:1	Quintet
5	1:5:10:10:5:1	Sextet

TABLE 3.15: Pascal's Triangle.

Proton	Multiplicity	Peak Intensity	Predicted shift (ppm)	Observed shift (ppm)	%Error
C-1, 2, 3	Triplet	1:2:1	7.25	7.50	3.40
C-4, 6	Doublet	Equivalent	7.75	8.00	3.20
C-8	Quartet	1:3:3:1	4.00	NA	NA
N-9	Quartet	1:3:3:1	3.25	NA	NA
C-12	Quartet	1:3:3:1	2.50	2.75	10.0

TABLE 3.16: Different types of protons in N-Ethylhexedrone.

Proton	Multiplicity	Peak Intensity	Predicted shift (ppm)	Observed shift (ppm)	%Error
C-3	Doublet	Equivalent	6.75	7.00	3.70
C-4	Doublet	Equivalent	7.50	7.75	3.30
C-6	Singlet	NA	7.25	7.50	3.40
C-8	Singlet	NA	6.00	6.25	4.20
C-12	Quartet	1:3:3:1	4.00	NA	NA
N-14	Quartet	1:3:3:1	3.25	NA	NA
C-15	Quartet	1:3:3:1	2.50	3.00	20.0

TABLE 3.17: Different types of protons in N-Ethylpentylone.

Proton	Multiplicity	Peak Intensity	Predicted shift (ppm)	Observed shift (ppm)	%Error
C-3	Doublet	Equivalent	7.00	7.00	NA
C-4	Doublet	Equivalent	7.50	7.75	3.30
C-6	Singlet	NA	7.50	7.50	NA
C-8	Singlet	NA	6.00	6.25	4.20
C-12	Quintet	1:4:6:4:1	5.00	NA	NA
C-13	Doublet	Equivalent	1.25	1.50	20.0
N-14	Quintet	1:4:6:4:1	4.00	NA	NA
C-15	Doublet	Equivalent	2.25	2.75	22.0

TABLE 3.18: Different types of protons in Methylone.

Proton	Multiplicity	Peak Intensity	Predicted shift (ppm)	Observed shift (ppm)	%Error
C-1, 2, 3	Triplet	1:2:1	7.25	7.50	3.40
C-4, 6	Doublet	Equivalent	7.75	8.00	3.20
C-8	Quintet	1:4:6:4:1	4.00	NA	NA
C-9	Doublet	Equivalent	1.25	1.75	40.0
N-10	Quintet	1:4:6:4:1	5.00	NA	NA
C-11	Doublet	Equivalent	2.25	2.75	20.0

TABLE 3.19: Different types of protons in Methcathinone.

References

[1] S. Schuette, R. Smith, L. Holden, and J. Graham, "Solid-phase extraction of herbicides from well water for determination by gas chromatography-mass spectrometry," *Analytica Chimica Acta* 1990, 236, 141–144.

[2] K. Robards, K. Robards, P. Haddad, P. Haddad, P. Jackson, P. Jackson, and P. Haddad, *Principles and practice of modern chromatographic methods*, Academic Press, San Diego, California, 1994.

[3] H. Kalász, *Displacement chromatography*, Oxford University Press, England, 2003.

[4] J. Płotka-Wasylka, N. Szczepańska, M. de la Guardia, and J. Namieśnik, "Modern trends in solid phase extraction: new sorbent media," *TrAC Trends in Analytical Chemistry* 2016, 77, 23–43.

[5] M.-R. Lee, S.-C. Yu, C.-L. Lin, Y.-C. Yeh, Y.-L. Chen, and S.-H. Hu, "Solid-phase extraction in amphetamine and methamphetamine analysis of urine," *Journal of Analytical Toxicology* 1997, 21, 4, 278–282.

[6] D. D. Perrin, *Dissociation constants of organic bases in aqueous solution: supplement 1972*, Butterworths, 1972.

[7] Z. Huang and S. Zhang, "Confirmation of amphetamine, methamphetamine, mda and mdma in urine samples using disk solid-phase extraction and gas

chromatography–mass spectrometry after immunoassay screening," *Journal of Chromatography B* 2003, 792, 2, 241–247.

[8] P. C. Falcó, C. M. Legua, A. S. Cabeza, and R. P. Serrano, "Derivatization of amphetamine and methamphetamine with 1, 2-naphthoquinone 4-sulfonic acid into solid-phase extraction cartridges. determination of amphetamine in pharmaceutical and urine samples," *Analyst* 1997, 122, 7, 673–677.

[9] T. H. Boles and M. J. Wells, "Analysis of amphetamine and methamphetamine as emerging pollutants in wastewater and wastewater-impacted streams," *Journal of Chromatography A* 2010, 1217, 16, 2561–2568.

[10] J. Dai, S. D. Mendonsa, M. T. Bowser, C. A. Lucy, and P. W. Carr, "Effect of anionic additive type on ion pair formation constants of basic pharmaceuticals," *Journal of Chromatography A* 2005, 1069, 2, 225–234.

[11] M. A. Bezerra, Q. O. dos Santos, A. G. Santos, C. G. Novaes, S. L. C. Ferreira, and V. S. de Souza, "Simplex optimization: a tutorial approach and recent applications in analytical chemistry," *Microchemical Journal* 2016, 124, 45–54.

[12] S. N. Deming, L. R. Parker Jr, and M. Bonner Denton, "A review of simplex optimization in analytical chemistry," *CRC Critical Reviews in Analytical Chemistry* 1978, 7, 3, 187–202.

[13] R. L. Plackett and J. P. Burman, "The design of optimum multifactorial experiments," *Biometrika* 1946, 33, 4, 305–325.

[14] K. Vanaja and R. Shobha Rani, "Design of experiments: concept and applications of plackett burman design," *Clinical Research and Regulatory Affairs* 2007, 24, 1, 1–23.

[15] H. E. Wiik, *Methods for Analyzing the 12 Run Plackett-Burman Design*, Master's thesis, Institutt for matematiske fag, 2014.

[16] S. P. Jain, P. P. Singh, S. Javeer, and P. D. Amin, "Use of placket–burman statistical design to study effect of formulation variables on the release of drug from hot melt sustained release extrudates," *Aaps Pharmscitech* 2010, 11, 2, 936–944.

[17] P. F. Stanbury, A. Whitaker, and S. J. Hall, *Principles of fermentation technology*, Elsevier, Amsterdam, Netherlands, 2013.

[18] A. AnalyticalMethodsCommittee, "Experimental design and optimisation (4): Plackett-burman designs," *Analytical Methods* 2013, 5, 8, 1901–1903.

[19] R. Fahmy, R. Kona, R. Dandu, W. Xie, G. Claycamp, and S. W. Hoag, "Quality by design i: application of failure mode effect analysis (fmea) and plackett–burman design of experiments in the identification of "main factors" in the formulation and process design space for roller-compacted ciprofloxacin hydrochloride immediate-release tablets," *AAPS PharmSciTech* 2012, 13, 4, 1243–1254.

[20] D. L. Beres and D. M. Hawkins, "Plackett–burman technique for sensitivity analysis of many-parametered models," *Ecological modelling* 2001, 141, 1-3, 171–183.

[21] W. Spendley, G. R. Hext, and F. R. Himsworth, "Sequential application of simplex designs in optimisation and evolutionary operation," *Technometrics* 1962, 4, 4, 441–461.

[22] J. Gabrielsson, N.-O. Lindberg, and T. Lundstedt, "Multivariate methods in pharmaceutical applications," *Journal of Chemometrics: A Journal of the Chemometrics Society* 2002, 16, 3, 141–160.

[23] S. L. Morgan and S. N. Deming, "Simplex optimization of analytical chemical methods," *Analytical chemistry* 1974, 46, 9, 1170–1181.

[24] D. MacDougall, W. B. Crummett, et al., "Guidelines for data acquisition and data quality evaluation in environmental chemistry," *Analytical Chemistry* 1980, 52, 14, 2242–2249.

[25] C. Xiao, F. Hao, X. Qin, Y. Wang, and H. Tang, "An optimized buffer system for nmr-based urinary metabonomics with effective ph control, chemical shift consistency and dilution minimization," *Analyst* 2009, 134, 5, 916–925.

[26] D. A. Skoog, F. J. Holler, and S. R. Crouch, *Principles of instrumental analysis*, Cengage learning, Boston, MA, 2017.

[27] R. M. Silverstein and G. C. Bassler, "Spectrometric identification of organic compounds," *Journal of Chemical Education* 1962, 39, 11, 546.

[28] J. Ruscika, *Flow Injection Analysis*, 2019 (accessed March 11, 2020), URL `http://flowinjectiontutorial.com/index.html`.

Chapter 4

Conclusions and Future Work

The goal of the thesis was three-fold. First, to develop and optimized a method for isolation of Cathinones by SPE-SIA NMR. Second, to apply the SPE-SIA-NMR method to apply the method to authentic casework samples provided by the WSCL in Milwaukee. Third, to rationalize the differences found in a comparison of the observed and predicted proton NMR spectra for four of the WSCL samples.

In the first part of the study, three types of amphetamine simulants were used to develop the SPE-SIA method: Phenylpropanolamine (PPA), Phenylephrine (PEP), and Methylephedrine (MEP) representing primary, secondary, and tertiary amines, respectively. Various types of resins were examined for these three analytes: mixed cation exchange (MCAX), reversed-phase (C18), strong cation exchange (SCX), and hydrophilic-lipophilic balance (HLB) resins. Three types of column were studied for the project: wide cylindrical (bed volume of 2.7 mL), narrow cylindrical (bed volume of 2.3 mL), and tapered (bed volume of 27 μL). The SCX resin had greater capacity for the Cathinone simulants in the wide cylindrical column, with a 100 mM phosphate buffer (pH 6.00) as mobile phase and 200 mM NaCl / 100 mM HCl as eluent. The final part of the first phase was to apply the SIA-NMR method to authentic samples at the WSCL.

137

Several case samples were studied, and the method was successful for determining primary and secondary Cathinones. However, tertiary amines were found to be more difficult to quantitatively elute than primary and secondary amines.

In the second phase of the study, the method was rigorously optimized by first using a Plackett-Burman screening design followed by Simplex optimization. The Plackett-Burman screening design was carried out with eleven factors to identify the most interacting factors in the SPE-SIA method. Out of the eleven factors, seven factors were found to have the greatest impact on the response. Those seven factors were: sample volume, sample aspiration flowrate, sample loading flowrate, concentration of NaCl in the eluent, concentration of HCl in the eluent, volume of eluent, and elution flowrate. The efficiency of the original method was compared to the optimized method. The LOD for the optimized method was found to be 0.023 mM (70% lower than observed for the original method). The sensitivity of the method increased by 66% as compared to the original method, and the %RSD improved from 1.47% to 0.10% which is a 93% improvement.

In the third and final phase of the study, four Cathinones that had been study at WSCL were studied by examining their NMR spectra: Methylone, Methcathinone, N-Ethylhexedrone, and N-Ethylpentylone, which are secondary amines. The predicted NMR spectra was created by using the Mnova software. It was interesting to observe that there were some peaks in experimental NMR spectra which were not found in the

predicted ones. Also, some predicted peaks were absent in observed spectra.

In the future, the SPE-SIA-NMR method could be applied to other amphetamines as well as explored for the determination of other"drugs of abuse" such as Fentanyls. Alternatives to SPE such as liquid-liquid extraction could be also examined for improving preconcentration and matrix removal. While SCX was the optimal stationary phase resin for this study, other types of SPE resins should be examined such as chemically modified resins. In optimizing the method, the eluent could also be examined more closedly, and organic modifiers could be included to more efficiently elute the analytes in a smaller volume to realize a preconcentration effect.

Future work could also focus on a study of the molecular mechanism of the ion-exhange process. A better understanding of the orientation of the analyte molecule to the sulfonic acid group on the SCX resin would allow for the design of a more efficient eluent. The structure of the Cathinone molecule with the lowest energy will determine the orientation of the molecule during retention. Computational studies using Density Functional Theory (DFT) could be undertaken to predict the molecular structure.